An Anatomical Approach to Lower Extremity Reconstructive Surgery

DISSERTATION

Presented to the Graduate Council of the

University of North Texas Health Science Center at Fort Worth

For the Degree of

DOCTOR OF PHILOSOPHY

Structural Anatomy and Rehabilitative Science

By

Addison R. Wood

Fort Worth, Texas

April 4, 2017

Abstract

Orthopaedic surgery of the lower extremity can be approached in several ways, but many times it is divided into soft tissue and boney reconstructive modalities. Orthopaedic sports surgery subspecialists tend to focus on soft tissue reconstruction; often with the goal of restoring as much natural motion as possible. Adult reconstructive orthopaedic surgery subspecialists often focus on boney alignment and use implants to replace degenerated cartilage and bone. There is significant overlap in these subspecialties as both make use of implants to mimic the structure and function of native anatomy to drive stability and motion. This dissertation focuses on the intersection of biomechanics, anatomy, and clinical orthopaedics of these two subspecialties. These areas are addressed through investigation of anatomical variation, muscular architecture, simulator design and construction, and comparative effectiveness via in vitro simulation.

Native anatomy directs all functions of the lower extremity via muscle forces, bone, and soft tissue. We demonstrate first that native anatomy is variable and is largely subject specific through a simple case report on bilateral tendinous foramina to serve as an example as one of many variations that can occur with anatomy. Many generalities are made with anatomy in assuming everything looks like a textbook, but in reality surgeons approach and consider each patient's specific anatomy when performing surgery. This translates over to the basic science research realm where experimental input and methods should subject specific as well in attempts to simulate kinematics of in vivo subjects.

Muscle forces are integral to proper kinematics and in vitro simulation. We describe the muscular architecture of the popliteus muscle with physiological cross sectional area (PCSA) and muscle trajectory data. Analysis revealed that females are capable of producing more force in their

popliteus muscle in proportion to their semimembranosus muscle than males. In addition, significant differences were found between male and female PCSA. The popliteus muscle trajectory data when combined with muscle force data suggests the popliteus muscle plays a significant dynamic role in knee kinematics. The popliteus has only been studied as a static muscle in prior literature. Our data suggests that treating the popliteus muscle as a dynamic figure in the knee would allow improved simulations focused on native knee kinematics and kinetics.

During cruciate retaining total knee arthroplasty (TKA) the posterior cruciate ligament (PCL) is an important structural determinant of motion. The PCL is at risk for damage during surgery as one of the tibial bone cuts is directly oriented towards the tibial PCL attachment. An effectiveness study was performed to examine prevention of iatrogenic PCL injuries using an osteotome in a simulated surgical environment using cadavers. The use of an osteotome was found to have an absolute risk reduction of 50% when compared to the control group which did not use an osteotome to protect the PCL. The use of an osteotome to preserve the PCL during CR TKA by forming a bone island was found to be an effective means of protecting the PCL over standard technique. This method is hypothesized to reduce the incidence of instability and knee joint laxity after CR TKA by maintaining the PCL and therefore kinematic quality.

Simulators enable mimicry of clinically relevant maneuvers performed in vivo with expanded potential to perform research considered unethical on living subjects. The creation of 3 separate simulators enabled description of clinically relevant kinematic situations in the knee and ankle. The University of North Texas Health Science Center (UNT HSC) ankle rig was designed to mimic an external rotational stress test of the ankle by an examiner. It allows simultaneous measurement of torque about the ankle, ultrasound imaging, and 3-dimensional motion tracking as a moment is applied to the ankle. This rig was of novel design and allows for controlled static positioning of the ankle with 6 degrees of freedom of control. In addition, it can allow 6 degrees of freedom to occur unconstrained if necessary. The UNT HSC ankle rig was used to stress test syndesmosis fixation using suture-button and internal brace constructs. The other 2 simulators represent a progression of improvement from a basic passive knee rig to a more advanced muscle loading knee rig. The initial simulator loaded the quadriceps and hamstrings through 1 line of action each while allowing the knee to passively flex and extend. The second-generation design was based on the muscle loading rig from The University of Kansas. It uses 3 lines of action to load the quadriceps and 2 lines of action to load the hamstrings with anatomically correct trajectories while allowing the knee to passively flex and extend. These simulators were built to enable in vitro simulations of the knee and ankle to describe kinematic changes from lower extremity reconstructive surgery.

Ankle syndesmosis injuries are common and are traditionally treated with simple cortical screw fixation. Newer implants like the suture-button and internal brace seek to restore physiological motion at the syndesmosis by mimicking native structure and function. We used the UNT HSC ankle rig to demonstrate the ability of combinational fixation constructs to restore physiological motion at the syndesmosis. The results indicate a combined suture-button and internal brace construct more closely resembles physiologic ankle syndesmosis kinematics than the suture-button alone. In addition, we described the mechanism through which this occurs. The suture-button or internal brace alone do not adequately restrain motion, but together they do. This is due to the external rotation of the fibula. As the fibula externally rotates it allows the fibula to translate posteriorly more with the suture-button only construct. The internal brace is added to the initial suture-button only construct and restricts external rotation and the resultant vector of restraint from both implants prevents posterolateral directed forces from inducing movement of the fibula.

In conclusion, we have described factors effecting physiologic motion through our anatomical variation and muscle architecture data that were applied to in vitro simulations to produce clinically relevant results. These data also show that careful restoration of native anatomical structure can produce more physiological kinematics in the knee and ankle.

Acknowledgements

First, I would like to give my immense gratitude to my three pillars of support throughout this long journey: Dr. Rita Patterson, Dr. Russell Wagner, and Dr. Rustin Reeves. These three mentors have provided me the best guidance a physician-scientist could ask for in basic and clinical science. Throughout my medical and graduate school education I always had someone to turn to for expert advice in biomechanics, orthopaedic surgery, and anatomy.

I must acknowledge the excellent guidance and patience of Dr. Patterson for always deepening my science and sharpening my objective mind. I am incredibly thankful to have met Dr. Reeves early in my studies as I am not sure this journey would have ever begun without him. Dr. Wagner has been a mentor and a role model for me. He has defined the principles I want to live up to as a surgeon with his incredible devotion and integrity to do what is right for those around him.

I would also like to thank the members of my committee: Dr. Nicoleta Bugnariu, Dr. Tristian Tayag, and Dr. Michael Forster for all their contributions they have given me over the years.

Without any doubt, I would not be capable of success if it were not for my wonderful fiancé and family. They have always let me lean on them if I ever needed to and I owe my survival to them for supporting me while I am at my worst and always seeing the best in me.

Table of Contents

1. INTRODUCTION

1.1 An Anatomical Approach to Kinematics: Overview

A common theme in anatomical science is the interrelationship of structure and function. A similar and popular thought in reconstructive surgery is to restore function through changing structure to achieve physiologic kinematics and stability. The theory is to manipulate the anatomical restraints of the body to guide motion back to what was once normal. Currently, attempts are made to achieve this through implant design, implant alignment, soft tissue modification, and/or modification of boney anatomical structures.

Restoring physiological kinematics and stability in the lower extremity is not a new concept and is the grounded basis of most orthopaedic reconstructive surgeries. However, the modalities for restoration of physiological kinematics and stability are largely situationally and patient specific. Many procedures focus on restoring soft tissue restraints of a joint through varied constructs dependent upon what is deficient and how they became deficient in function. Ankle syndesmosis fixation is an excellent model for adapting treatment to the mechanism of injury and patient factors in addition to the injury itself. An associated Lauge-Hansen supination-external rotation ankle fracture in an older adult may imply syndesmosis injury and direct treatment towards a more rigid stability focused construct to foster bone healing. In a different situation, a high-performance athlete may only have symptoms of instability and pain with a syndesmosis injury; directing treatment towards restoring physiological motion and stability to the syndesmosis to foster a soft tissue environment amenable to healing and expedited return to function. While with other modalities, such as total knee arthroplasty (TKA), the goal is to reduce pain while maintaining a functionally stable knee joint. In this procedure, a polyethylene bearing is used in conjunction with cobalt chrome to resurface cartilaginous interfaces to remove pain generators. In the process, this artificial resurfacing allows a surgeon to correct joint alignment deformity, make soft tissue balancing adjustments, and modify other factors effecting knee joint kinematic characteristics and stability. Additionally, both of these widely-used treatment modalities in orthopaedic reconstructive surgery frequently fail to fully achieve physiologic kinematics and stability.

Many treatment modalities prioritize stability over restoration of kinematics and in others a reverse prioritization is made. This relationship highlights a balance or compromise that is frequently made when choosing a treatment modality. Native joint kinematics are inherently “physiologic” and stable. As with other fields of science and engineering, striving to attain natural biological efficiency and function is difficult to achieve. In reconstructive surgery, the inefficiency comes out in the form of the inverse relationship of trading reduced stability for improved physiologic kinematics or vice versa. As improvements in reconstructive surgery are made this inefficiency is diminished. In theory, this increased efficiency brings a combined improvement in joint kinematics and stability while improving patient outcomes, satisfaction, and function.

Biomechanical studies are a primary source for innovation and advancement in orthopaedic surgery. In vitro simulations are a backbone for these biomechanical experiments in orthopaedic surgery. Cadaver specimens are connected to mechanical apparatuses to simulate real world functional tasks performed by in vivo joints. Major focus has been placed on alignment, implant design, and anatomical constraints in recent in vitro simulations focused on achieving physiologic kinematics. The work described here within focuses on two models for achieving physiological kinematics in the knee and ankle using in vitro joint simulation. In addition, the basic mechanical and anatomical determinants of joint kinematics are described.

1.2 Ankle Joint Model

Syndesmosis injuries are common with up to 25% of all ankle injuries being reported to involve an associated syndesmosis injury.[1-3] These injuries are even more common in athletic patient populations with an incidence reported up to 25% in specific sports.[2, 3] The ankle syndesmosis ligaments prevent diastasis of the syndesmosis and contribute some stability to the ankle joint as a whole. The ligaments of that comprise the syndesmosis are the anterior-inferior tibiofibular ligament (AITFL), interosseous ligament (IOL), posterior-inferior tibiofibular ligament (PITFL), and the inferior transverse ligament (ITL). The diagnosis and treatment of the syndesmosis are typically focused on the AITFL and PITFL as they have repeatedly been found to be the major contributors to syndesmosis integrity.[4-9]

Management of syndesmosis injuries historically involves treatment with either nonoperative stabilization or screw constructs as both treatments provide good results.[10] However, these traditional methods of treatment do have major deficiencies. Non operative management and screw fixation can both leave a patient non weight bearing for as long as 6-12 weeks in many protocols.[10] Additionally, syndesmotic screws frequently need removal and in some cases have been found to be a source of improved patient outcomes once the screw breaks or is removed.[11, 12] Therefore, current advances in syndesmosis fixation have focused on expediting the return of patients back to function and improving patient outcomes with fixation. These advances are largely driven by sports focused surgeons and researchers looking to return eager athletes to full play earlier. This has led to the evolution of syndesmosis fixation ideology to take aim at achieving physiologic motion and stability. It is theorized that restoration of stability and motion to the native state would promote an environment optimal for ligamentous healing and faster return to play. Suture-button constructs were created with this in mind, but they have not quite proven to be the fixation construct that achieves physiologic stability and motion.[13-16] The internal brace is an implant used to augment ligamentous injuries in the foot and ankle that uses two suture anchors to tether bones together through a tension mechanism, but has yet to be studied in the ankle syndesmosis.

Specific Aim 1: To evaluate the ability of an internal brace to add sagittal plane translational and transverse plane rotational constraint to suture-button constructs. It is hypothesized that the internal brace oriented in parallel with the fibers of an injured AITFL in addition to a suture-button construct would achieve physiological motion and stability at the syndesmosis through increased rotational and translational constraint of the fibula.

The goal of the ankle model is to provide a dynamic, mechanistic understanding of ankle syndesmosis kinematics in 3 different states: Native, injured, and repaired. Specifically, I evaluate syndesmosis kinematics and reduction dynamically to find the fixation construct that best restores physiologic motion after injury. In addition, this 3-state comparison allows for the investigation of the underlying mechanisms of injury of Lauge-Hansen SER ankle fractures and description of native ankle kinematics. There is a paucity of literature on ankle kinematics when compared to the knee and hip. Further understanding of the mechanisms of function, injury, and treatment of the ankle syndesmosis may reveal clinically meaningful information. Currently, there are a wide variety of implants available for syndesmosis fixation and a wide-ranging variety of fixation constructs proposed to use them in. This work provides evidence for which combination of implant and construct provide the most physiological restoration of motion through a stair stepped approach. Specimens will have 3D kinematics recorded and undergo ultrasound evaluation in all 3 states with the repaired state having multiple levels of repair and evaluation. This enables the assessment of 6 different fixation constructs consisting of different combinations of tightrope and internal brace implants to restore physiological kinematics. This is highly valuable information for orthopaedic surgeons and may lead to earlier return to function for patients through higher quality motion and stability. To competently assess the impact of these implants the ankles must be evaluated in their native and injured forms to act as controls. The native state will first be evaluated using the same methodology described above for the implants. In the injured state a stepwise artificially induced injury pattern is performed. This stepwise approach allows the delineation between different structural contributions to kinematic control of the syndesmosis, which has yet to be described in the literature. Overall, the mechanistic understanding of syndesmosis function and fixation comparison will contribute to a greater understanding of the ankle to research scientists and orthopaedic surgeons.

1.3 Knee Joint Model- Future and Current Work

Total knee arthroplasty (TKA) is most commonly performed on patients aged 50-80 years old for chronic knee pain and disability. It is considered one of the most successful surgeries performed. The long-term survival of TKA implants are generally over 90% at 15 years of follow up [17, 18]. Advances over the past 20 years in implant design, surgical technique, and patient selection have led to these outstanding outcomes. Today, orthopaedic surgeons are faced with an increasingly younger patient population with severe joint degeneration. This new demographic of patients does not achieve the same level of success with TKA as prototypical patients [19-23]. This population is expected to increase over the next decade which presents new challenges for TKA [24]. Younger patients have higher average physical activity levels and require a wider range of functional motion than their older peers [21]. These patients deserve definitive treatment, but TKA does not achieve that level of success with current methods. To accomplish this, the knowledge base on the effects of posterior tibial slope (PTS) and implant design must be further elucidated.

The primary objective of this study is to provide a conceptual strategy for better knee flexion using a combination of implant design and surgical technique. Younger patients demand physiologic motion of their prosthetic knees to keep up with their activity levels. Surgeons take advantage of PTS and implant design to increase the functional range of motion of the prosthetic knee. However, the literature provides a limited view of the collective effects of these two variables. This study can provide objective data to orthopaedic surgeons on the appropriate combination of prosthesis and PTS to achieve physiologic motion during TKA. Furthermore, future prosthesis design may be influenced by our findings to improve tibiofemoral (TF) and patellofemoral (PF) interaction. I propose a hypothesis in which maintaining more native anatomy and geometry during TKA provides the most physiological motion of the knee. This study focuses on 4 major implant designs currently used in the United States. These designs encompass the divergent methodologies of constraining the knee via implant to control motion versus using native anatomic structures to control motion. Bicruciate retaining (BCR) and posterior cruciate retaining (PCR) implants make use of native structures to help guide TF and PF motion. Anterior stabilized (AS) designs retain the PCL, but makes use of an anterior polyethylene lip to constrain motion. Posterior stabilized (PS) designs do not retain native cruciate structures and attempt to control motion through a cam-post mechanism. Data acquired from this study can be used to implement implant design changes and guide surgeons on decision making.

Specific Aim 1: To determine the combination of implant design and posterior tibial slope that provides the most physiological motion during TKA. Hypothesis: Cruciate retaining implant designs provide the most physiological motion by retaining the PTS found in the native knee. Sequential TKA with 4 different implant designs is performed on cadaver specimens utilizing each specimen's native motion as a control. Deep knee flexion is simulated from 0-120 degrees using a knee rig used by Shalhoub et al [25]. Dynamic motion is recorded by an electromagnetic tracking system with 6 degrees of freedom. PF motion and TF motion is then reconstructed and analyzed after each design is tested at 0, 4, and 8 degrees of PTS using a shim system from our previous work. We expect the BCR and PCR designs to be the most similar to the native knee with the AS and PS bearings being the least similar. We also postulate the mechanism of this increased physiologic motion to be the retention of native cruciate anatomy.

*Specific Aim 2: To assess changes in cruciate ligament strain as a function of posterior tibial slope and implant design***.** Hypothesis: Minimalizing PTS will provide the most benefit to the BCR design and maximizing PTS will benefit PCR, AS, and PS designs. Experimentation takes place using the same model as specific aim 1 with the addition of strain sensors. Synchronized data will be collected in the dynamic model as the knee completes a cycle of deep knee flexion. Cruciate strain is assessed for an increased risk of rupture as indicated by increased strain at different combinations of PTS and implant design. We expect the BCR design to benefit the most from restricting PTS at or below the native PTS to reduce ACL strain. All other designs are expected to benefit the most from having a PTS at or above the level of native. The point at which PTS becomes detrimental to cruciate strain in each implant design is of crucial importance to implant survivability.

1.4 References

1. Gerber JP, Williams GN, Scoville CR, Arciero RA, Taylor DC. Persistent disability associated with ankle sprains: a prospective examination of an athletic population. *Foot Ankle Int.* 1998;19:653-660.

2. Hunt KJ, George E, Harris AH, Dragoo JL. Epidemiology of syndesmosis injuries in intercollegiate football: incidence and risk factors from National Collegiate Athletic Association injury surveillance system data from 2004-2005 to 2008-2009. *Clin J Sport Med.* 2013;23:278-282.

3. Waterman BR, Belmont PJ, Jr., Cameron KL, Svoboda SJ, Alitz CJ, Owens BD. Risk factors for syndesmotic and medial ankle sprain: role of sex, sport, and level of competition. *Am J Sports Med.* 2011;39:992-998.

4. McCullough CJ, Burge PD. Rotatory stability of the load-bearing ankle. An experimental study. *J Bone Joint Surg Br.* 1980;62-b:460-464.

5. Ogilvie-Harris DJ, Reed SC, Hedman TP. Disruption of the ankle syndesmosis: biomechanical study of the ligamentous restraints. *Arthroscopy.* 1994;10:558-560.

6. Ramsey PL, Hamilton W. Changes in tibiotalar area of contact caused by lateral talar shift. *J Bone Joint Surg Am.* 1976;58:356-357.

7. Rasmussen O. Stability of the ankle joint. Analysis of the function and traumatology of the ankle ligaments. *Acta Orthop Scand Suppl.* 1985;211:1-75.

8. Scranton PE, Jr., McMaster JG, Kelly E. Dynamic fibular function: a new concept. *Clin Orthop Relat Res.* 1976:76-81.

9. Xenos JS, Hopkinson WJ, Mulligan ME, Olson EJ, Popovic NA. The tibiofibular syndesmosis. Evaluation of the ligamentous structures, methods of fixation, and radiographic assessment. *J Bone Joint Surg Am.* 1995;77:847-856.

10. Van Heest TJ, Lafferty PM. Injuries to the ankle syndesmosis. *J Bone Joint Surg Am.* 2014;96:603-613.

11. Manjoo A, Sanders DW, Tieszer C, MacLeod MD. Functional and radiographic results of patients with syndesmotic screw fixation: implications for screw removal. *J Orthop Trauma.* 2010;24:2-6.

12. Song DJ, Lanzi JT, Groth AT, et al. The Effect of Syndesmosis Screw Removal on the Reduction of the Distal Tibiofibular Joint: A Prospective Radiographic Study. *Foot Ankle Int.* 2014;35:543-548.

13. Clanton TO, Whitlow SR, Williams BT, et al. Biomechanical Comparison of 3 Current Ankle Syndesmosis Repair Techniques. *Foot Ankle Int.* 2017;38:200-207.

14. Forsythe K, Freedman KB, Stover MD, Patwardhan AG. Comparison of a novel FiberWire-button construct versus metallic screw fixation in a syndesmotic injury model. *Foot Ankle Int.* 2008;29:49-54.

15. LaMothe JM, Baxter JR, Murphy C, Gilbert S, DeSandis B, Drakos MC. Three-Dimensional Analysis of Fibular Motion After Fixation of Syndesmotic Injuries With a Screw or Suture-Button Construct. *Foot Ankle Int.* 2016;37:1350-1356.

16. Teramoto A, Suzuki D, Kamiya T, Chikenji T, Watanabe K, Yamashita T. Comparison of different fixation methods of the suture-button implant for tibiofibular syndesmosis injuries. *Am J Sports Med.* 2011;39:2226-2232.

17. Le DH, Goodman SB, Maloney WJ, Huddleston JI. Current modes of failure in TKA: infection, instability, and stiffness predominate. *Clin Orthop Relat Res.* 2014;472:2197-2200.

18. Sharkey PF, Lichstein PM, Shen C, Tokarski AT, Parvizi J. Why are total knee arthroplasties failing today--has anything changed after 10 years? *J Arthroplasty.* 2014;29:1774-1778.

19. Parvizi J, Nunley RM, Berend KR, et al. High level of residual symptoms in young patients after total knee arthroplasty. *Clin Orthop Relat Res.* 2014;472:133-137.

20. Matsuda S, Kawahara S, Okazaki K, Tashiro Y, Iwamoto Y. Postoperative alignment and ROM affect patient satisfaction after TKA. *Clin Orthop Relat Res.* 2013;471:127-133.

21. Keeney JA, Eunice S, Pashos G, Wright RW, Clohisy JC. What is the evidence for total knee arthroplasty in young patients?: a systematic review of the literature. *Clin Orthop Relat Res.* 2011;469:574-583.

22. Kurtz S, Mowat F, Ong K, Chan N, Lau E, Halpern M. Prevalence of primary and revision total hip and knee arthroplasty in the United States from 1990 through 2002. *J Bone Joint Surg Am.* 2005;87:1487-1497.

23. Wainwright C, Theis JC, Garneti N, Melloh M. Age at hip or knee joint replacement surgery predicts likelihood of revision surgery. *J Bone Joint Surg Br.* 2011;93:1411-1415.

24. Kurtz SM, Lau E, Ong K, Zhao K, Kelly M, Bozic KJ. Future young patient demand for primary and revision joint replacement: national projections from 2010 to 2030. *Clin Orthop Relat Res.* 2009;467:2606-2612.

25. Shalhoub S, Maletsky LP. Variation in patellofemoral kinematics due to changes in quadriceps loading configuration during in vitro testing. *J Biomech.* 2014;47:130-136.

2. BACKGROUND, METHODS, AND REVIEW

2.1. Lower Extremity Structure and Function

2.1.1 General Principles of Lower Extremity Anatomy

The musculoskeletal system of the lower extremity is very complex and functions to provide stability and motion to the entire body. The hip, knee, and ankle are the three major joints of the lower extremity with the knee and ankle being the primary focus of the research presented in this dissertation. Rudimentary portrayals of the knee and ankle joints classify them as hinge joints, but both joints have 6 degrees of freedom of motion. The character of the motion largely determines the stability, function, and survivability of the joints. In both the knee and ankle are several anatomical features that determine the character of motion in addition to forces produced by body weight and muscle action. To better understand these processes, it is important to first understand the structure and function of the native knee and ankle joints.

Most proximally, the innominate acts as a rigid structure that transfers forces from the spinal column and musculature to the lower extremity. The innominate is formed from the fusion of the ilium, ischium, and pubis bones which sit atop the femur at the hip joint. The hip joint is where we begin to discuss the focus of the current work. The center of the hip joint or femoral head is a common point to begin measurement of several aspects of lower extremity alignment. The mechanical axis of the lower extremity is formed from adjoining a point from the center of the femoral head to the center of the talus in the ankle. The anatomical axis of the femur is formed by a line passing through the center of the medullary canal. In the femur, the mechanical axis and the anatomical axis do not overlap; this forms a typical valgus angulation of the femur of approximately 5-7 degrees. The mechanical and anatomical axis also do not overlap in the tibia, but is less pronounced than the femur with a typical angulation of 2-3 degrees in the opposite direction in varus. This gives the knee a slight natural valgus angle of 2-5 degrees.

This axis can be used as an approximation of ground reactive forces transmitted from the ground up through the lower extremity in bilateral stance. As the lower extremity moves to unilateral stance these forces are shifted medially in the joint to cause compression in the medial compartment of the knee and tension in the lateral compartment. This contrasts with resting bilateral stance where loads in the medial and lateral compartments are more equally distributed as both lower limbs provide a larger base of support. This provides an excellent rudimentary example of how the lower extremity distributes forces to maintain stance as body weight is negated by ground reactive force. A subject at rest creates motion by producing a force through muscular contraction which creates an equal and opposite reactionary ground reaction force greater than the weight of the subject creating an acceleration. These are simple applications of Newtons laws to lower extremity kinetics, but are sufficient for a simple understanding of how motion is created in the lower extremity. The lower extremity musculoskeletal system creates muscular force and uses bones, ligaments, and joints to create mechanical advantage to produce directed motion and stability.

To further understand driving forces behind joint structure and function it is important to define the axes in which movement occurs at the knee and ankle. The tibiofemoral joint’s main function is to perform flexion/extension about the epicondylar axis in the sagittal plane and normally ranges from 5 degrees of hyperextension to 155 degrees of maximum flexion depending on the individual. The knee internally/externally rotates in the transverse plane about a vertical axis, located between the tibial intercondylar eminences, allowing the knee to rotate 10 degrees in either direction while the knee is extended and approximately 20-30 degrees more while flexed. There is little varus/valgus movement of the knee with approximately 2 degrees present while the knee is flexed and none while extended. Translations in the knee occur in all 3 planes, but medial/lateral and superior/inferior translations are rarely reported on with the greatest clinical interest being in anterior/posterior translation between the tibia and femur[1]. The patellofemoral joint of the knee has simpler axis definitions. All three axes of rotation of the patella pass through the centroid connecting the superior/inferior, medial/lateral, and anterior/posterior poles of the patella. Although there are several different methods for establishing a joint coordinate system that is clinically meaningful this work uses the Grood and Suntay system.[1] The rotation occurring about the superior/inferior axis is patellar tilt. The medial/lateral poles form the axis where flexion/extension occurs. Internal/external rotation of the patella occurs about the anterior/posterior axis. Due to the nature of the patella being sesamoid and fixed at either end by the patellar tendon and quadriceps, the only translations of clinical interest are medial/lateral and anterior/posterior[2]. Interestingly, the normal ranges of motion for the patellofemoral joint are debatable and have variability when comparing different individuals[3]. The normal ranges of motion for the tibiofemoral joint are well agreed upon and suffer from interindividual variability to a lesser degree than the patellofemoral joint.

Approaching lower extremity anatomy is best done from a modern method of an application based perspective. Classical anatomy curriculum of the musculoskeletal system generally focused on 5 key elements of muscular anatomy: 1. Origin, 2. Insertion, 3. Innervation, 4. Action, 5. Blood Supply. Classical bone anatomy typically focuses on surface prominences, orientation, and the relative position of soft tissue structures to bone features. In the modern approach, different audiences would receive presentations tailored to suit their area of application. Therefore, the lower extremity anatomy presented in this work will focus on biomechanical and orthopaedic surgical applications. Special attention is made to structures that are commonly encountered clinically, provide mechanical advantage, coupled in function, or have compound actions. However, classical musculoskeletal anatomy provides an excellent foundation to build upon and all the key muscular elements of the lower extremity can be referenced in Table 1.

Muscle	Origin	Insertion	Innervation	Action	Special
Gluteus Maximus	Outer Ilium, Posterior Sacrum, Coccyx, Sacrotuberous Ligament	Iliotibial Tract, Gluteal Tuberosity of Femur	Inferior Gluteal Nerve L5, S1-S2	Extends and Externally Rotates Femur	Assists in Rising from Seated Position
Gluteus Medius	Outer Ilium, Below Iliac Crest and Between Posterior and Anterior Gluteal Lines	Superolateral Surface of Greater Trochanter	Superior Gluteal Nerve L4-5, S1	Abduction and Internal Rotation of Femur	Keeps Pelvis Level, Important for Gait
Gluteus Minimus	Outer Ilium, Between Anterior and Inferior Gluteal Lines	Anterior Surface of Greater Trochanter	Superior Gluteal Nerve L4-5, S1	Abduction and Internal Rotation of Femur	Keeps Pelvis Level
Tensor Fasciae Latae	Outer Edge of Iliac Crest, Between	Iliotibial Tract	Superior Gluteal Nerve L4-5, S1	Flexion and Internal Rotation of Femur	Assists in Knee Extension Through

	ASIS And Iliac Tubercle				Iliotibial Tract
Piriformis	Anterior Surface of S2-4	Upper Border of Greater Trochanter Anteriorly	Ventral Rami of S1-2	External Rotation of Extended Femur; Abduction of Flexed Femur	Passes Through Greater Sciatic Foramen
Superior Gemellus	Ischial Spine	Obturator Internus Tendon and Into Greater Trochanteric Fossa	Nerve to Obturator Internus L5 S1-2	External Rotation of Extended Femur; Abduction of Flexed Femur	May Be Absent
Obturator Internus	Margins of Obturator Foramen and Internal Surface of Obturator Membrane	Superior Greater Trochante, Near Fossa	Nerve to Obturator Internus L5 S1-2	External Rotation of Extended Femur; Abduction of Flexed Femur	Passes Through Lesser Sciatic Foramen

Inferior Gemellus	Superior Ischial Tuberosity	Obturator Internus Tendon and Into Greater Trochanteric Fossa	Nerve to Quadratus Femoris L4-5, S1	External Rotation of Extended Femur; Abduction of Flexed Femur	
Quadratus Femoris	Lateral Ischial Tuberosity	Quadrate Tubercle	Nerve to Quadratus Femoris L4-5, S1	External Rotation of Femur	
Sartorius	ASIS	Proximal, Medial Tibia	Femoral Nerve L2-4	Flexion, Abduction, External Rotation of Femur and Flexion of Knee	Most Superficial Portion of Pes Anserinus
Psoas	Transverse Process T12-L5 And Vertebral Bodies	Lesser Trochanter of Femur	L2-3	Flexion of Femur	Common Insertion with Iliacus

Iliacus	Superior 2/3 Iliac Fossa, Ala of Sacrum, Anterior Sacroiliac Ligaments	Lesser Trochanter of Femur	L2-3	Flexion of Femur	Common Insertion with Iliacus
Pectineus	Superior Ramus of Pubis	Superior Section of Linea Aspera Of Femur	Femoral Nerve L2-4	Adduction, Flexion, Internal Rotation	Action Changes Depending on Hip Position
Rectus Femoris	AIIS And Ilium Superior to Acetabulum	Tibial Tuberosity Via Quadriceps Tendon	Femoral Nerve L2-4	Extension of Knee, Flexion of Hip	
Vastus Lateralis	Proximal, Lateral Femoral Shaft	Tibial Tuberosity Via Quadriceps Tendon	Femoral Nerve L2-4	Knee Extension	
Vastus Medialis	Proximal, Medial Femoral Shaft	Tibial Tuberosity Via	Femoral Nerve L2-4	Knee Extension	

		Quadriceps Tendon			
Vastus Intermedius	Anterior Femoral Shaft	Tibial Tuberosity Via Quadriceps Tendon	Femoral Nerve L2-4	Knee Extension	
Gracilis	Anterior Pubis and Ischium	Proximal, Medial Tibia	Obturator Nerve L3-4	Adduction of Thigh, Flexion and Internal Rotation of Knee	Middle Layer of Pes Anserinus
Adductor Longus	Body of Pubis, Inferior Pubic Tubercle	Linea Aspera	Obturator Nerve L3-4	Adduction, Flexion, Internal Rotation of Thigh	
Adductor Brevis	Inferior Pubic Rami	Posterior Femoral Shaft	Obturator Nerve L3-4	Adduction, Flexion, And Internal Rotation of Thigh	
Adductor Magnus	Ischiopubic Ramus and	Posterior Femoral Shaft	Obturator Nerve L3-4	Adduction, Flexion,	

	Ischial Tuberosity	and Adductor Tubercle	And Tibial Div. Of Sciatic Nerve L4	Extension, Internal and External Rotation of Thigh	
Obturator Externus	Margins of Obturator Foramen and External Obturator Membrane	Trochanteric Fossa	Obturator Nerve L3-4	External Rotation of Femur	XXX
Biceps Femoris	Short Head- Distal Posterolateral Femur, Long Head- Ischial Tuberosity	Head of Fibula	Long Head- Tibial DivS1-2, Short Head- Common Fibular Div. L5 S1-2	Extension of Thigh, Flexion of Leg, And Externally Rotates Knee	
Semitendinosus	Ischial Tuberosity	Proximal, Medial Tibia	Tibial Div. L5, S1-2	Extension of Hip While Knee Extended, Flexes and Internally	Deepest Layer of Pes Anserinus

				Rotates Tibia While Knee Is Flexed	
Semimembranosus	Ischial Tuberosity	Posteromedial Tibia	Tibial Div. L5, S1-2	Extends Thigh While Knee Extended, Flexes and Internally Rotates Tibia While Knee Is Flexed	
Tibialis Anterior	Lateral Tibia and Interosseous Membrane	Plantar Medial Cuneiform, Base Of 1st MTP	Deep Fibular Nerve L4-5, S1	Dorsiflexion and Inversion of Foot	
Extensor Digitorum Longus	Medial Surface of Fibula and Interosseous Membrane	Extensor Expansion of Lateral 4 Toes	Deep Fibular Nerve L4-5, S1	Extension of Toes 2-5 And Dorsiflexion of Foot	
Extensor Hallucis Longus	Anteromedial Fibula And	Distal Phalanx Of 1st Toe	Deep Fibular	Extension Of 1st Toe,	

	Interosseous Membrane		Nerve L4-5, S1	Inversion and Dorsiflexion of Foot	
Fibularis Tertius	Fibula, Interosseous Membrane	Dorsum Of 5th Metatarsal	Deep Fibular Nerve L4-5, S1	Dorsiflexion and Eversion of Foot	May Be Absent
Fibularis Longus	Proximal 2/3 Fibula	Base Of 1st MTP, Medial Cuneiform	Superficial Fibular Nerve L4-5, S1	Plantar Flexion and Eversion of Foot	
Fibularis Brevis	Distal 2/3 Of Fibula	Tuberosity Of 5th MTP	Superficial Fibular Nerve L4-5, S1	Plantar Flexion and Eversion of Foot	
Gastrocnemius	Lateral and Medial Condyles of Femur	Calcaneous Via Achilles Tendon	Tibial Nerve S1-2	Plantar Flexion of Foot and Flexion of Knee	
Soleus	Posterior Surface of Proximal	Calcaneous Via Achilles Tendon	Tibial Nerve S1-2	Plantar Flexion	

	Tibia and Fibula				
Plantaris	Lateral Supracondylar Ridge of Femur	Calcaneous Via Achilles Tendon	Tibial Nerve S1-2	Plantar Flexion Foot and Flexion of Knee	May Be Absent, Tendon Runs Medial
Tibialis Posterior	Posterior Fibula, Interosseous Membrane, And Tibia	Navicular, 3 Cuneiforms, Cuboid And 2-4 MTP	Tibial Nerve S1-2	Plantar Flexion and Inversion of Foot	
Flexor Digitorum Longus	Posterior Tibia	Distal Phalanx Of 2-5 Toes	Tibial Nerve S1-2	Plantar Flexion of Distal 2-5 Toes and Foot, Inversion of Foot	Unipennate
Flexor Hallucis Longus	Median Fibula	Distal Phalanx Of 1st Toe	Tibial Nerve L5, S1-2	Plantar Flexion, Inversion of Foot and Flexes 1st Distal Phalanx	

Popliteus	Lateral Condyle of Femur	Posteromedial Tibia	Tibial Nerve L4-5, S1	Closed Chain- External Rotation of Femur, Open Chain- Internal Rotation of Tibia	Intra Articular
Extensor Digitorum Brevis	Calcaneous	Extensor Tendons 2-4 Toes	Deep Fibular Nerve L4-5, S1	Extends Toes 2-4	
Dorsal Interosseous	1-5 Metatarsal Bases	Base of Proximal Phalanx 2-4	Lateral Plantar Nerve S1-2	Abduction 2-4	
Abductor Hallucis	Calcaneous, Flexor Retinaculum	Base Of 1st Proximal Phalanx	Medial Plantar Nerve L4-5	Flexion, Abduction 1st Toe	
Flexor Digitorum Brevis	Calcaneous	Toes 2-5 Distal Phalanx	Medial Plantar Nerve L4-5	Flexes Toes 2-5	Bipennate
Abductor Digiti Minimi	Calcaneous	Base Of 5th Toe Proximal Phalanx	Lateral Plantar Nerve S1-2	Flexion, Abduction 5th Toe	

Quadratus Plantae	Calcaneous	Tendons of Flexor Digitorum Longus	Lateral Plantar Nerve S1-2	Flexion 2-5 Toes	
Lumbricals of Foot	Tendons of Flexor Digitorum Longus	Dorsal Extensor Expansion and Bases of Proximal Phalanx 2-5	1st Lumbrical- Medial Plantar Nerve L4-5, 2-4 Lumbrical- Lateral Plantar Nerve S1-2	Extends Toe at IP	Split Innervation
Flexor Hallucis Brevis	Cuboid and Lateral Cuneiform	Medial and Lateral 1st Toe	Medial Plantar Nerve L4-5	Flexes MTP of 1st	
Adductor Hallucis	2-4 MTP, Plantar Ligaments	Proximal Phalanx 1st Toe	Lateral Plantar Nerve S1-2	Adduction 1st Toe	
Flexor Digit Minimi Brevis	5th MTP	Proximal Phalanx Of 5th Toe	Lateral Plantar Nerve S1-2	Flexion Of MTP	

Plantar Interosseous	Base Of 3-5 MTP	Base of Proximal Phalanx 3-5	Lateral Plantar Nerve S1-2	Adduction 3-5 Toes and Flexion Of MTP	

2.1.2 Muscle Structure and Function

Lower extremity muscles function to provide the forces necessary for stability and mobility of the boney framework they are connected to and surround. To understand these functions, it is best to look at the underlying structure first. Muscles are composed of contractile and non-contractile elements that together form a capable mechanism of responding to and producing force. Contractile elements are mostly proteinaceous and respond to chemical, mechanical, and electrical stimuli to produce force. Skeletal muscle is composed of many fascicles surrounded by non-contractile connective tissue. Each fascicle is composed of many muscle fibers or cells and each cell is composed of many myofibrils. Each myofibril is composed of filaments that are organized into sarcomeres that are joined from end to end. The sarcomeres are the smallest contractile unit of muscle at approximately 2 μm in length and approximately 100,000 of them can be found per a muscle fiber depending on the muscle examined. These sarcomeres are activated via neuronal stimulation in bulk at the muscle fiber level.

However, each muscle fiber is not activated individually, but in motor units. The number of sarcomeres aligned in parallel or side by side determines the maximal amount of force a muscle can produce. Physiological cross-sectional area (PCSA) of a muscle is an indirect measurement of the number of sarcomeres in parallel and is directly proportional to the potential maximal force generation of a muscle. This PCSA is calculated from muscle fiber length, orientation of the fibers, and muscle fiber volume Formula 1.

$$\text{Physiological Cross sectional area (PCSA)} = \frac{Muscle\ volume \times \cos(Pennation\ Angle)}{Fiber\ Length}$$

Formula 1.

Muscle fiber length is proportional to the number of sarcomeres found in series and is directly related to the length of excursion a muscle can perform. The orientation of the muscle fibers in relationship to the direction of action the tendon takes is the pennation angle. The pennation angle decreases the amount of force production a given fiber can produce as it is not in line with the tendon. However, a pennate muscle can have higher fiber density due to the angle and produce more force; overriding the loss of force due to pennation angle. Pennated muscles do have less potential for excursion length in comparison to non pennated muscles. Long muscles without pennation have longer excursion distances and have the potential to boost their force effects through moment arms rather than through higher fiber density. There are also two major muscle fiber types and one intermediate type: I slow oxidative, II fast glycolytic, and IIA fast intermediate. Type I fibers do not fatigue as quickly due to their energy supply being sustained by oxidation and are found in higher proportion in muscle maintaining stability and posture. Type II fibers fatigue quicker, but have higher force production per a fiber than type I. These fibers are typically found in higher proportions in muscles of mobility that operate joints requiring a broad range of motion changes. In addition, type II fibers produce force at a higher velocity than type I. The type IIA fibers are an intermediary fiber consisting of characteristics found in both type I & II. The non-contractile components of muscle structure are the connective tissues are passive elastic tissues in function. The connective tissues that are in and around muscle fibers that produce a passive tension in parallel with the contractile elements. The total tension produced by a muscle includes this parallel passive tension in addition to the contractile components. The tendinous connective tissues of a muscle are in series with the contractile elements and cause a reduction of tension produced as slack must be taken up within the tendon to propagate the force to the bone. Although the net effect of this extensibility may store potential energy, maintain optimal sarcomere length, lower shortening velocity, and in the end produce more force depending on the situation. These microscopic architectural features of muscle constitute the basis of how muscles of the lower extremity meet the force demands of motion and stability. The muscles, however, must receive input to produce this motion and stability.

Motor units are the smallest unit of contractile activation and consist of a single alpha neuron and all the muscle fibers it innervates. A single muscle is not activated in its entirety by one motor unit, but has separate motor units activated asynchronously to produce force. The number of muscle fibers per an alpha neuron can vary from several thousand to less than 10. Smaller motor units are activated for finer movements and larger motor units are suited for producing sudden large magnitudes of force. In addition, magnitude of force can be controlled through the number of motor units activated and frequency at which they are activated.

The muscles of the eye have a large number of motor units, but each motor unit consists of very few muscle fibers per a neuron. The gastrocnemius muscle is in sharp contrast to the eye with very few motor units, but each unit contains thousands of muscle fibers. This makes the eye physiologically better at finer movements and lower force production while the gastrocnemius is well suited to quickly produce large amounts of force with less dexterous control. In addition, smaller motor units are typically activated first with advancement to larger motor unit activation as force generation requirements increase. Electromyography (EMG) can be used to determine the frequency and amplitude of motor unit activation in a muscle. Combining EMG and muscular architecture data can provide insight into the magnitude and timing of muscular force production and serves as the basis for many leading lower extremity muscle force prediction models.[4, 5]

2.1.3 Knee Structure and Function

At first glance, the knee can appear to be one of the most simply described joints in the body with its large size, easily visible anatomical structures, and seemingly simple function. Delving further reveals a joint that has one of the most complex systems of soft tissue restraint and motion in the body. The knee consists of the patellofemoral and the tibiofemoral joints which are connected in function and lubricated from within the same synovial envelope. There are 3 main bones interacting in the knee the femur, tibia, and patella with the fibula and fabella being closely related to the joint via ligaments and tendons.

The medial and lateral tibiofemoral compartments articulate through opposing hyaline cartilage surfaces of the femoral condyles and the tibial plateau. The medial plateau has a larger contact surface area and is concave with an average posterior slope of 8. The lateral tibial plateau has a smaller contact surface area is convex with a slightly higher posterior slope.[6] The femoral condyles have a stark contrast in geometry between the medial and lateral sides as well. The medial condyle is larger and projects further distally with a greater radius of curvature than the lateral femoral condyle. However, due to the difference between the mechanical and anatomic axis of the femur being valgus; the distal most points of the femoral condyles are nearly horizontal. The femoral condyles also have a decreased radius of curvature as they track posteriorly. In addition, the actual surface area of the femur that is in articular contact with the tibia is larger and extends more anteriorly with the medial condyle than the lateral. The asymmetries between the medial and lateral compartments is continued when examining the tibial plateau. To accommodate the larger articular surfaces of the medial femoral condyle the medial tibial plateau is larger in the anteroposterior direction and overall surface area than the lateral side. The menisci are found in the medial and lateral compartments and serve to increase contact surface area between the femoral condyles and the tibia to distribute forces over a wider area. This reduces focal areas of joint stress and increases the survivability of the cartilage to withstand the daily demands of body[7]. The medial meniscus has more capsular and ligamentous restraint to motion as compared to the lateral side. In addition, the medial meniscus is connected to the medial collateral ligament and the lateral meniscus to the popliteus muscle. It is thought both structures help stabilize movement of the menisci. The asymmetries in anatomy between the medial and lateral compartments of the knee play a major role in internal/external rotation kinematics and stability. The medial side of the knee is less mobile and translates from anterior to posterior less; creating a medially oriented center of rotation. The medial compartment can be thought of as dished and during dynamic activity receives higher loads than its lateral counterpart.[8] This restrained medial side is also the most common side for the development of osteoarthritis. The lateral femoral condyle translates posteriorly during flexion to "unlock the knee". The femur is "locked" in full extension by the seating of the medial and lateral condyles of the femur into the tibial plateau. As the knee is brought into flexion the femoral contact point on the tibia moves posterior (translation) in the lateral compartment and the femur is rotated externally in relation to the tibia. These actions unseat the femoral condyles and allow flexion to occur past 30 degrees. Most restraints to motion in the knee are due to the collateral and cruciate ligaments. The medial collateral ligament (MCL) has two bands, superficial and deep, that connect the medial femoral epicondyle to the medial face of the tibia. Its primary purpose is to resist valgus angulation at the knee. It also has a secondary function to restrain external rotation of the tibia. The lateral collateral ligament (LCL) is found connecting the lateral femoral epicondyle to the fibular head. The primary role of the LCL is to resist varus and has a minor role in limiting external rotation of the tibia. The cruciate ligaments are the primary restraints to anterior-posterior translation of the knee with the collateral ligaments playing a secondary role. The anterior cruciate ligament (ACL) connects the medial tibial spine to the posteromedial aspect of the lateral femoral condyle. It consists of two bundles, the anteromedial and posterolateral bundles. The bundles act separately to prevent anterior translation of the tibia depending the amount of flexion in the knee. The anteromedial bundle is most active during flexion and the posterolateral bundle functions mostly in extension. This keeps one bundle or the other taut and active throughout most of the knees range of motion. The ACL prevents tibial translation maximally in extension whereas with approximately 30 degrees of flexion neither bundle of the ACL are particularly active. The oblique orientation of the ACL from superolateral to inferomedial provides a secondary restraint to internal rotation and valgus loading of the tibia. The posterior cruciate ligament (PCL) has a superomedial to inferolateral orientation as it attaches to the lateral face of the medial femoral condyle to the tibia between the posterior horns of the menisci situated slightly lateral to the midline of the tibia. Similar to the ACL, the PCL has two bundles: posteromedial and anterolateral bundles. These bundles act to prevent posterior translation of the tibia at different intervals along knee flexion/extension. The posteromedial bundle is most taut and active during full extension while the anterolateral bundle is most active in flexion. Additionally, the PCL may act to induce an external rotation of the tibia as posterior translation of the tibia is occurring. The PCL also has secondary function in restraining varus/valgus stress. These characteristics give the PCL greatest ability to restrain posterior translation of the tibia while the knee is flexed. The MCL, LCL, PCL, and ACL work in concert alongside muscle forces and geometry to guide motion and provide stability. As structures of primary restraint are damaged, secondary structures tend to compensate and carry the increased strain. The posterolateral corner of the knee contains the popliteal complex, LCL, arcuate ligament, Iliotibial (IT) band, joint capsule, and a host of smaller ligaments known to provide primary and secondary stability. The popliteal complex is composed of the popliteus muscle with its associated tendon (PLT) and the popliteofibular ligament (PFL). The 3 main stabilizers of the posterolateral knee are the PLT, LCL, and the PFL. They function as static structures to stabilize the knee in external rotation, varus angulation, and posterior to anterior translations of the femur in relation to the tibia. The PLT functions as a dynamic muscle, but the effects of its dynamic function are unknown.[9, 10]

The patellofemoral joint is the third compartment of the knee joint and functions to transfer extensor force to the tibia from the quadriceps muscles. The quadricep muscles are the primary producers of extension moment at the knee. The vastus lateralis, vastus medialis, vastus intermedius, and rectus femoris converge as they all attach to the patella. Force produced from the quadriceps are transmitted through the patella and patellar ligament to the tibial tuberosity anteriorly. This extensor mechanism acts as a pulley to direct the lines of force away from the epicondylar axis for flexion/extension which in turn increases the moment arm. At initial flexion of the knee, the patella is the farthest from the center of rotation and increases the moment arm and as the knee nears full flexion the patella can be found closest to the center of rotation and the moment arm effect decreases. The extensor mechanism is also responsible for an increasing anterior tibial translation as the knee extends. As the knee flexes the force vector directed anteriorly decreases and has less of an effect on tibial translation. The major group of muscles responsible for knee flexion are the hamstring muscles found posteriorly. The hamstrings are comprised of the semitendinosus, semimembranosus, and biceps femoris muscles, but there are 8 total muscles that cross the knee posteriorly and contribute to flexion. These 5 other muscles are the popliteus, sartorius, gastrocnemius, gracilis, and plantaris muscles. In addition, biceps femoris contributes to external rotation of the tibia and the semimembranosus, semitendinosus, gracilis, sartorious, and popliteus can contribute internal rotation. The anterior/posterior translation and internal/external rotation of the tibiofemoral joint are driven by the forces of these muscles working in coordination. The anterior/posterior translation and internal/external rotation of the tibia are coupled as muscle forces are introduced and soft tissue joint constraints are engaged. During the initiation of knee flexion, the tibial contact point of the lateral femoral condyle moves posteriorly and the knee unlocks. As the knee continues to flex, in a closed chain, the femur must simultaneously glide anteriorly to stay on the tibia as the femur rolls backward. The radius of curvature of the femoral condyles decreases from anterior to posterior; requiring the femur to glide anteriorly to maintain the same contact position on the tibia in the transverse plane as the femur rolls back. The rolling, gliding, and internal/external rotation of the knee all work together to put the femur in optimal position to perform flexion/extension in accordance to soft tissue restraint, surface geometry, and muscle force.

2.1.4 Ankle Joint Structure and Function

The three major segments of the foot complex are categorized into the hindfoot, midfoot, and forefoot. However, the current work only explores the more proximal structures of the tibiofibular and tibiotalar joints. Specifically, the medial malleolus of the tibia, tibial plafond, and lateral malleolus of the fibula are conjoined at the distal tibiofibular joint and make up the ankle mortise. The domed talus with its three articular facets sits within the mortise and comprises the tibiotalar joint. The lateral malleolus projects further distally and is found more posteriorly than the medial malleolus and articulates with the lateral articular facet of the talus. The medial malleolus articulates with the medial articular facet of the talus and has the deltoid ligament complex attached to the distal end. The trochlea of the talus is the largest and most proximal facet that articulates with the tibial plafond. The ankle largely depends on ligamentous structures for support. The medial deltoid and lateral collateral ligaments of the ankle are significant stabilizers of the ankle joint.

The deltoid ligament provides restraint to plantar flexion, external rotation, and pronation of the ankle through its attachments from the medial malleolus to the navicular, calcaneous, and talus. The lateral ankle receives stability from the calcaneofibular and talofibular ligaments. The calcaneofibular ligament restrains inversion and talar tilt. The anterior and posterior talofibular ligaments (ATFL and PTFL) are composed of anterior and posterior slips that should not be confused with the tibiofibular ligaments. The ATFL connects the fibula to the talus and restrains inversion and anterolateral translation of the talus. The PTFL plays a secondary role in ankle stability, but is under the greatest stress during dorsiflexion and posterior translation of the talus. Plantar flexion of the ankle is primarily limited by active muscles force produced from the anterior compartment of the leg. Dorsiflexion can be limited by both active and passive muscle forces of the gastrocnemius and soleus muscles. The gastrocnemius muscle crosses both the knee and ankle joints causing the passive restriction in dorsiflexion when the knee is extended. The gastrocnemius lengthens in this scenario and cannot provide any further excursion to act as a restraint to dorsiflexion. The majority of ankle stability is determined by muscle forces, collateral ligaments, and the mortise.

The stability of the mortise relies on the proximal and distal tibiofibular joints to keep the lateral malleolus conjoined about the plafond. The proximal tibiofibular joint has a mildly convex tibia abutting a mildly concave fibula to form a mostly planar synovial joint surrounded by the anterior and posterior superior tibiofibular ligaments. This joint has little motion and is only indirectly related to ankle and knee structure and function. Although, the proximal and distal tibiofibular joints do depend on one another for stability as the instability of one would directly affect the other through a very long moment arm. The distal tibiofibular joint has a concave tibia abutting a convex fibula at the incisura of the tibia. This joint is known as the ankle syndesmosis due to the fibrous union of the tibia and fibula at the site. The ankle syndesmosis is comprised of the anterior inferior tibiofibular (AITFL), posterior inferior tibiofibular (PITFL), and interosseous ligaments (IOL) in order of descending contribution to syndesmosis stability.[11] The AITFL is the largest contributor to syndesmosis stability and functions as a restraint to posterior translation and external rotation of the fibula. The PITFL is the second largest contributor to stability and functions to restrain internal fibular rotation. The IOL can be found extending from the proximal tibiofibular joint to the distal tibiofibular joint and mostly contributes stability as a restraint to lateral translation of the fibula. Maximal stress to the syndesmosis is found during combined movements of dorsiflexion and external rotation of the talus. During ankle dorsiflexion, the wider anterior dimensions of the talus are brought into closer contact within the mortise as the talus translates posteriorly in dorsiflexion. As external rotation of the ankle is added the talus wedges itself between the medial and lateral facets of the mortise creating a lever arm effect oriented to cause posterior translation, lateral translation, and external rotation of the fibula. These interactions occur during physiological maneuvers in vivo and during the external rotational stress test of the ankle. The stability of the ankle is greatest in dorsiflexion due to the high congruity of the widened anterior body of the talus wedging itself into the mortise. The tibiofibular and medial clear spaces can be monitored for widening as the ankle is stressed in this manner using fluoroscopy, ultrasound, or arthroscopy. Any widening greater than 6 mm of the tibiofibular space or medial clear space widening greater than 4 mm is indicative of a syndesmosis injury. The widening becomes problematic as contact surface area decreases and focal areas of high contact surface pressure form. These areas of high pressure likely lead to an increased rate of cartilage degeneration and incidence of osteoarthritis.[12] The excellent ability of the ankle joint to distribute forces through large contact surface areas allows lower incidences of osteoarthritis as compared to the knee and hip.[13] In addition, instability of the mortise can lead to loss of weight-bearing function of the ankle and pain. There is, however, some motion at the syndesmosis that is normal, but it is highly variable between individuals.[11] Injured syndesmoses are repaired classically with a cortical screw and newer methods using a suture-button construct. The goal of both constructs is to stabilize the syndesmosis to allow healing, but the suture-button attempts to do this by allowing some motion to mimic the physiological condition.[14, 15] However, the suture-button construct has yet to achieve restoration of physiologic motion and the cortical screw method still prevails as the most commonly used construct for syndesmosis repair. These methods further highlight the need for stability of the syndesmosis and therefore ankle mortise for proper ankle function. Overall, a stable ankle mortise is vital to a well-functioning and long lasting tibiotalar joint.

2.2 In Vitro Simulation

2.2.1 General Principles of In Vitro Simulation

In vitro simulations of the lower extremity provide an opportunity to test hypothesis impossible for in vivo studies to perform due to ethical considerations. They also have the advantage of anatomic variability and complexity that provide a more realistic model for simulation than many of the constraining computational models. In general, in vitro simulation involves securing a cadaveric specimen to an apparatus to apply loads to bone and muscle to simulate a specific motion or task. Typically, motion is 3 dimensionally tracked using an optical or electromagnetic system as a main outcome variable in addition to collecting some type of kinetic data (force, pressure, strain, moment arm length). However, in vitro simulations are frequently limited by cadaveric specimen integrity, system control over mechanical factors, repeatability, and quality of input data.

Replicating a relevant maneuver from in vivo is the goal of in vitro simulation. A simulation is only as good as its control of the system and the input parameters put in to control. Good control starts with aligning the specimen properly with the system. The muscular forces, ground reactive forces, and positional alignment of the specimen need to match the simulator. This is a key element often overlooked in current simulators. Often the speed and force magnitudes of an in vivo maneuver are scaled back to prevent specimen damage or meet simulator restrictions. Most simulators are not capable of attaining 100% physiological loads or speed which can affect strain rate dependent processes. A simulator can be over and under constrained by trying to control too many or too few degrees of freedom. It is common practice to only control an aspect of force or an aspect of position/rotation for a given degree of freedom to prevent over-constraining the system. For example: A simulator may apply a valgus moment about the knee and not control the positions or rotations of the femur and tibia in the coronal plane. Most simulators apply a vertical load to simulate body weight through the mechanical axis and control muscle forces to allow freedom of movement of the joints in response.

Cadaveric materials used for simulations can be problematic, but provide the closest model for comparison to in vivo situations. Cadaveric specimens are biologically inactive and are in a constant state of decay. To further this problem, only fresh frozen cadavers should be used as the embalming process changes tissue properties. Material longevity can be improved with flash freezing specimens as soon as possible and maintaining a temperature of less than ## degrees. In addition, if the simulation involves cyclic loading, high numbers of trials, or long experimentation times it can be expected that the data will change as the tissues degrade. If forces are being applied to a specimen they should be scaled based on body weight or matched to the mechanical aspects of the particular specimen for higher quality simulation and specimen integrity. Attempts at recreating any mechanical aspects of the in vivo situation should be made and may have a significant impact on results. For instance, using synthetic synovial fluid in joints, loss of hydration, or ensuring temperature control of tissues can all play a role in how tissues respond to force and can induce changes in motion. Specimens should also undergo preconditioning of tissue through cycles of maximal motion in three planes to prevent changes in tissue properties from stretch. When at all possible it is best to use each specimen as its own control as matched pairs of specimens can show intraspecimen variability from left to right sides and large samples sizes are often not feasible.

2.2.2 UNT HSC Ankle Joint Simulator

The impetus for the creation of the UNT HSC Ankle Joint Simulator was to enable controlled cadaveric testing of the ankle syndesmosis with a dynamic external rotational stress test. The rig controls the position of the foot with 6 degrees of freedom while maintaining the tibia in a fixed position. The fibula is left with 6 degrees of freedom of movement. The leg is fixated using 5-6 half pins drilled into the tibia that lock into 2 aluminum clasps. The foot is secured to a wooden wheel using 3-6 decking screws with the center of the talus aligning to the center of the wooden wheel. The wheel is then secured to the mounting block that contains the torque sensor Figure 11. This foot-wheel-mounting block combination are aligned such that the center of the talus aligns to the center of the torque sensor's center of rotation. This mounting block is attached to the control arm of the rig which controls the position of the foot through the foot-wheel-mounting block combination Figure 12.

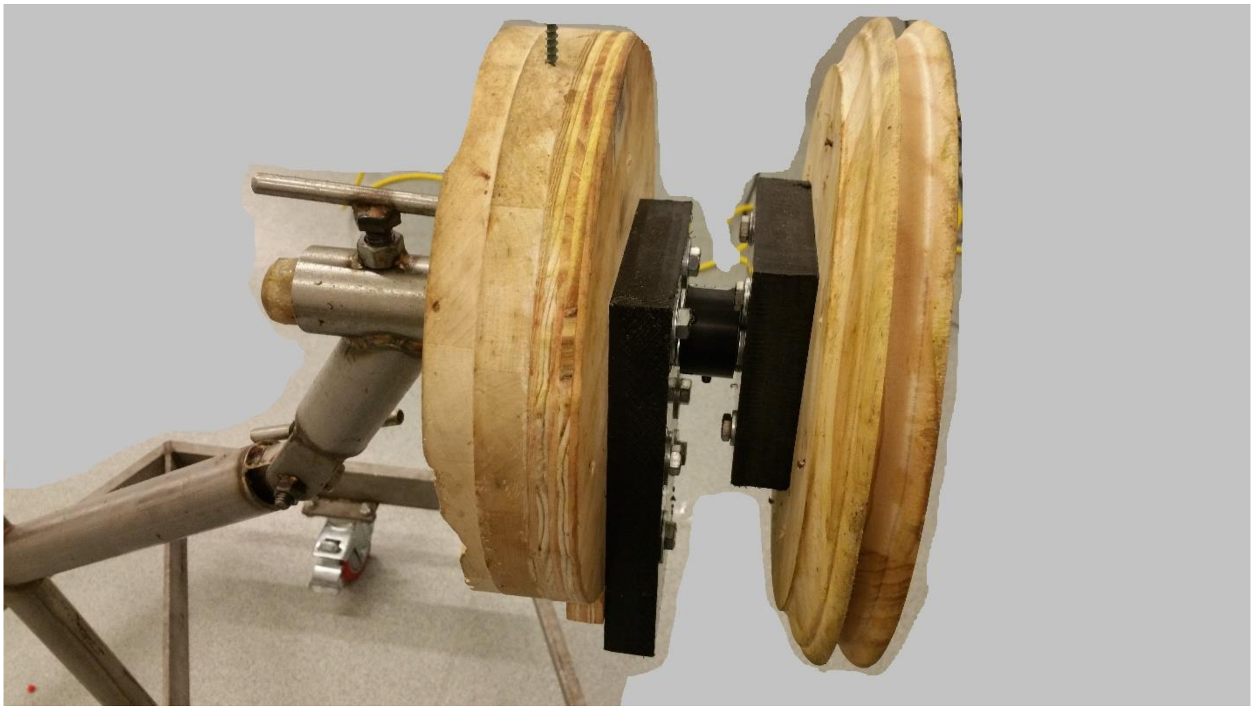

Figure 11- Mounting block with torque sensor connected to control arm

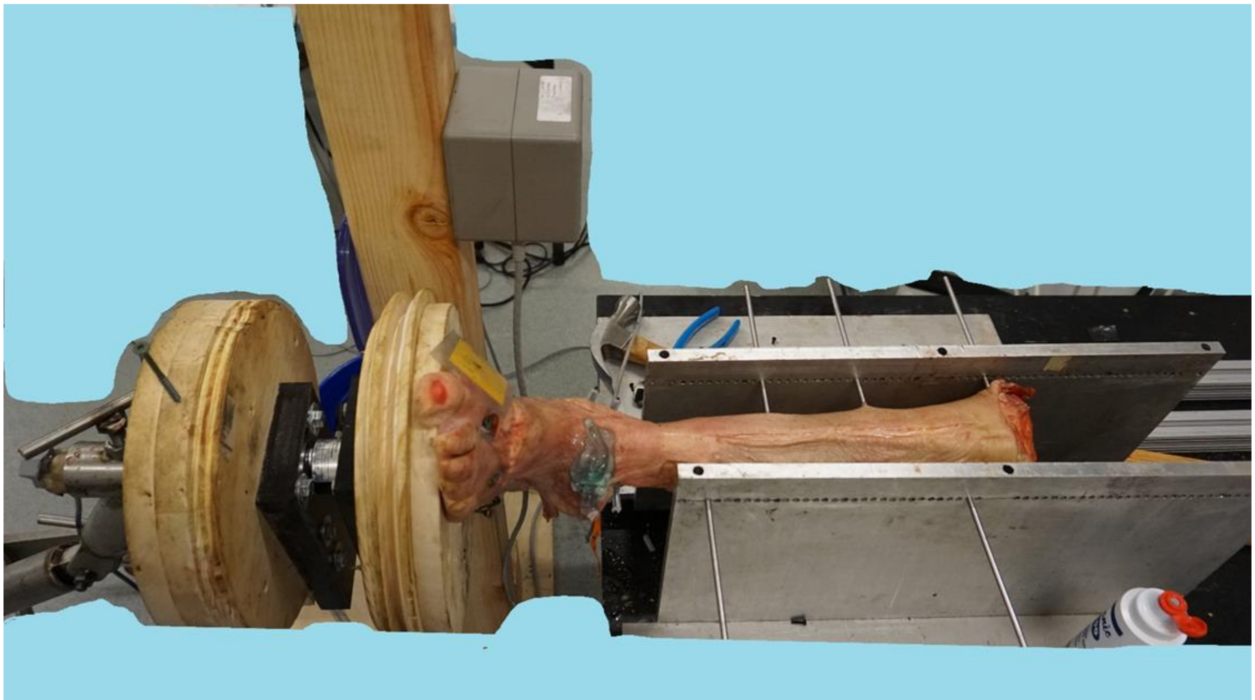

Figure 12- Ankle rig displaying fixation, rotation wheel, and tracking system

An examiner can then apply rotational force to the foot by rotating the wheel which is recorded by the torque sensor. At the same time, the motion tracking sensors that are attached to the tibia, fibula, and control arm spindle enable simultaneous recording of the positions and rotations of all three objects. Additionally, there is space to record ultrasound or fluoroscopy imaging as the force is applied to the ankle. This setup best mimics a standard clinical scenario where a patient undergoes an ankle stress examination to diagnose a syndesmosis injury through tibiofibular clear space measurement. In addition, it does provide some insight to syndesmosis stress during in vivo maneuvers involving external rotation. However, the rig does not attempt to recreate aspects of a dynamic in vivo maneuver and assumptions made concerning in vivo maneuvers based on rig results are limited. The rig does not recreate any ground reaction force or muscle force and functions to mostly to allow the foot to be static in all degrees of freedom except internal/external rotation. Although there are several other possible functions of the ankle rig, these have not been utilized yet. Even with the limitations of the rig, it provides an excellent representation of syndesmosis function during external rotations of the tibiotalar joint in vivo. Several similar simulators have been used to describe syndesmosis kinematics in prior literature and our results have been similar to theirs when comparisons could be made.[11, 15]

2.2.3 UNT HSC Knee Simulator

The current UNT HSC Knee Simulator was built based on the design of the Kansas muscle loading knee rig.[3] The first generation UNT HSC knee rig was an independent design that allowed passive range of motion of the knee while under single quadriceps and hamstring loads Figure 13. This initial design had too many limitations and the Kansas design provided a cost-effective means of improving our simulations.

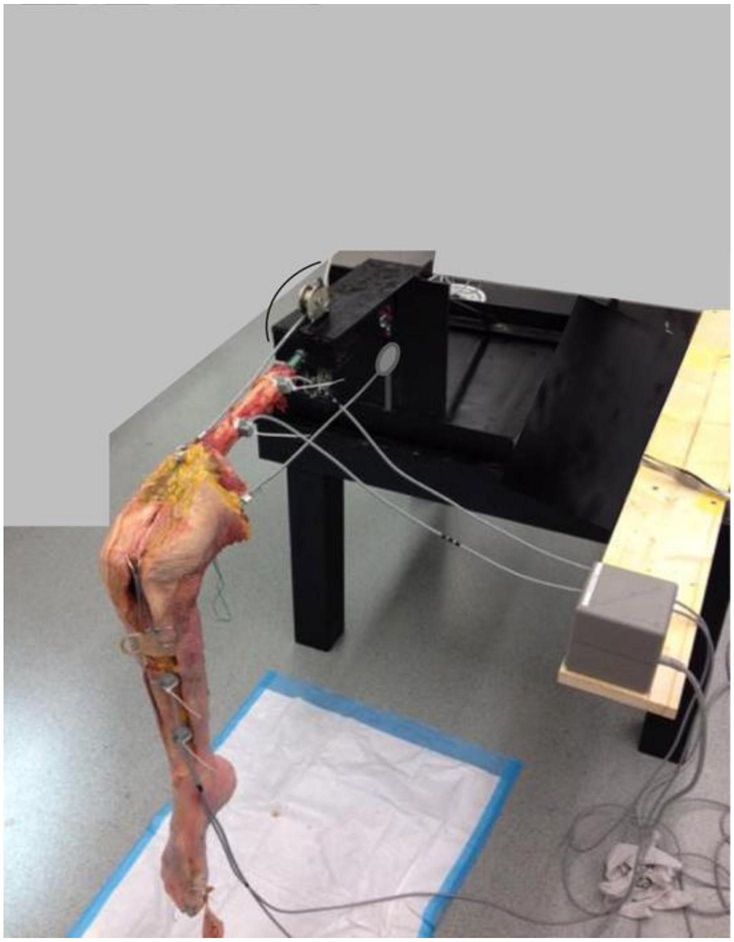

Figure 13. First Generation UNT HSC Knee Simulator

The Kansas design has the exceptional capability to control the trajectory of muscle loads on the quadriceps and hamstrings. In the first generation UNT HSC rig there was a single line for the quadriceps and a single line for the hamstrings to apply load through. The Kansas design allows for 3 separate trajectories of load for the quadriceps for independent loading of the vastus medialis, vastus lateralis, and the rectus femoris. The hamstrings are also controlled through 2 separate lines of action loading the semimembranosus and biceps femoris. The design provides static muscle loads and does not consider physiological muscle activation patterns. The muscles are scaled proportionally based upon the PCSA of each muscle and loaded using a weight and pulley system that recreates the anatomical trajectory of each muscle Figure 14-15.[16]

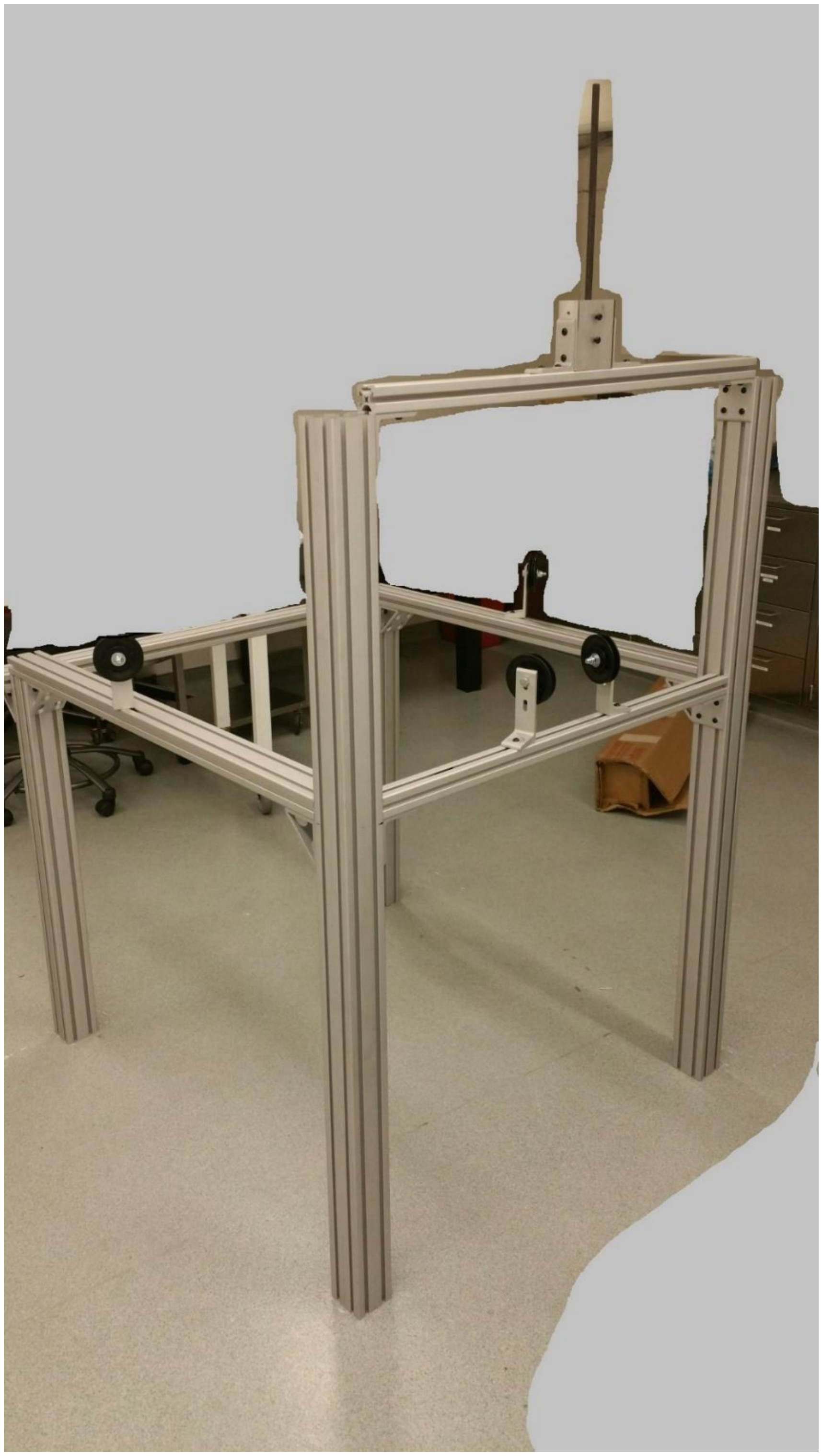

Figure 14 UNT HSC Knee Simulator based upon the design of the Kansas University Muscle Loading Rig.

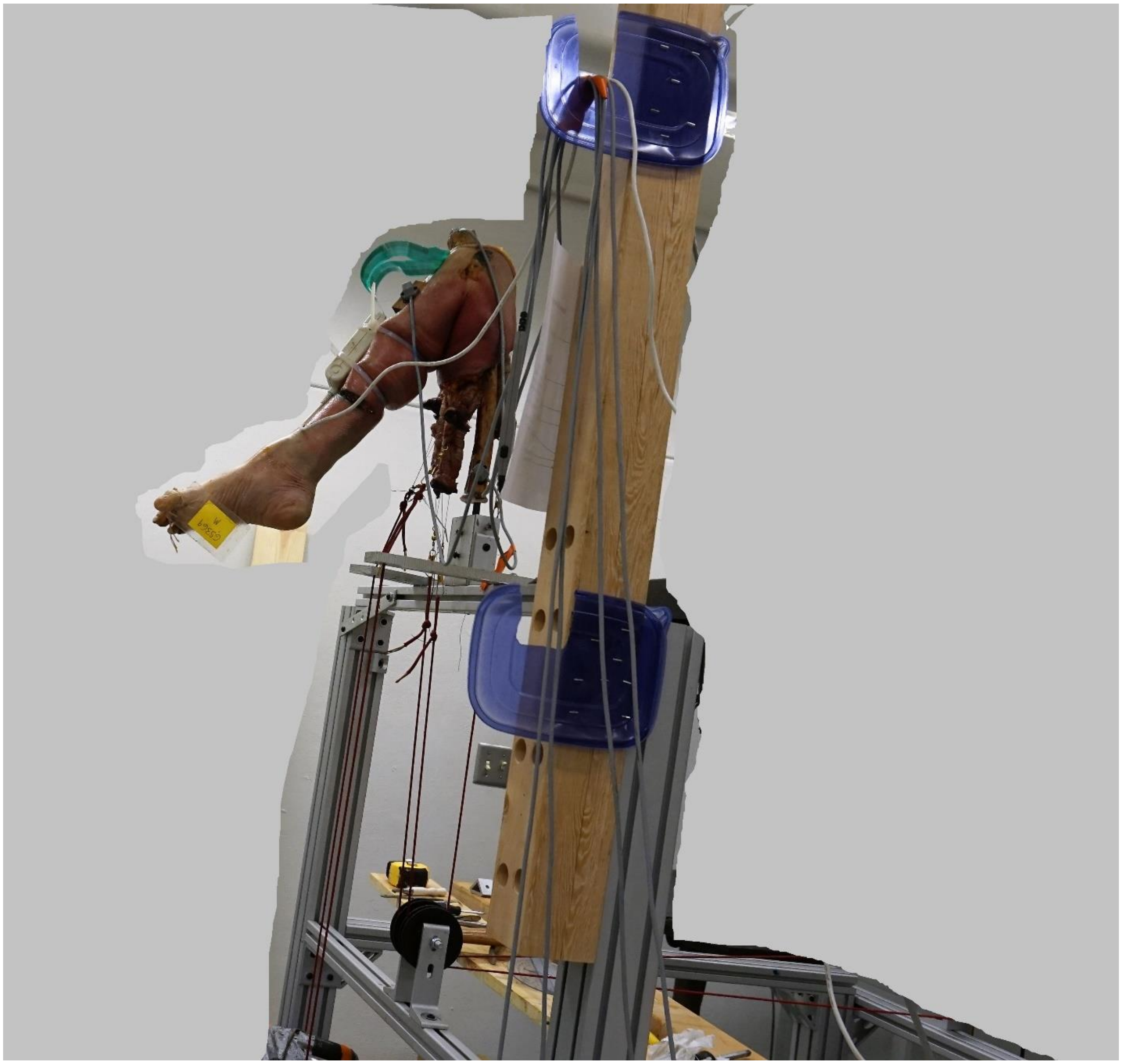

Figure 15 UNT HSC Knee Simulator with all sensory attached and muscles loaded

The specimen is attached via a carbon fiber rod that is cemented into the medullary canal of the femur. This rod can be adjusted rotationally and can be used to artificially lengthen the femur. All specimens have the same femur length due to adjusting the carbon fiber rod. The muscle trajectories can be adjusted once the carbon fiber rod is fixed to forgo the need to align the specimen's mechanical axis with the rig. Other aspects of alignment are completed through the establishment of a joint coordinate system using the digitizing pen of the motion tracking system.[1] The muscles are then loaded and the knee is actively moved into full extension where the quadriceps extensor moment maintains full extension about the knee. When the trial is ready to begin, the leg is brought into flexion gently until the flexion moment takes over allowing the knee to flex on its own. The rigid bodies formed through the fixation of the sensor to the bone have their kinematics recorded with 6 degree of freedom. Application of the rigid body motion is then transformed using the joint coordinate system and clinically relevant joint angles are calculated.

The UNT HSC Knee Simulator is a cost effective and easy to use rig with several benefits and limitations. The rig does not simulate any ground reactive forces or vertical load and does not produce dynamic muscle forces that are found in vivo. However, it is a valid, cost effective rig capable of loading the quadriceps and hamstring muscles with static loads during a simulated deep knee bend.

2.3 References

1. Grood ESE. A joint coordinate system for the clinical description of three-dimensional motions: application to the knee. *Journal of biomechanical engineering.*105:136-144.

2. Bull AM, Katchburian MV, Shih YF, Amis AA. Standardisation of the description of patellofemoral motion and comparison between different techniques. *Knee Surg Sports Traumatol Arthrosc.* 2002;10:184-193.

3. Shalhoub S, Maletsky LP. Variation in patellofemoral kinematics due to changes in quadriceps loading configuration during in vitro testing. *J Biomech.* 2014;47:130-136.

4. Serrancol, iacute, G. G. Neuromusculoskeletal Model Calibration Significantly Affects Predicted Knee Contact Forces for Walking. *Journal of biomechanical engineering.*138:081001.

5. Manal KK. An electromyogram-driven musculoskeletal model of the knee to predict in vivo joint contact forces during normal and novel gait patterns. *Journal of biomechanical engineering.*135:021014.

6. de Boer JJ, Blankevoort L, Kingma I, Vorster W. In vitro study of inter-individual variation in posterior slope in the knee joint. *Clin Biomech (Bristol, Avon).* 2009;24:488-492.

7. Mononen MEME. Effects of radial tears and partial meniscectomy of lateral meniscus on the knee joint mechanics during the stance phase of the gait cycle--A 3D finite element study. *Journal of orthopaedic research.*31:1208-1217.

8. Fregly BJBJ. Grand challenge competition to predict in vivo knee loads. *Journal of orthopaedic research.*30:503-513.

9. LaPrade RF, Morgan PM, Wentorf FA, Johansen S, Engebretsen L. The anatomy of the posterior aspect of the knee. An anatomic study. *J Bone Joint Surg Am.* 2007;89:758-764.

10. Stensdotter AK, Dalen T, Holmgren C, Hager-Ross C. Knee angle and force vector-dependent variations in open and closed kinetic chain for M. popliteus activation. *J Orthop Res.* 2008;26:217-224.

11. Clanton TO, Williams BT, Backus JD, et al. Biomechanical Analysis of the Individual Ligament Contributions to Syndesmotic Stability. *Foot Ankle Int.* 2017;38:66-75.

12. Hunt KJ, Goeb Y, Behn AW, Criswell B, Chou L. Ankle Joint Contact Loads and Displacement With Progressive Syndesmotic Injury. *Foot Ankle Int.* 2015;36:1095-1103.

13. Snedeker JGJG. Biomechanics of the normal and arthritic ankle joint. *Foot and ankle clinics.*17:517-528.

14. Clanton TO, Whitlow SR, Williams BT, et al. Biomechanical Comparison of 3 Current Ankle Syndesmosis Repair Techniques. *Foot Ankle Int.* 2017;38:200-207.

15. LaMothe JM, Baxter JR, Murphy C, Gilbert S, DeSandis B, Drakos MC. Three-Dimensional Analysis of Fibular Motion After Fixation of Syndesmotic Injuries With a Screw or Suture-Button Construct. *Foot Ankle Int.* 2016;37:1350-1356.

16. Farahmand F, Senavongse W, Amis AA. Quantitative study of the quadriceps muscles and trochlear groove geometry related to instability of the patellofemoral joint. *J Orthop Res.* 1998;16:136-143.

Chapter 3

Muscular Architecture of the Popliteus Muscle and the Basic Science Implications

Addison Wood[1], Morgan Smith[1], Taylor Dodgen[2], Russell Wagner[2], Rita M. Patterson[1]

From the [1]Department of Structural Anatomy and Rehabilitative Science,

University of North Texas Health Science Center, Fort Worth, Texas;

[2]John Peter Smith Hospital, Fort Worth, Texas

3.1 Abstract

The function of the popliteus muscle is largely treated as a static stabilizer of the posterolateral knee and has a lack of robust basic muscular architectural data to enable study of its dynamic function. A large volume of literature supports its static function and reconstruction in the posterolateral knee as vital to overall knee stability. A robust collection of foundational popliteus architectural data was collected from 28 cadaver knee specimens (mean (SD) 76 years (11)) to support future dynamic simulations of knee kinematics and kinetics. Physiological cross-sectional area of the popliteus and semimembranosus muscles were calculated from muscle volume and fiber length to power future muscle force prediction models. Posterior knee muscle trajectories were measured with respect to the longitudinal axis of the tibia as well. A 2-tailed T test was performed to test for significant differences amongst the 14 female and 14 male cadaver specimens. Significant differences between males and females were found for both the popliteus (p=1.1E-05) and semimembranosus (p=2.0E-05) volumes. Significant differences between males and females were also found in PCSA for the popliteus (p=0.005) and semimembranosus (p=4.1E-05) muscles. There were no significant differences found between males and females in fiber length, overall muscle length excluding tendon, age, and orientation. Further consideration should be given to include the popliteus muscle as a dynamic entity in the knee given its mechanical properties, trajectory, and prior biomechanical evidence showing when and how it is activated.

3.2 Introduction

Musculoskeletal computational modelling and in vitro simulations play an integral role in predicting clinically relevant kinetics and kinematics of the knee joint. To simulate the physiological motion of different tasks the simulations use a mixture of cadaveric, EMG, and in vivo biomechanical data to supply the models with input. Most muscle force prediction models include physiological cross-sectional area (PCSA) as a major determinant variable and use anatomical muscle trajectories to determine moment arms about the knee. Many times simulations circumvent this substantial hurdle and are often simplified and scaled without the use of subject specific data and do not include all muscles.[1] The overall quality of a simulation is highly dependent on the input data it uses as the results are only as valid as the input data and a system's ability to control the aspects of the test.[2]

The muscular architecture of the posterior knee is often overlooked with respect to in vitro simulations and computational models. This is of no surprise as the posterolateral corner of the knee is anatomically complicated, small, and situated in the deepest layer of the posterior knee. Clinically, the posterior knee structures, like the popliteus muscle, can play an important role in knee mechanics and balancing.[3-7] However, there are no studies addressing the dynamic effects of the popliteus muscle on knee kinetics and kinematics as the literature has focused on the static effects. Additionally, there is a lack of robust basic muscular architecture data on the popliteus in the literature. There is an increased focus on knee simulations recreating physiological motion in current literature; which has made internal/external rotation and contact forces important outcome measures of emphasis. These models rarely include posterolateral knee structures; which leads to questions about model validity when concerning internal/external rotation and contact forces about the knee.[2, 8-13] We hypothesize that the popliteus muscle is more significant as a dynamic presence in the knee with a meaningful PCSA and trajectory focused on internal/external rotation rather than as a static fixture. All prior simulation studies have treated the popliteus as a static structure and found it to be a contributor to external rotational stability.[5-7, 14-16] This is valuable information, but likely does not portray a full understanding of the effects of the popliteus muscle on dynamic internal/external rotation and contact forces about the knee. The primary goal of the present study is to provide foundational evidence and useful experimental input data to support the inclusion of the popliteus muscle as a dynamic force contributor in computational modelling and in vitro simulations of the knee focused on physiologic kinetics and kinematics.

3.3 Materials & Methods

The structure of the popliteus and semimembranosus muscles were examined in 12 female and 13 male embalmed cadaver specimens. An overall total of 28 popliteus and semimembranosus muscles with a mean age of 76 (female mean 75, male mean 76) were examined with 14 being female and 14 male. Prior to dissection, 12 of the original 25 cadavers had the orientations of their popliteus, medial and lateral gastrocnemius muscles recorded with respect to the long axis of the tibia as shown in Figure 1. Of the specimens with orientations measured, 5 were male and 7 female. A 36-inch metal rod was nailed to the proximal and distal centers of the tibia to act as a representative of the long axis of the tibia. A goniometer was then used to measure all orientations of the popliteus muscle using the metal rod as reference. The muscles were then dissected from their origin and insertion and placed into a shared container with humidity and temperature control for cold storage (35°F). Great care was taken to remove excess soft tissues and tendinous components without compromising muscle tissue. All specimens were embalmed using the same fixation solutions and stored in the same manner prior to dissection. Muscle volume was then measured using a water displacement canister with a visual accuracy of 1 ml using a graduated cylinder.[17] This measurement was repeated 3 times and an average taken to reduce the effect of observer error. Longitudinal incisions were then made in the midline, superior, and inferior portions of the muscle belly to extract muscle fibers from the corresponding areas of the muscle using a dissecting scope. A single fiber from each area was then measured under scope magnification using a transparent ruler to determine length to the nearest millimeter and averaged. The physiological cross sectional areas were then calculated by dividing the volume of each muscle by the measured fiber length. The physiological cross sectional areas of popliteus and semimembranosus were analyzed without the use of a pennation angle as it was not found to produce a significant change in PCSA during preliminary calculations.[18] Results were analyzed initially using descriptive statistics. Statistically significant differences amongst groups were determined by a 2-tailed T test with an alpha of .05.

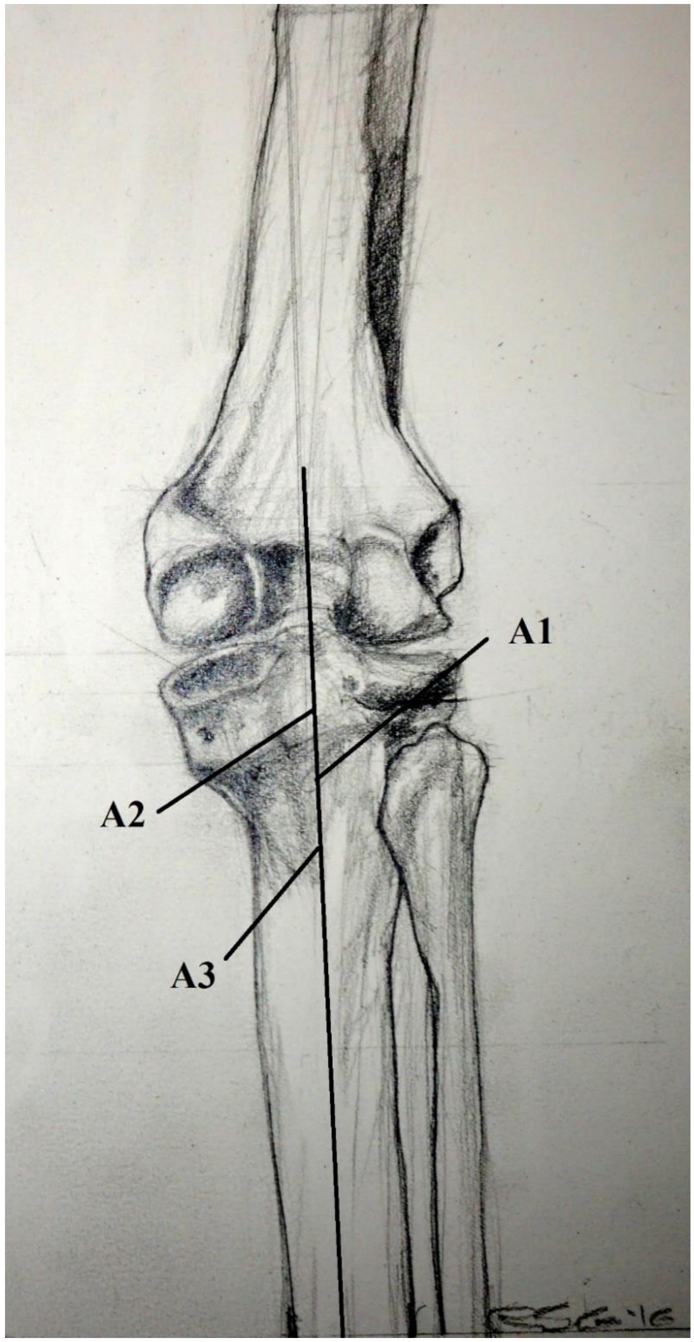

Figure 1. Illustration of the posterior knee without soft tissue. A1-Trajectory of the popliteal tendon as measured from the long axis of the tibia through the middle of the muscle body and tendon; A2-Trajectory of the superior most border of the muscle body of popliteus as measured from the long axis of the tibia; A3- Trajectory of the inferior most border of the popliteus as measured from the long axis of the tibia.

3.4 Results

Mean muscle volumes of the 14 female specimens were 13.9 ml for popliteus and 84.1 ml for semimembranosus. Mean muscle volumes of the 14 male specimens were 21.7 ml for popliteus and 154.4 ml for semimembranosus Tables 1-2. Significant differences between males and females were found for both the popliteus and semimembranosus volumes p=1.1E-05 and p=2.0E-05 respectively Table 3. Significant differences between males and females were also found in PCSA for the popliteus and semimembranosus muscles p=0.005 and p=4.1E-05 respectively Table 3. There were no significant differences found between males and females in fiber length, overall muscle length excluding tendon, and orientation in the 12 specimens found in Tables 3-5. The mean orientations of the popliteus, medial gastrocnemius, and lateral gastrocnemius with respect to the long axis of the tibia were 145.3 degrees (A1), 163.8 degrees (A4), and 162.4 degrees (A5) respectively Figure 1, Table 4-5. The tibial attachment site of the popliteus muscle spanned between 38.3 degrees (A2) and 25.5 degrees (A3) in relation to the long axis of the tibia Figure 1, Table 4-5. There was no significant difference in age between the male and female groups (P value= 1).

Female							
Age	ID	V pop	V semi	Pop L	Semi L	PCSA pop	PCSA semi
83	1	8.0	50.0	20.3	51.7	3.9	9.7
83	1	11.5	45.0	38.3	65.3	3.0	6.9
71	2	15.9	84.6	31.7	60.8	5.0	13.9
44	3	15.2	118.8	25.8	74.8	5.9	15.9
62	4	15.3	115.9	21.7	56.0	7.1	20.7
91	5	11.3	49.0	23.3	39.0	4.9	12.6
86	6	8.5	58.5	19.7	44.7	4.3	13.1
63	7	16.5	79.0	32.0	83.3	5.2	9.5
84	8	14.5	54.5	31.0	60.0	4.7	9.1
76	9	21.4	138.8	28.7	67.0	7.5	20.7
72	10	13.0	42.9	15.0	163.3	8.7	2.6
84	11	14.0	107.0	20.3	54.7	6.9	19.6
84	11	15.5	92.5	21.0	56.3	7.4	16.4
71	12	14.0	141.0	20.3	75.3	6.9	18.7

Table 1

Male							
Age	ID	V pop	V semi	Pop L	Semi L	PCSA pop	PCSA semi
75	13	18.0	204.0	22.0	54.7	8.2	37.3
75	13	23.5	224.0	24.0	81.3	9.8	27.5
60	14	22.5	174.0	20.7	50.7	10.9	34.3
59	15	17.5	160.0	24.0	63.3	7.3	25.3
83	16	21.0	109.0	28.7	68.3	7.3	16.0
70	17	17.6	185.3	30.1	63.7	5.8	29.1
70	17	18.0	157.2	34.0	73.8	5.3	21.3
78	18	21.3	99.9	35.3	67.8	6.0	14.7
78	18	23.5	148.2	31.7	42.7	7.4	34.7
93	19	15.8	117.0	26.7	41.3	5.9	28.3
86	20	24.2	180.1	25.7	65.0	9.4	27.7
80	21	30.2	143.8	29.7	54.3	10.2	26.5
85	22	27.8	130.8	33.7	61.3	8.3	21.3
70	23	23.3	127.8	34.7	83.7	6.7	15.3

Table 2

	Overall		Male		Female			
	Mean	Std Dev	Mean	Std Dev	Mean	Std Dev	P-Value	P-Value < .05
Age	75.6	11	75.8	9.2	75.2	12.6	0.9	N
Volume Popliteus*	17.8	5.5	21.7	4	13.9	3.4	1.10E-05	Y*
Volume Semimembranosus*	119.2	50.2	154.4	35	84.1	35.3	2.00E-05	Y*
Popliteus Length	26.8	5.9	28.6	4.7	24.9	6.5	0.102	N
Semimembranosus Length	65.2	22.8	62.3	12.3	68	29.9	0.518	N
PCSA Popliteus*	6.8	1.9	7.8	1.7	5.8	1.6	0.0052	Y*
PCSA Semimembranosus*	19.6	8.8	25.7	7	13.5	5.5	4.00E-05	Y*
Pop to Semi PCSA Ratio	1 : 2.9	NA	1 : 3.3	NA	1 : 2.3	NA		

Table 3

	Female							Male				
A1	143	141	142	153	141	146	148	142	153	146	143	145
A2	42	36	40	31	43	41	41	38	22	48	35	42
A3	26	20	24	21	25	30	24	30	28	25	19	34
A4	x	163	165	166	160	165	163	151	163	162	163	165
A5	x	167	170	161	168	162	167	156	159	167	156	169

Table 4 Trajectories of posterior knee structures. A1-Trajectory of the popliteal tendon; A2-Trajectory of the superior most border of the muscle body of popliteus; A3- Trajectory of the inferior most border of the popliteus; A4- Trajectory of the medial head of gastrocnemius as measured from the long axis of the tibia; A5- Trajectory of the lateral head of the grastrocnemius muscle as measured from the long axis of the tibia.

	Overall		Male		Female			
	Mean	Std Dev	Mean	Std Dev	Mean	Std Dev	P-Value	P-Value < .05
A1	145.3	4.2	145.8	4.3	144.9	4.5	0.72	N
A2	38.3	6.7	37.0	9.7	39.1	4.2	0.66	N
A3	25.5	4.4	27.2	5.6	24.3	3.3	0.34	N
A4	162.4	4.1	160.8	5.6	163.7	2.2	0.33	N
A5	163.8	5.2	161.4	6.2	165.8	3.5	0.20	N

Table 5 Mean muscle trajectories of the posterior knee. A1-Trajectory of the popliteal tendon; A2-Trajectory of the superior most border of the muscle body of popliteus; A3- Trajectory of the inferior most border of the popliteus; A4- Trajectory of the medial head of gastrocnemius; A5-Trajectory of the lateral head of the grastrocnemius muscle a.

3.5 Discussion

The posterolateral corner of the knee contains several structures, but the 3 essential structures to knee stability include the popliteus muscle tendon (PLT), popliteofibular ligament (PFL), and the fibular collateral ligament (FCL).[19] The popliteus muscle belly is triangular in shape at its origin on the posteromedial tibial cortex which tapers to a slender tendon as it progresses towards its insertion just anterior and inferior to the FCL on the lateral femoral condyle. The PFL and popliteal capsular expansion (PCE) acts to tether the popliteus at its musculotendinous junction to the fibular styloid. The FCL attaches to the femur just proximal and posterior to the lateral epicondyle and attaches to the lateral aspect of the fibula distal to the fibular styloid Figure 2. The orientation of the PLT deep to the FCL, PCE, and the PFL acts as a soft tissue constraint to PLT bowstringing motion.[19] Although, there are no biomechanical studies on the effects of the PCE. The primary role of the popliteus muscle is to internally rotate the tibia in relation to the femur in open-chain and stabilization of external rotation of the femur in relation to the tibia in closed chain situations.

The FCL, PFL, and PLT structures function in combination to provide stability to the lateral knee and are the target for reconstruction clinically.[3, 7] Prior biomechanical literature has shown these posterolateral corner structures to be primary stabilizers against varus stress, external rotation, and coupled to posterolateral tibial translations.[6, 7, 15, 19] The PLT itself was implicated as a significant static contributor to external rotational stability of the knee in addition to varus stress, external rotation, and tibial translation.[7, 14, 15] In addition, the PLT was found to have the highest stiffness and ultimate failure of the 3 primary posterolateral corner structures with an ultimate failure strength of 700 N and a stiffness of 83 N/m.[16] Clinically, concomitant injuries of posterolateral corner structures with a cruciate injury leads to an increased incidence of ACL and PCL reconstruction failures.[22, 23] Biomechanically, this higher rate of cruciate graft failure was due to increased force transmitted through the cruciate ligaments if a concomitant posterolateral corner injury was not fixed alongside the cruciate injury.[22-24] Clearly the literature supports the PLT and popliteus complex as being important static structures for knee stability.

The focus on achieving physiologic kinematics is thought to be the ultimate goal for knee surgery in order to restore function. Orthopaedic sports surgeons routinely attempt to restore physiologic motion during soft tissue or implant reconstruction and implant designers have sought after an implant that mimics a native knee for arthroplasty patients. The popularity of restoring physiologic motion via surgery is derived from hopes to improve patient satisfaction, improve function, and reduce negative long term sequela of the injury or surgery.[11, 13] To properly test hypotheses and achieve these goals, simulations must continue to increase in complexity to match the increased precision demanded by the interventions used by surgeons. Defining what drives physiologic kinematics of the knee is variable with complex anatomy, muscle activation patterns, and muscle forces being largely specific to an individual.[1, 18, 25] However, there are a few general patterns considered by most to be physiologic for an average knee. Most knees have a medialized center of rotation in the transverse plane for internal-external rotation during deep knee flexion.[11, 13, 26] There is also variation in the location of the center of rotation depending upon the activity that is being performed.[27] In addition, the medial femoral condyle has less posterior translation than its lateral condylar counterpart as the medial tibial plateau is concave and the lateral tibial plateau is convex. This contrasting tibial surface anatomy restricts translational motion medially and promotes it laterally. Dynamically, the rotational contribution of the popliteus is not linear as the FCL, PCE, and PFL form a pulley or tethering mechanism with a biomechanical effect on dynamic popliteus function that is still unknown.[19, 21] Furthermore, the trajectory data gathered from the present study may aid future model development as a significant moment arm is likely formed at this pulley junction as the knee is flexed and the tether holds the distal popliteus tendon in place. The proximal portion of the PLT then follows the rotation of the epicondyle and forms two different trajectories from the popliteus tendon as it is bent around the tether and creates a moment arm Figure 3.[21] Buford et al. found the moment arm of the popliteus to peak at 30° and 50° of knee flexion and reached up to 10.4 mm in length and these results were without consideration of the possible tethering effect of the PFL and PCE. Additionally, the popliteus moment arm was greatest while the knee was at neutral position in internal/external rotation in the transverse plane. For comparison, Buford et al. also found all other knee muscle moment arms to be maximal at 70° or 90° of flexion and the semimembranosus had a moment arm range from 10.1-11.6 mm while the knee was in 30° of flexion.[28] A popliteus moment arm similar to semimembranosus at 30° of flexion combined with the surprisingly low ratio of 1 : 2.9 popliteus to semimembranosus PCSA found in this study make a compelling argument that the popliteus is a significant dynamic contributor to joint reaction forces at the knee Table 3. To complicate matters, consistently accurate calculation of individual muscle forces has been recalcitrant to research, with widespread variations in prediction models and predictions being reported.[29] The majority of these muscle force prediction models use physiological cross sectional area, EMG data, and in vivo kinetic data as essential variables in their calculations. Overall, the combined interactions of femoral and tibial surface geometries, muscle forces, and soft tissue restraints are the primary determinants of physiologic kinematics and internal-external tibial rotation.[11, 13, 29]

The current study focused on the muscular architecture and trajectory of the popliteus muscle as they directly correspond to the mechanical performance of muscles. Cadaveric material provides a detailed description of the physiological cross sectional area (PCSA), volume, and trajectory of muscles. The PCSA of popliteus and semimembranosus found in this study were analyzed for differences in volume and fiber length due to specimen sex Table 3. Interestingly, when looking at the ratio of popliteus to semimembranosus PCSA in males vs females, females were found to have a lower ratio. Females had a ratio of 1 : 2.3 whereas males had a ratio of 1 : 3.3 suggesting female popliteus muscles contribute more force in proportion to their semimembranosus than males Table 3. Although this finding could be due to sample size, but the study was adequately powered and to date there are no studies focused on finding differences in popliteus function between males and females. There were also significant differences found between males and females in PCSA and volume Table 3. These findings could find value in the future as muscle force predictions are known to be highly sensitive to changes in PCSA.[30] These models use PCSA to estimate peak muscle force production and use EMG data with in vivo force measurement to determine how much and when a muscle is activated. Stensdotter et al provided evidence that the direction of force vectors within the knee and particular knee kinematics drive when the popliteus is activated and can be influenced by behavioral context. Additionally, they ruled out anticipatory activation and found the peak RMS or magnitude of activation to increase as the knee became more unstable and additionally controlled by the biomechanics of a particular task.[31, 32] The basic muscle parameter data presented in Tables 1-5 along with prior EMG data provides sufficient evidence that the popliteus is significant as a dynamic muscle that is activated during perturbations and specific movements.[31-33]

There are several limitations to this study. Foremost, this study was purely descriptive in nature using cadaveric specimens to gather useful biomechanical information and providing a logical argument for future simulations including a dynamically acting popliteus muscle. The PCSA and trajectory data are subject to observer error through the use of the goniometer and water displacement canister. However, these methods were used in prior studies with success and when comparisons were possible our results were found to be very similar to other studies using different methods.[17, 18] Additionally, cadaveric specimens are subject to changes in hydration, density, fixation methods, and drying time when calculating PCSA. To minimize these sources of error we controlled temperature, humidity, and used direct volume measurements instead of density measurements for our calculation of PCSA. Furthermore, there were two matched pairs of data in each of the male and female groups, but calculation of significance with and without the matched pairs caused minimal changes in results and maintained significance and were therefore included in our results. Finally, this study was meant to provide valuable input data on the popliteus muscle for use in dynamic simulations and computational modeling of the knee and does not disprove the validity of any prior knee simulations or models.

3.6 Conclusion

To date, our study results provide the largest and most diverse sample of popliteus muscle anatomical information that may have implications on mechanical performance. The trajectory and PCSA data may be of value for reference and further investigation for use in computer models with the continued focus on physiologic motion. Further consideration should be given to include the popliteus muscle as a dynamic entity in the knee given its mechanical properties, trajectory, and prior biomechanical evidence showing when and how it is activated. In addition, subject specific input may be of value as there are variations between individuals for PCSA and differences in PCSA due to gender can be found.

3.7 References

1. Carbone V, van der Krogt MM, Koopman HF, Verdonschot N. Sensitivity of subject-specific models to Hill muscle-tendon model parameters in simulations of gait. *J Biomech.* 2016;49:1953-1960.

2. Maletsky LL. In Vitro Experimental Testing of the Human Knee: A Concise Review. *The Journal of knee surgery.*29:138-148.

3. Chahla JJ. Midterm outcomes following anatomic-based popliteus tendon reconstructions. *Knee surgery, sports traumatology, arthroscopy : official journal of the ESSKA.*

4. Chun YM, Kim SJ, Kim HS. Evaluation of the mechanical properties of posterolateral structures and supporting posterolateral instability of the knee. *J Orthop Res.* 2008;26:1371-1376.

5. Cottino U, Bruzzone M, Rosso F, Dettoni F, Bonasia DE, Rossi R. The role of the popliteus tendon in total knee arthroplasty: a cadaveric study: SIGASCOT Best Paper Award Finalist 2014. *Joints.* 2015;3:15-19.

6. James EW, LaPrade CM, LaPrade RF. Anatomy and biomechanics of the lateral side of the knee and surgical implications. *Sports Med Arthrosc.* 2015;23:2-9.

7. LaPrade RF, Wozniczka JK, Stellmaker MP, Wijdicks CA. Analysis of the static function of the popliteus tendon and evaluation of an anatomic reconstruction: the "fifth ligament" of the knee. *Am J Sports Med.* 2010;38:543-549.

8. Jacobs WC, Clement DJ, Wymenga AB. Retention versus removal of the posterior cruciate ligament in total knee replacement: a systematic literature review within the Cochrane framework. *Acta Orthop.* 2005;76:757-768.

9. Keeney JA, Eunice S, Pashos G, Wright RW, Clohisy JC. What is the evidence for total knee arthroplasty in young patients?: a systematic review of the literature. *Clin Orthop Relat Res.* 2011;469:574-583.

10. Li N, Tan Y, Deng Y, Chen L. Posterior cruciate-retaining versus posterior stabilized total knee arthroplasty: a meta-analysis of randomized controlled trials. *Knee Surg Sports Traumatol Arthrosc.* 2014;22:556-564.

11. Victor J, Bellemans J. Physiologic kinematics as a concept for better flexion in TKA. *Clin Orthop Relat Res.* 2006;452:53-58.

12. Heyse TJTJ. Kinematics of a bicruciate-retaining total knee arthroplasty. *Knee surgery, sports traumatology, arthroscopy : official journal of the ESSKA.*

13. Bates NANA. Anterior cruciate ligament biomechanics during robotic and mechanical simulations of physiologic and clinical motion tasks: a systematic review and meta-analysis. *Clinical biomechanics (Bristol).*30:1-13.

14. Kim YH, Purevsuren T, Kim K, Oh KJ. Contribution of posterolateral corner structures to knee joint translational and rotational stabilities: a computational study. *Proc Inst Mech Eng H.* 2013;227:968-975.

15. LaPrade RF, Tso A, Wentorf FA. Force measurements on the fibular collateral ligament, popliteofibular ligament, and popliteus tendon to applied loads. *Am J Sports Med.* 2004;32:1695-1701.

16. LaPrade RF, Bollom TS, Wentorf FA, Wills NJ, Meister K. Mechanical properties of the posterolateral structures of the knee. *Am J Sports Med.* 2005;33:1386-1391.

17. Farahmand F, Senavongse W, Amis AA. Quantitative study of the quadriceps muscles and trochlear groove geometry related to instability of the patellofemoral joint. *J Orthop Res.* 1998;16:136-143.

18. Fukunaga T, Roy RR, Shellock FG, et al. Physiological cross-sectional area of human leg muscles based on magnetic resonance imaging. *J Orthop Res.* 1992;10:928-934.

19. LaPrade RF, Morgan PM, Wentorf FA, Johansen S, Engebretsen L. The anatomy of the posterior aspect of the knee. An anatomic study. *J Bone Joint Surg Am.* 2007;89:758-764.

20. LaPrade RFRF. The anatomy of the posterior aspect of the knee. An anatomic study. *Journal of bone and joint surgery. American volume.*89:758-764.

21. LaPrade RFRF. The posterolateral attachments of the knee: a qualitative and quantitative morphologic analysis of the fibular collateral ligament, popliteus tendon, popliteofibular ligament, and lateral gastrocnemius tendon. *The American journal of sports medicine.*31:854-860.

22. LaPrade RF, Resig S, Wentorf F, Lewis JL. The effects of grade III posterolateral knee complex injuries on anterior cruciate ligament graft force. A biomechanical analysis. *Am J Sports Med.* 1999;27:469-475.

23. LaPrade RF, Muench C, Wentorf F, Lewis JL. The effect of injury to the posterolateral structures of the knee on force in a posterior cruciate ligament graft: a biomechanical study. *Am J Sports Med.* 2002;30:233-238.

24. Harner CD, Vogrin TM, Hoher J, Ma CB, Woo SL. Biomechanical analysis of a posterior cruciate ligament reconstruction. Deficiency of the posterolateral structures as a cause of graft failure. *Am J Sports Med.* 2000;28:32-39.

25. Bolsterlee B, Vardy AN, van der Helm FC, Veeger HE. The effect of scaling physiological cross-sectional area on musculoskeletal model predictions. *J Biomech.* 2015;48:1760-1768.

26. Komistek RD, Dennis DA, Mahfouz M. In vivo fluoroscopic analysis of the normal human knee. *Clinical Orthopaedics and Related Research.* 2003:69-81.

27. Koo SS. The knee joint center of rotation is predominantly on the lateral side during normal walking. *Journal of biomechanics.* 2008;41:1269-1273.

28. Buford WLW. Internal/external rotation moment arms of muscles at the knee: moment arms for the normal knee and the ACL-deficient knee. *The knee.*8:293-303.

29. Fregly BJBJ. Grand challenge competition to predict in vivo knee loads. *Journal of orthopaedic research.*30:503-513.

30. Brand RA, Pedersen DR, Friederich JA. The sensitivity of muscle force predictions to changes in physiologic cross-sectional area. *J Biomech.* 1986;19:589-596.

31. Stensdotter AK, Holmgren C, Dalen T, Hager-Ross C. The role of M. popliteus in unpredictable and in self-initiated balance provocations. *J Orthop Res.* 2006;24:524-530.

32. Stensdotter AK, Dalen T, Holmgren C, Hager-Ross C. Knee angle and force vector-dependent variations in open and closed kinetic chain for M. popliteus activation. *J Orthop Res.* 2008;26:217-224.

33. Schinhan MM. Electromyographic study of the popliteus muscle in the dynamic stabilization of the posterolateral corner structures of the knee. *The American journal of sports medicine.*39:173-179.

Chapter 4

Protecting the PCL during Total Knee Arthroplasty using a Bone Island Technique

Addison Wood, MS*[1]; Tebyan Rabbani[1]; Benjamin Sheffer MD[2]; Russell Wagner MD[1,2]; Hugo Sanchez MD, PhD[1,2]

From the [1]Department of Structural Anatomy and Rehabilitative Science,

University of North Texas Health Science Center, Fort Worth, Texas;

[2]John Peter Smith Hospital, Fort Worth, Texas

4.1. Abstract

Background: Prior studies have shown the PCL may be partially resected during cruciate retaining (CR) total knee arthroplasty (TKA) using highly experienced hands and standard surgical technique, therefore, proper surgical technique is aimed at preservation and balance of the PCL during CR TKA. The central objective of this study is to evaluate the effectiveness of a simple surgical technique to prevent PCL damage during performance of a CR TKA.

Methods: 60 embalmed cadaver specimens were randomized into two groups, experimental and control. The control group consisted of standard tibial resection without the use of an osteotome. The experimental group utilized an osteotome in addition to standard technique to preserve a bone island anterior to the tibial attachment of the PCL.

Results: In the control group, PCL damage was noted in 73% (22/30) of specimens. In the experimental group, where an osteotome was used, PCL damage was found in 23% (7/30) specimens. The use of an osteotome was found to have an absolute risk reduction of 50% when compared to the control group which did not use an osteotome to protect the PCL.

Conclusion: In the setting of minimal surgical experience, the use of an osteotome to preserve the PCL during CR TKA by forming a bone island was found to be an effective means of protecting the PCL over standard technique. In addition, standard technique with the use of a Y-shaped PCL retractor was found to provide questionable protection to the PCL.

4.2. Introduction

Total knee arthroplasty (TKA) has shown high rates of long term success for both posterior cruciate retaining (CR) and posterior stabilized (PS) implant designs. There is great debate as to whether either of these designs provide any benefit over the other. Both CR and PS knees have shown similar functional scores and a wide variability in achieving more physiological kinematics while both maintain similar long term survivability.[1-16] A well-functioning PCL is the goal of the CR surgical technique and plays an important role in proper CR implant function as well. A functional PCL in a CR TKA is believed to provide proprioceptive feedback and drive more physiological knee kinematics by reducing paradoxical roll forward enabling the femur to perform a controlled rollback during flexion.[2, 17, 18] Although the portion of intact PCL required to maintain adequate function of a CR TKA is not defined; several studies have sought to describe the amount of PCL footprint injury during CR TKA. These studies have revealed that the PCL may be partially resected in the majority of cases, maybe even completely resected, using highly experienced hands and standard surgical technique.[19-24] Preservation of 100% of the PCL has been reported as low as 9% in the literature when not using a PCL protecting technique, but 100% of the PCL is not likely required for adequate function.[25] Therefore, surgical technique is aimed at the preservation and balance of the PCL during CR TKA.

Aside from a well experienced hand there are few methods in practice today that protect the PCL from injury and a complete lack of studies on the effectiveness of these methods. One such method works by maintaining a bone island for the PCL tibial attachment site so not to disturb it during tibial resection. The central objective of this study is to evaluate the effectiveness of this simple surgical technique to prevent PCL damage during performance of a CR TKA. This technique involves placement of an osteotome to prevent iatrogenic injury to the PCL by the sagittal bone saw blade during tibial resection. To our knowledge, this method has yet to be studied for effectiveness.

4.3. Materials and Methods

60 lower extremities from embalmed cadaveric specimens were prepared via dissection in the University of North Texas Health Science Center Anatomy Department gross laboratory. Specimens' age ranged from 44 to 95 with a mean age of 76. Of the 60 specimens used, 25 were bilateral and 10 were unilateral. There were 33 female and 27 male specimens used. A unique surgical exposure was performed, which allowed full visualization of the tibial plateau by reflecting the patella superiorly from the tibia by cutting the patellar tendon. Standard surgical exposure for CR TKA was then followed to remove the menisci, ACL, and any remaining soft tissues that impeded the performance of a standard tibial resection. The PCL, posterior capsule, and femur were left fully intact while the MCL and LCL were partially resected to allow for increased visibility. The specimens were mounted on a triangular apparatus to maintain knee flexion to fully expose the tibial plateau.

To simulate the worst-case scenario for surgeon performance and reduce bias from surgeon surgical technique preference, 60 medical students were used as blinded participants. Specimens were equally randomized into two groups, an experimental group and a control group. The control group consisted of standard tibial resection technique using a Y-shaped PCL retractor without the use of an osteotome. The experimental group used an osteotome in addition to standard technique used in the control group. Participants were blinded to which group they were in and given instructions from a board certified adult reconstructive orthopaedic surgeon on how to perform the resection and observed one example prior to making the cut themselves. A standard vanguard tibial preparation set (Biomet), sagittal surgical saw (Stryker), saw blade (1.3 mm thickness), Hohmann retractors, and a PCL retractor were used. The senior surgeon aligned the extramedullary tibial resection guide, positioned the Y-shaped PCL retractor posterior to the tibia, and inserted the osteotome for the experimental group if indicated. Once the guide was in place the senior surgeon was required to leave and not provide advice to reduce bias. The posterior tibial slope and resection depth were held constant at 3 degrees and 2mm from the medial plateau respectively for all specimens. The varus/valgus angle of the tibial cut was set to each specimen to achieve a 0 degree overlap of the anatomical and mechanical axis. When the ¼ inch osteotome was used in the experimental protocol, a penetration depth of 1 cm and A-P position of 5 mm anterior to the PCL were held constant across all experimental group trials (Figure 1).

Figure 1 Anterior to Posterior view of a left knee with osteotome and Y-shaped retractor in position

Posterior cruciate ligaments were independently assessed before and after completion of the procedures by 3 separate individuals to assess PCL condition. There were two states defined: PCL intact and PCL damaged. PCL damaged state was defined as approximately >20% of the ligament diameter being lacerated. PCL intact was defined as approximately <20% of the ligament being lacerated.

We estimated how deep to place the osteotome into the tibial plateau by making the following calculations found in Table 1 using a mean A-P tibial diameter of 57 mm, saw blade thickness of 1.3 mm, and assuming a simplified geometric shape of a cube with a lateral tibial plateau PTS of 8.7 degrees. Pythagoreans theorem was used to find posterior tibial resection depth while subtracting the effect of the native PTS. Recommended osteotome depth was calculated based upon a 57 mm A-P diameter and did not factor in the native PTS and added in an additional 1.7 mm of depth to ensure a larger margin of safety.

Posterior Tibial Slope (PTS)	Posterior Depth Solely Due to Saw Blade PTS	Total Lateral Tibial Plateau Posterior Resection with 8mm Guide Depth (mm)	Suggested Minimum Protective Osteotome Penetration Depth with 8mm Guide Depth (mm)	Total Lateral Tibial Plateau Posterior Resection with 9mm Guide Depth (mm)	Suggested Minimum Protective Osteotome Penetration Depth with 9mm Guide Depth (mm)	Total Lateral Tibial Plateau Posterior Resection with 10mm Guide Depth (mm)	Suggested Minimum Protective Osteotome Penetration Depth with 10mm Guide Depth (mm)
0	0.00	-0.58	-11.00	-1.58	-12.00	-2.58	-13.00
1	-0.99	-1.57	-12.00	-2.57	-13.00	-3.57	-14.00
2	-1.99	-2.57	-13.00	-3.57	-14.00	-4.57	-15.00
3	-2.99	-3.57	-14.00	-4.57	-15.00	-5.57	-16.00
4	-3.99	-4.57	-15.00	-5.57	-16.00	-6.57	-17.00
5	-4.99	-5.57	-16.00	-6.57	-17.00	-7.57	-18.00
6	-5.99	-6.57	-17.00	-7.57	-18.00	-8.57	-19.00
7	-7.00	-7.58	-18.00	-8.58	-19.00	-9.58	-20.00

Table 1. Geometric calculations based upon a mean A-P tibial diameter of 57 mm, saw blade thickness of 1.3 mm, and a mean native lateral plateau PTS of 8.7 degrees. Based upon use of an extramedullary tibia cutting guide set to cut based upon the highest point in the lateral tibial plateau and assumes no presence of pathology.

4.4. Results

In the control group, PCL damage was noted in 73% (22/30) of specimens. In the experimental group, where an osteotome was used for protection, PCL damage was found in 23% (7/30) specimens. The use of an osteotome to maintain a bone island was found to have an absolute risk reduction of 50% when compared to the control group which did not use an osteotome to protect the PCL.

4.5. Discussion

Using a randomized partially blinded study, we have shown the effectiveness of using an osteotome to protect the PCL during CR TKA. This technique preserves a small bone island for the tibial PCL footprint by preventing the saw blade from cutting in the anterior to posterior direction during tibial resection. It is an undemanding technique that requires little to no training and requires an additional minute in operative time to perform. This technique is not new and is relatively well known yet there are no studies showing the effectiveness of the technique to prevent PCL damage until now. Our results show that maintaining a bone island can have an absolute risk reduction of damaging the PCL by 50%. In addition, our study indicated the Y-shaped PCL retractor provides questionable protection to the PCL. Interestingly, in our study, 23% of the experimental group that used an osteotome for protection still had PCL damage. This suggests that 1 cm of osteotome penetration is not deep enough. With hindsight, we suggest that the osteotome be at least as deep as the estimated posterior tibial resection depth in Table 1 to reduce the risk of the blade passing underneath the osteotome. This may further reduce the incidence of iatrogenic PCL damage. Using this technique, surgeons may avoid damaging the PCL in most patients where standard technique has shown to be variably effective at preserving the PCL footprint and highly dependent upon the surgeon’s proficiency. In addition, the bone island technique has broad applicability from the senior joint surgeon down to the novice resident looking to be adept at performing a CR TKA with adequate preservation of the PCL.

Damaging the PCL during tibial resection is largely dependent upon the experience of the surgeon, anatomy, and geometry of the cut that is performed. The posterior tibial slope and initial resection depth can greatly affect the end posterior tibial resection thickness and PCL fiber integrity.[20, 24, 26] The mean native PTS for the lateral tibial plateau is 8.7 degrees and medial tibial plateau is 8.2

degrees with an overall mean of 8.4 degrees and a range of -3 degrees to 16 degrees.[27] In addition, the medial plateau is concave in shape while the lateral plateau is convex in shape (Figures 2 and 3). As the native knee PTS increases, it decreases the overall posterior tibial resection depth. This is an important note to make when choosing resection parameters. A standard posterior tibial slope angle and resection depth does not truly exist for TKA. Parameter recommendations for tibial resection vary widely between implant manufacturers, implant design, and surgeon preference. Based purely from the average tibial morphology and pure geometry calculations, for every 1 degree of posterior slope increase during resection you get approximately 1 mm average increase in end posterior tibial resection thickness from the starting depth of the cut, assuming an average A-P tibial diameter of 57 mm. The average A-P distance from the anterior border of the tibia to the anterior most border of the PCL footprint is 41 mm, putting the footprint in the direct path of a bone saw blade.[28] As the A-P distance increases, with the target PTS set greater than 0, the deeper the posterior resection will become. The tibial PCL footprint has been reported to begin its proximal attachment from 0 mm to 3 mm deep to the articular surface and extending to its distal most attachment on tibia of up to 20 mm (Figures 1 and 2).[29, 30] In one cadaveric study, 68.8% of the PCL footprint was removed when performing a 9 mm tibial cut at 3 degrees of posterior tibial slope without use of a PCL protective technique.[21] In an MRI study, it was found that cutting the posterior tibial slope at 0 degrees reduced the PCL attachment by 45% in men and 46% in women without use of a PCL protective technique. When the slope was increased to 7 degrees, it increased the amount of PCL attachment loss in men to 69% and 67% in women without use of a PCL protective technique.[23] Although the amount of tolerable PCL damage that allows normal function and stability is unknown, we considered damage to the PCL footprint of greater than 20% to be relevant. Anecdotally, this 20% cut off is a conservative approximation, with the PCL likely to function with less than 80% integrity. Ochsner et al found that the PCL failed under physiological loads after an average of 8.6 mm of resected tibial bone, with most failures occurring in the 7-10 mm resection range.[31] One common limitation of many of the prior iatrogenic PCL injury studies is they are theoretical and do not involve actual bone cuts to test the hypothesis. An experienced surgeon is likely able to perform a tibial resection while maintaining a small bone island without the use of an osteotome by controlling the depth of saw blade penetration. However, many of the findings do suggest PCL injury during standard TKA tibial resection may be more common than once thought and places even more importance on techniques that preserve the PCL such as the one described in this study.

Figure 2 Lateral view of a right knee section in the sagittal plane at the midline of the tibia

Figure 3 Posterior to anterior view of the right knee

The importance of a competent PCL during CR TKA focuses on the ligament's debated ability to help drive a more physiological kinematic motion and aid in stability. An increased incidence of anteroposterior knee laxity and posterior instability have been reported in CR TKA as compared to PS designs.[32, 33] Prior evidence suggests these incidences have a connection to a compromised PCL footprint due to the surgical intervention itself.[19, 21, 23] This can present in patients as frank instability, persistent swelling, and/or anterior knee pain. However, Misra et al found results questioning the need for a competent PCL in the CR design all together when they found no difference in outcomes when retaining or resecting the PCL in CR designed knees.[17] Despite those results, it is unlikely that the PCL plays no role in kinematic control of the knee as found from a large cohort of literature.[8, 17, 18, 34, 35] Failure of the PCL in a CR TKA is rarely clearly reported in the literature, but typically leads to a revision surgery with a more constrained design if symptomatic.[32, 36] Revision surgery is not always necessary as not all patients are symptomatic and do not complain of instability with an incompetent PCL. Although this would require further study to confirm, we hypothesize that widespread use of the PCL bone island technique during CR TKA would reduce the incidence of instability and laxity.

There are several limitations to our study. This study replicated the worst-case scenario by using minimally trained medical students to perform the tibial resections. This was done to remove a situation in which a bone island was created by the skillful use of the bone saw and to remove surgeon bias. It also simulated a situation that is commonly found during orthopaedic surgical residency training whereby a novice resident is taught to perform a CR TKA. Bending of the saw blade may have also influenced the depth of cut and participants had varying levels of experience using a bone saw. The strengths of this study include a large sample size, in vitro tibial resections, and real world instruments being used.

4.6. Conclusion

The use of an osteotome to preserve the PCL during CR TKA by forming a bone island was found to be an effective means of protecting the PCL over the standard technique. Standard technique with the use of a Y-shaped PCL retractor was found to provide questionable protection to the PCL as 73% of the control group had at least 20% of the PCL damaged with only the use of the retractor. By implementing the simple method described from this study and following the recommended osteotome depth in Table 1, the incidence of iatrogenic PCL resection may be reduced. In addition, this method is hypothesized to reduce the incidence of instability and knee joint laxity after CR TKA.

4.7. References

1. Beaupre LA, Sharifi B, Johnston DW. A Randomized Clinical Trial Comparing Posterior Cruciate-Stabilizing vs Posterior Cruciate-Retaining Prostheses in Primary Total Knee Arthroplasty: 10-Year Follow-Up. *J Arthroplasty.* 2016.

2. Cates HE, Komistek RD, Mahfouz MR, Schmidt MA, Anderle M. In vivo comparison of knee kinematics for subjects having either a posterior stabilized or cruciate retaining high-flexion total knee arthroplasty. *J Arthroplasty.* 2008;23:1057-1067.

3. Gotz J, Beckmann J, Sperrer I, et al. Retrospective comparative study shows no significant difference in postural stability between cruciate-retaining (CR) and cruciate-substituting (PS) total knee implant systems. *Int Orthop.* 2016;40:1441-1446.

4. Hino K, Oonishi Y, Kutsuna T, et al. Preoperative varus-valgus kinematic pattern throughout flexion persists more strongly after cruciate-retaining than after posterior-stabilized total knee arthroplasty. *Knee.* 2016;23:637-641.

5. Hunt NC, Ghosh KM, Blain AP, Rushton SP, Longstaff LM, Deehan DJ. No statistically significant kinematic difference found between a cruciate-retaining and posterior-stabilised Triathlon knee arthroplasty: a laboratory study involving eight cadavers examining soft-tissue laxity. *Bone Joint J.* 2015;97-b:642-648.

6. Jiang C, Liu Z, Wang Y, Bian Y, Feng B, Weng X. Posterior Cruciate Ligament Retention versus Posterior Stabilization for Total Knee Arthroplasty: A Meta-Analysis. *PLoS One.* 2016;11:e0147865.

7. Verra WC, van den Boom LG, Jacobs W, Clement DJ, Wymenga AA, Nelissen RG. Retention versus sacrifice of the posterior cruciate ligament in total knee arthroplasty for treating osteoarthritis. *Cochrane Database Syst Rev.* 2013:CD004803.

8. Swanik CB, Lephart SM, Rubash HE. Proprioception, kinesthesia, and balance after total knee arthroplasty with cruciate-retaining and posterior stabilized prostheses. *J Bone Joint Surg Am.* 2004;86-a:328-334.

9. Singh G, Tan JH, Sng BY, Awiszus F, Lohmann CH, Nathan SS. Restoring the anatomical tibial slope and limb axis may maximise post-operative flexion in posterior-stabilised total knee replacements. *Bone Joint J.* 2013;95-B:1354-1358.

10. Peters CL, Mulkey P, Erickson J, Anderson MB, Pelt CE. Comparison of total knee arthroplasty with highly congruent anterior-stabilized bearings versus a cruciate-retaining design. *Clin Orthop Relat Res.* 2014;472:175-180.

11. Pereira DS, Jaffe FF, Ortiguera C. Posterior cruciate ligament-sparing versus posterior cruciate ligament-sacrificing arthroplasty. Functional results using the same prosthesis. *J Arthroplasty.* 1998;13:138-144.

12. Parsley BS, Conditt MA, Bertolusso R, Noble PC. Posterior cruciate ligament substitution is not essential for excellent postoperative outcomes in total knee arthroplasty. *J Arthroplasty.* 2006;21:127-131.

13. Maruyama S, Yoshiya S, Matsui N, Kuroda R, Kurosaka M. Functional comparison of posterior cruciate-retaining versus posterior stabilized total knee arthroplasty. *J Arthroplasty.* 2004;19:349-353.

14. Li N, Tan Y, Deng Y, Chen L. Posterior cruciate-retaining versus posterior stabilized total knee arthroplasty: a meta-analysis of randomized controlled trials. *Knee Surg Sports Traumatol Arthrosc.* 2014;22:556-564.

15. Jacobs WC, Clement DJ, Wymenga AB. Retention versus removal of the posterior cruciate ligament in total knee replacement: a systematic literature review within the Cochrane framework. *Acta Orthop.* 2005;76:757-768.

16. Clark CR, Rorabeck CH, MacDonald S, MacDonald D, Swafford J, Cleland D. Posterior-stabilized and cruciate-retaining total knee replacement: a randomized study. *Clin Orthop Relat Res.* 2001:208-212.

17. Misra AN, Hussain MR, Fiddian NJ, Newton G. The role of the posterior cruciate ligament in total knee replacement. *J Bone Joint Surg Br.* 2003;85:389-392.

18. Wright JO, Skelley NW, Schur RP, Castile RM, Lake SP, Brophy RH. Microstructural and Mechanical Properties of the Posterior Cruciate Ligament: A Comparison of the Anterolateral and Posteromedial Bundles. *J Bone Joint Surg Am.* 2016;98:1656-1664.

19. Shannon FJ, Cronin JJ, Cleary MS, Eustace SJ, O'Byrne JM. The posterior cruciate ligament-preserving total knee replacement: do we 'preserve' it? A radiological study. *J Bone Joint Surg Br.* 2007;89:766-771.

20. Cinotti G, Sessa P, Amato M, Ripani FR, Giannicola G. Preserving the PCL during the tibial cut in total knee arthroplasty. *Knee Surg Sports Traumatol Arthrosc.* 2015.

21. Feyen H, Van Opstal N, Bellemans J. Partial resection of the PCL insertion site during tibial preparation in cruciate-retaining TKA. *Knee Surg Sports Traumatol Arthrosc.* 2013;21:2674-2679.

22. Jawhar A, Wasnik S, Scharf HP, Roehl H. Fibula head is a useful landmark to predict the location of posterior cruciate ligament footprint prior to total knee arthroplasty. *Int Orthop.* 2014;38:267-272.

23. Matziolis G, Mehlhorn S, Schattat N, et al. How much of the PCL is really preserved during the tibial cut? *Knee Surg Sports Traumatol Arthrosc.* 2012;20:1083-1086.

24. Sessa P, Fioravanti G, Giannicola G, Cinotti G. The risk of sacrificing the PCL in cruciate retaining total knee arthroplasty and the relationship to the sagittal inclination of the tibial plateau. *Knee.* 2015;22:51-55.

25. Liabaud B, Patrick DA, Geller JA. Is the posterior cruciate ligament destabilized after the tibial cut in a cruciate retaining total knee replacement? An anatomical study. *Knee.* 2013;20:412-415.

26. Amis AA, Senavongse W, Bull AM. Patellofemoral kinematics during knee flexion-extension: an in vitro study. *J Orthop Res.* 2006;24:2201-2211.

27. de Boer JJ, Blankevoort L, Kingma I, Vorster W. In vitro study of inter-individual variation in posterior slope in the knee joint. *Clin Biomech (Bristol, Avon).* 2009;24:488-492.

28. Osti M, Tschann P, Kunzel KH, Benedetto KP. Anatomic characteristics and radiographic references of the anterolateral and posteromedial bundles of the posterior cruciate ligament. *Am J Sports Med.* 2012;40:1558-1563.

29. Lee YS, Ra HJ, Ahn JH, Ha JK, Kim JG. Posterior cruciate ligament tibial insertion anatomy and implications for tibial tunnel placement. *Arthroscopy.* 2011;27:182-187.

30. Greiner P, Magnussen RA, Lustig S, Demey G, Neyret P, Servien E. Computed tomography evaluation of the femoral and tibial attachments of the posterior cruciate ligament in vitro. *Knee Surg Sports Traumatol Arthrosc.* 2011;19:1876-1883.

31. Ochsner JL, McFarland G, Baffes GC, Cook SD. Posterior cruciate ligament avulsion in total knee arthroplasty. *Orthop Rev.* 1993;22:1121-1124.

32. Montgomery RL, Goodman SB, Csongradi J. Late rupture of the posterior cruciate ligament after total knee replacement. *Iowa Orthop J.* 1993;13:167-170.

33. Matsuda S, Miura H, Nagamine R, Urabe K, Matsunobu T, Iwamoto Y. Knee stability in posterior cruciate ligament retaining total knee arthroplasty. *Clin Orthop Relat Res.* 1999:169-173.

34. Conditt MA, Noble PC, Bertolusso R, Woody J, Parsley BS. The PCL significantly affects the functional outcome of total knee arthroplasty. *J Arthroplasty.* 2004;19:107-112.

35. Cabuk H, Kusku Cabuk F. Mechanoreceptors of the ligaments and tendons around the knee. *Clin Anat.* 2016;29:789-795.

36. Waslewski GL, Marson BM, Benjamin JB. Early, incapacitating instability of posterior cruciate ligament-retaining total knee arthroplasty. *J Arthroplasty.* 1998;13:763-767.

Chapter 5

Three-Dimensional Comparison of Fibular Motion After Syndesmosis Fixation Using Combined Suture-Button and Internal Brace Constructs

Addison Wood[1,2], Arshad Seyed[1], Hannah Kim[2], Donald Stewart[3],

From the [1]Department of Structural Anatomy and Rehabilitative Science,

University of North Texas Health Science Center, Fort Worth, Texas;

[2]John Peter Smith Hospital, Fort Worth, Texas

[3]Arlington Orthopedic Associates, Mansfield, Texas

5.1. Introduction

Syndesmosis injuries are common with up to 25% of all ankle injuries being reported to involve an associated syndesmosis injury.[1-3] These injuries are even more common in athletic patient populations with an incidence reported up to 25% in specific sports.[2, 3] The ankle syndesmosis ligaments prevent diastasis of the syndesmosis and contribute some stability to the ankle joint as a whole through mortise stability. The ligaments of that comprise the syndesmosis are the anterior-inferior tibiofibular ligament (AITFL), interosseous ligament (IOL), posterior-inferior tibiofibular ligament (PITFL), and the inferior transverse ligament (ITL). The diagnosis and treatment of syndesmosis injuries are typically focused on the AITFL and PITFL as they have repeatedly been found to be the major contributors to syndesmosis integrity.[4-9]

Management of syndesmosis injuries historically involves treatment with either nonoperative stabilization or screw constructs as both treatments provide good results.[10] However, these traditional methods of treatment do have major deficiencies. Non operative management and screw fixation can both leave a patient non weight bearing for as long as 6-12 weeks in most protocols.[10] Additionally, syndesmotic screws frequently need removal and in some cases have been found to be a source of improved patient outcomes once the screw breaks or is removed.[11, 12] Therefore, current advances in syndesmosis fixation have focused on expediting the return of patients back to function and improving patient outcomes with fixation. These advances are largely driven by sports focused surgeons and researchers looking to return eager athletes to full play earlier. This has led to the evolution of syndesmosis fixation ideology to take aim at achieving physiologic motion and stability. It is theorized that restoration of stability and motion to the native state would promote an environment optimal for ligamentous healing and faster return to play. Suture-button constructs were created with this in mind, but they have not quite proven to be the fixation construct that achieves physiologic stability and motion.[13-16]

The purpose of this study was to evaluate the ability of an internal brace to add sagittal plane translational and transverse plane rotational constraint to suture-button constructs. It was hypothesized that the internal brace oriented in parallel with the fibers of an injured AITFL in addition to a suture-button construct would achieve physiological motion and stability at the syndesmosis through increased rotational and translational constraint of the fibula.

5.2. Materials Methods

Specimen Preparation and Testing Apparatus

15 all male fresh frozen cadaveric specimens were obtained and resected at the tibial plateau. There were 4 specimens that failed to complete the protocol due to early fracture of the fibular and 3 specimens failed to complete the last phase of testing due to late fracture of the fibula. There were 11 total specimens that adequately completed the protocol up to the last phase and were included in this study (mean age 59, range 48-65). We were unable to make statistical comparisons to the internal brace alone state due to specimen loss and it was therefore excluded from this study. Specimens had no known prior surgical history of lower extremity surgery, ankle injury, gross deformity, confounding pathology, and were screened for any prior surgical scars. All soft tissues were left intact prior to a lateral Kocher approach with care being taken to ensure all muscles, tendons, and ligaments were left intact. The ankle flexor retinaculum was released and the extensor digitorum longus was retracted medially to allow full visualization of the AITFL. The foot was then aligned and secured to a circular footboard via 4x 3-inch-long screws. The specimen was then mounted into a custom-made ankle rig that keeps the tibia rigid via 4-5x half pins while maintaining free fibular movement (Figure. 1). The lateral malleolus was prepared by minimal periosteal scrapping, without ligamentous damage, to allow attachment of a tracking sensor via nylon screws. The medial malleolus was also prepared in the same manner by window resection through soft tissue allowing sensor placement. A custom-made control arm stabilized ankle position through a bearing joint rigidly attached to the footboard. This control arm-bearing connection allowed control of ankle position with 6 degrees of freedom and when locked only allowed internal/external rotation of the ankle in the transverse plane. At the end of the spindle a third tracking sensor was placed to act as a goniometer for ankle positioning. In addition, a torque

sensor (TRT-200, Transducer Techniques, Temecula CA,) was embedded in the spindle-footboard-bearing apparatus to allow torque recording during stress examination. Due to the design of the control arm mechanism, this torque sensor was limited to record internal/external force applied through a controlled, known moment arm by the examiner. For all three-dimensional data recording a 3-sensor motion capture unit was used with known positional resolution of $5e^{-5}$ inches, orientation resolution of $4e^{-4}$ degrees, static positional accuracy of .76 mm RMS, and static orientation accuracy of .15 degrees RMS (Liberty EM Tracking System; Polhemus, Colchester, VT). An ultrasound unit was used to dynamically record and monitor tibiofibular clear space measurements 1 cm proximal from the tibial plafond (GE Venue 40, 4-13 MHz probe). Ultrasound videos were separated into images every .5 seconds and clear space measurements were made using Image J software (NIH, Bethesda, MD) and calibrated using the onscreen ruler. Tibiofibular clear space measurements were made by three independent examiners for each image up to the peak of torque at 10 Nm which signaled the end of the trial. Ultrasound gel was used to fill any empty spaces between structures and the skin draped over the AITFL area prior to probe use. Prior to testing, each ankle was stressed through 10 cycles of maximal range of motion in each degree of freedom to reduce error.

Protocol and Operative Technique

All measurements throughout protocol phases were repeated 3 times to establish a mean for each state. The ankle was held fixed with 10 degrees of dorsiflexion and all other orientations in neutral except for internal/external rotation which was allowed freedom of movement. The ankle had simultaneous recording of ultrasound video, 3D kinematics, and torque as the ankle was stressed by an examiner. The examiner applied a gradually increasing external rotational force to the footboard over a 10 second period until 10 Nm was reached. This was first performed on the intact ankle state and repeated for the injured state and the 5 different fixation constructs. For the injured state, the AITFL was sectioned first followed by section of the IOL 5 cm proximal to the proximal most point of the AITFL fibers with additional freeing of soft tissue within the incisura in this same area. The PITFL and ITL were left undisturbed. Fixation constructs were implemented in a stepwise manner in order with examination after each step. Prior to resecting the AITFL and IOL a k-wire was driven through the lateral cortex of the fibula into the tibia to ensure reduction of the syndesmosis between each step. During all implant placement reduction clamps were used and the ankle held in 10 degrees of dorsiflexion. The single suture-button construct was placed at 2 cm proximal to the tibial plafond following standard technique and angled 30 degrees to the frontal plane (Knotless Tightrope; Arthrex, Naples, FL).[17] The two suture-button construct was implemented with 15 degrees of divergence 1cm proximal to the first. The combined internal brace and suture-button construct then followed with placement of the suture anchors and fiber tape as per manufacturers technique guide with slight modification as detailed below (Internal Brace; Arthrex, Naples, FL). The internal brace was aligned in parallel with the AITFL fibers and anchors securely positioned at the middle of the tibial and fibular AITFL attachment sites. During tightening the manufacturers laser line was used to mark the fiber tape tensioning with one modification. The eyelet of the anchor driver was justified to one side of the marking for slightly increased tension over standard manufacturers technique. The specimen then underwent stress examination with the internal brace and two suture-buttons in place. Afterward, the removal of the proximal most tightrope was performed, followed by removal of the last tightrope, with examination after each removal.

Data Collection and Analysis

Results were analyzed initially using descriptive statistics. The maximum value during a trial was determined and a database was formed that underwent a Log10 transformation to lessen the effect of potential outliers and to normalize data. Significant differences were determined by one way repeated measures ANOVA with a post hoc TUKEY test to determine changes from the native fibular motion as compared to the stepwise addition of implant restraint. Kinematics, torque, and ultrasound data were recorded at every step of the experiment. Main outcome measures recorded were internal/external rotation, anterior/posterior translation, mediolateral translations of the fibula with relation to the tibia. The native fibula motion is considered physiologic and acts as the control for all comparisons made in the study.

5.3. Results

External Fibular Rotation

At 10 Nm of external rotational stress all ankle states were found to be significantly different than the intact state with external fibular rotation. Only the internal brace + 2x suture button and internal brace + 1x suture-button constructs were found to be significantly different than the injured state (p=.0003, p=.002). Mean external rotation: intact state (1.27 degrees), injured state (2.87 degrees), 1x suture-button (2.5 degrees), 2x suture-buttons (2.46 degrees), internal brace + 2x suture-buttons (1.82 degrees), internal brace + 1x suture-button (2.09 degrees) (Figure 1).

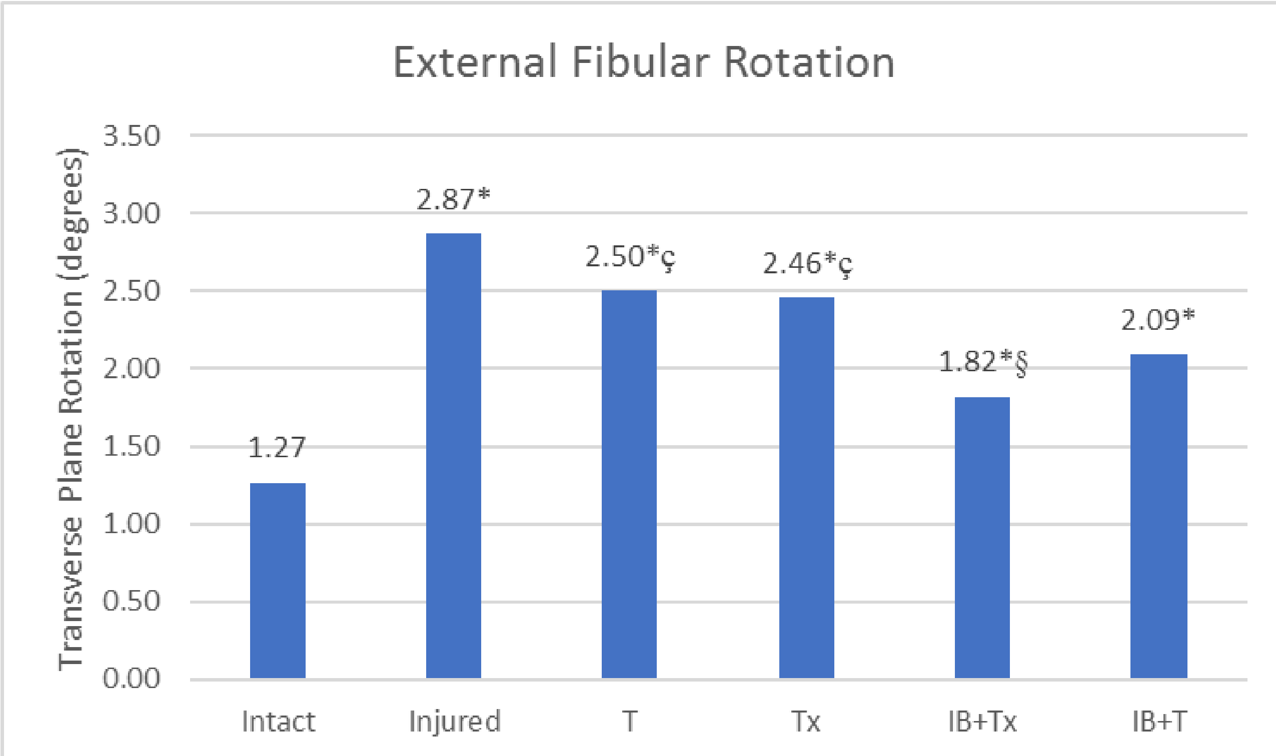

Figure 1. 3D Motion Tracking Data at 10 Nm of External Rotational Torque. 1x Suture-Button (T); 2x Suture-Button (Tx); 2x Suture-Buttons and Internal Brace (IB+Tx); 1x Suture-Button and Internal Brace (IB+T). (*P Value < .05 as Compared to Intact State; §P Value < .05 as Compared to Suture-Button Constructs; çP Value > .05 as Compared to Injured State)

Anterior to Posterior Fibular Translation

At 10 Nm of external rotational stress all ankle states were found to be significantly different than the intact state with anterior to posterior translation. All fixation constructs were significantly different than the injured state except for the single suture-button construct. Mean anterior to posterior translation: intact state (2.93 mm), injured state (6.27 mm), 1x suture-button (5.66 mm), 2x suture-buttons (4.88 mm), internal brace + 2x suture-buttons (4.85 mm), internal brace + 1x suture-button (5.09 mm) (Figure 2).

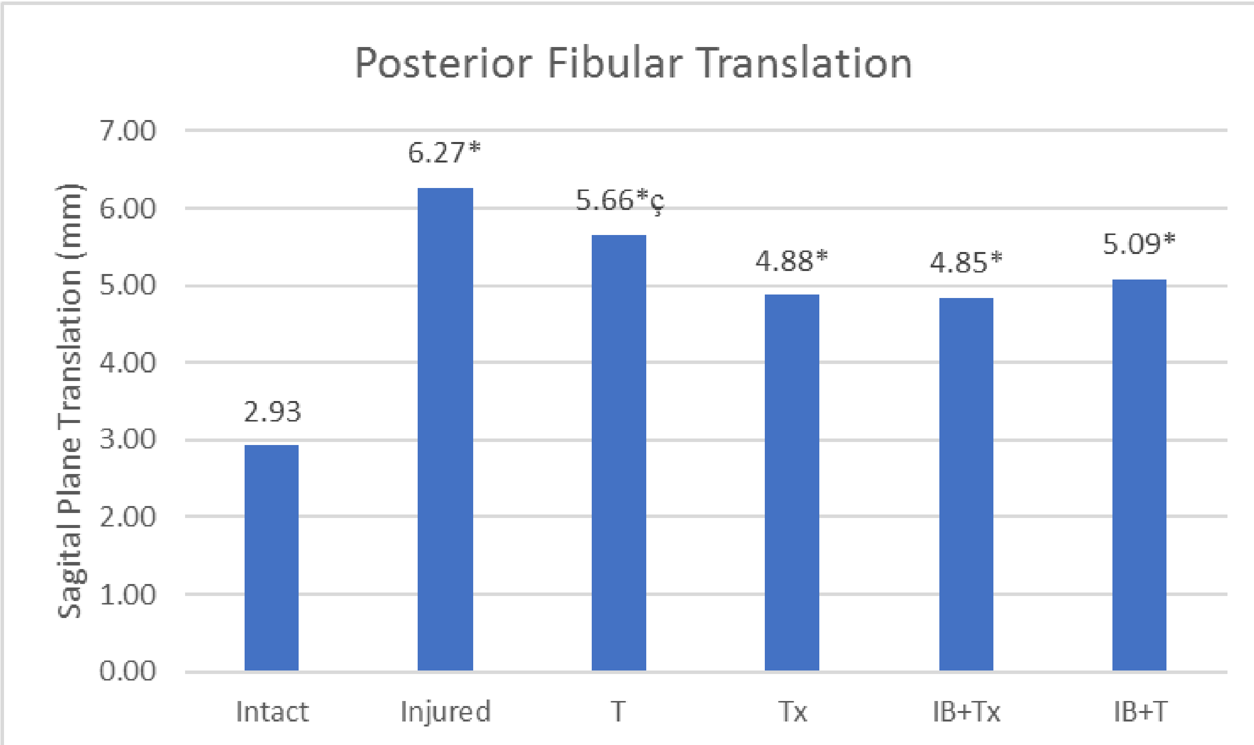

Figure 2. 3D Motion Tracking Data at 10 Nm of External Rotational Torque. 1x Suture-Button (T); 2x Suture-Button (Tx); 2x Suture-Buttons and Internal Brace (IB+Tx); 1x Suture-Button and Internal Brace (IB+T). (*P Value < .05 as Compared to Intact State; çP Value > .05 as Compared to Injured State)

Lateral Fibular translation

At 10 Nm of external rotational stress, all ankle states except one were not found to be different than the injured state with lateral fibular translation. Only the internal brace+ 2x suture button construct was found to be significantly different than the injured state (p=.028). Mean lateral fibular translation: intact state (2.1 mm), injured state (2.3 mm), 1x suture-button (2.2 mm), 2x suture-buttons (1.76 mm), internal brace + 2x suture-buttons (1.5 mm), internal brace + 1x suture-button (2.2 mm) (Figure 3).

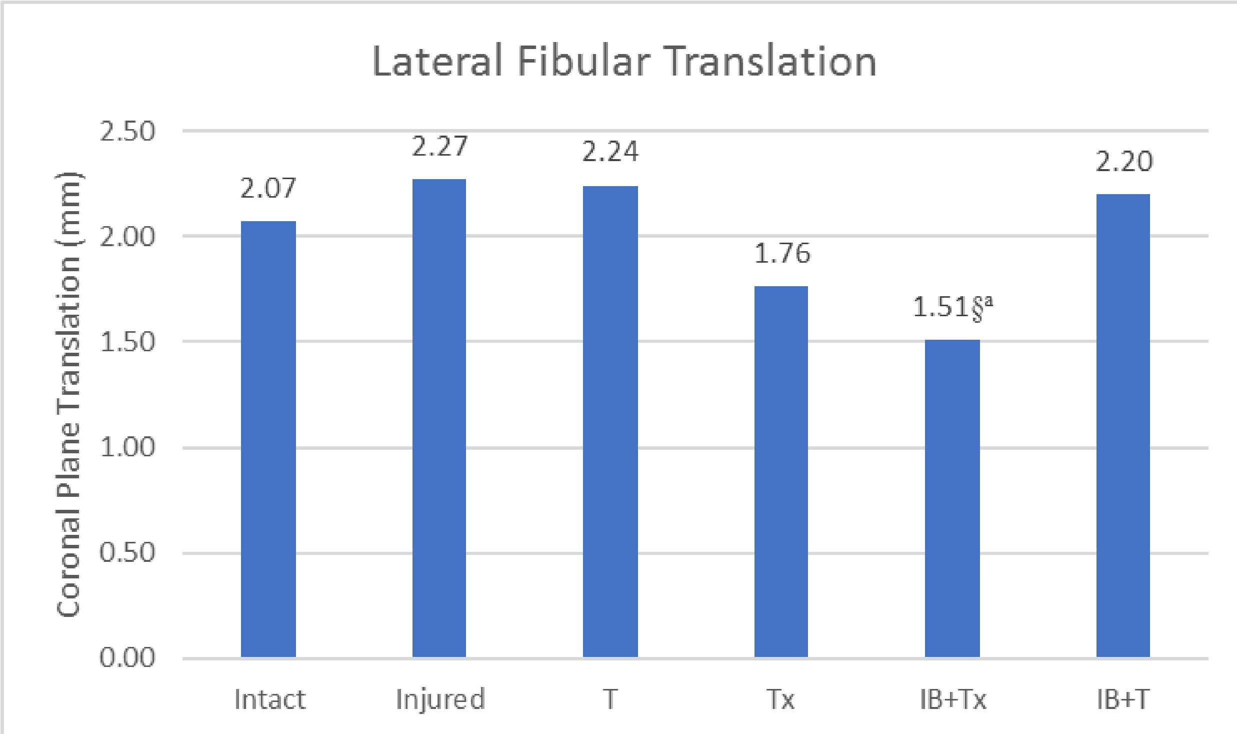

Figure 3. 3D Motion Tracking Data at 10 Nm of External Rotational Torque. 1x Suture-Button (T); 2x Suture-Button (Tx); 2x Suture-Buttons and Internal Brace (IB+Tx); 1x Suture-Button and Internal Brace (IB+T). (*P Value < .05 as Compared to Intact State; §P Value < .05 as Compared to Suture-Button Constructs; [a]P Value < .05 as Compared to Injured State)

Fibular Valgus Rotation

At 10 Nm of external rotational stress, all ankle states were found to be significantly different than the intact and injured states with fibular valgus rotation. Mean valgus rotation: intact state (1.0 degrees), injured state (2.6 degrees), 1x suture-button (1.8 degrees), 2x suture-buttons (1.8 degrees), internal brace + 2x suture-buttons (1.6 degrees), internal brace + 1x suture-button (1.7 degrees) (Figure 4).

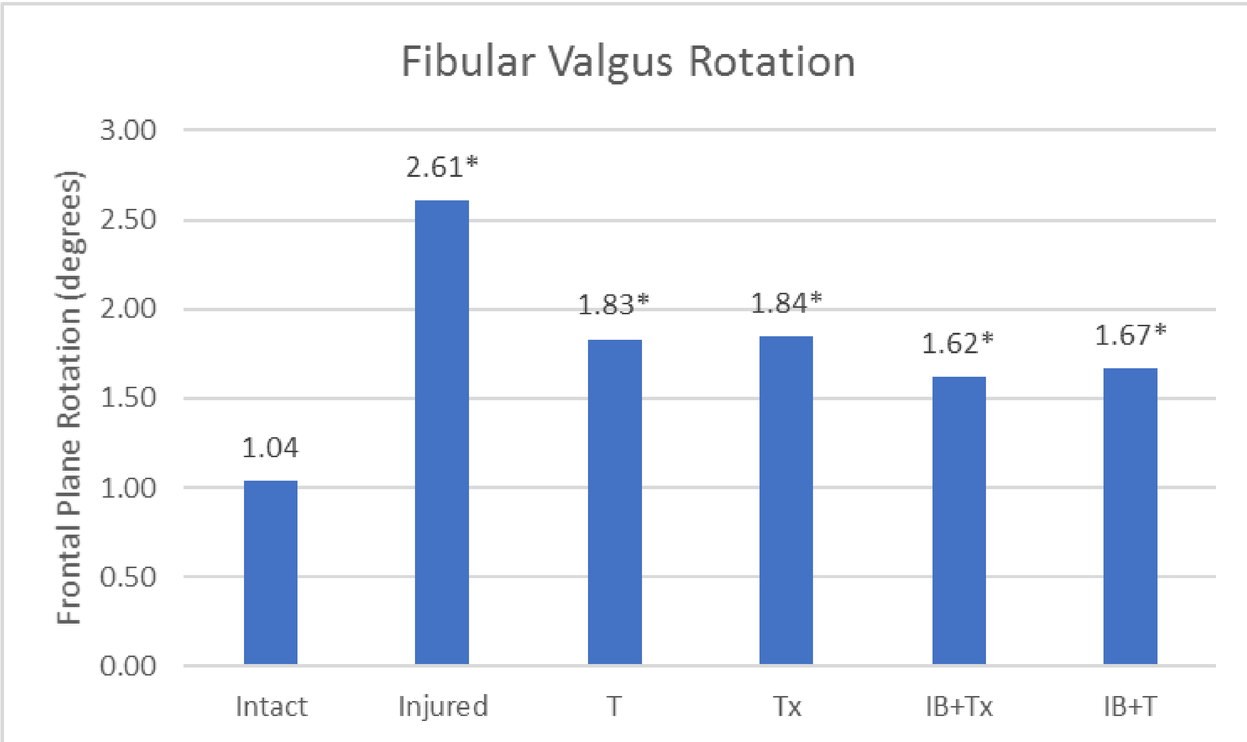

Figure 4. 3D Motion Tracking Data at 10 Nm of External Rotational Torque. 1x Suture-Button (T); 2x Suture-Button (Tx); 2x Suture-Buttons and Internal Brace (IB+Tx); 1x Suture-Button and Internal Brace (IB+T). (*P Value < .05 as Compared to Intact State)

Fibular Flexion Rotation

At 10 Nm of external rotational stress, all ankle states were found to be significantly different than the intact state with fibular flexion rotation. Both the 1x suture-button or the 2x suture-button were not found to be significantly different than the injured state (p=.99, p=.99). Mean flexion rotation: intact state (1.9 degrees), injured state (5.1 degrees), 1x suture-button-T (4.9 degrees), 2x suture-buttons (4.9 degrees), internal brace + 2x suture-buttons (4.1 degrees), internal brace + 1x suture-button (4.0 degrees) (Figure 5).

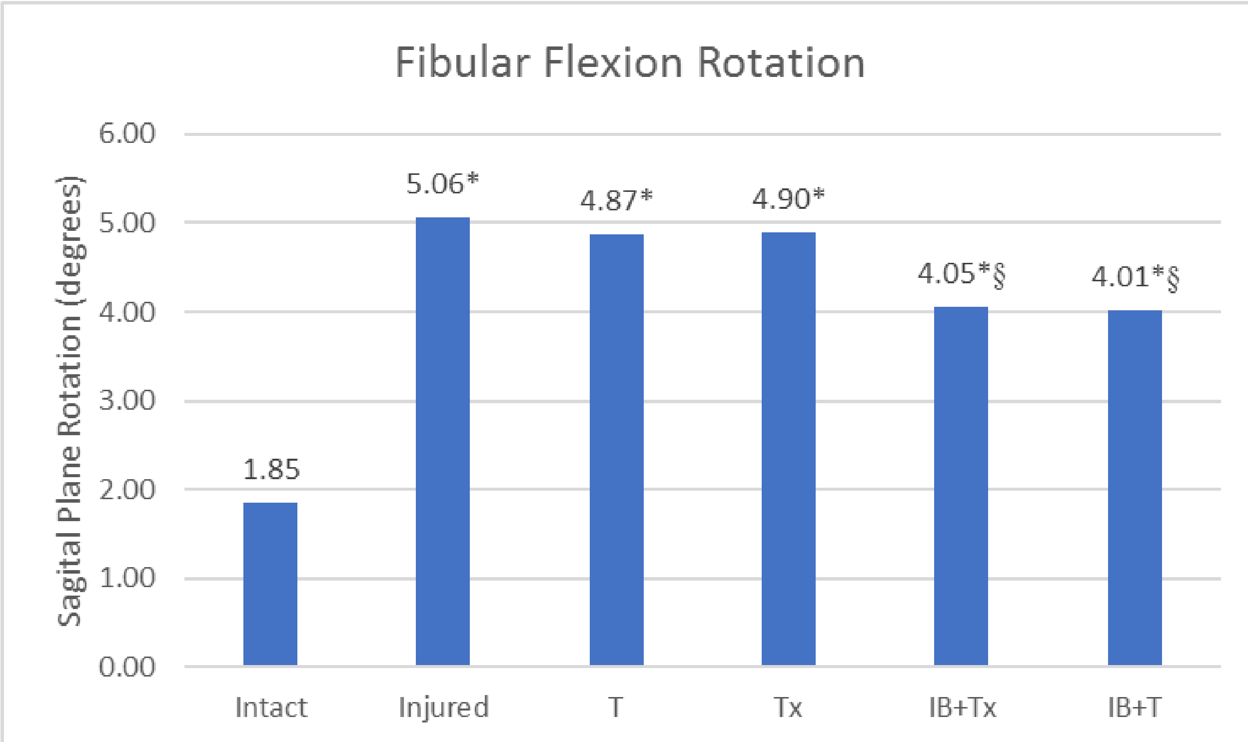

Figure 5. 3D Motion Tracking Data at 10 Nm of External Rotational Torque. 1x Suture-Button (T); 2x Suture-Button (Tx); 2x Suture-Buttons and Internal Brace (IB+Tx); 1x Suture-Button and Internal Brace (IB+T). (*P Value < .05 as Compared to Intact State; §P Value < .05 as Compared to Suture-Button Construct)

Proximal Fibular Translation

At 10 Nm of external rotational stress, all ankle states except repairs that included internal braces were not found to be different than the intact state with proximal fibular translation. Only the constructs that included the internal brace were found to be significantly different than the intact state (p=.03, p=.03). Mean proximal fibular translation: intact state (1.6 mm), injured state (2.1 mm), 1x suture-button (2.2 mm), 2x suture-buttons (2.0 mm), internal brace + 2x suture-buttons (2.3 mm), internal brace + 1x suture-button (2.3 mm) (Figure 6).

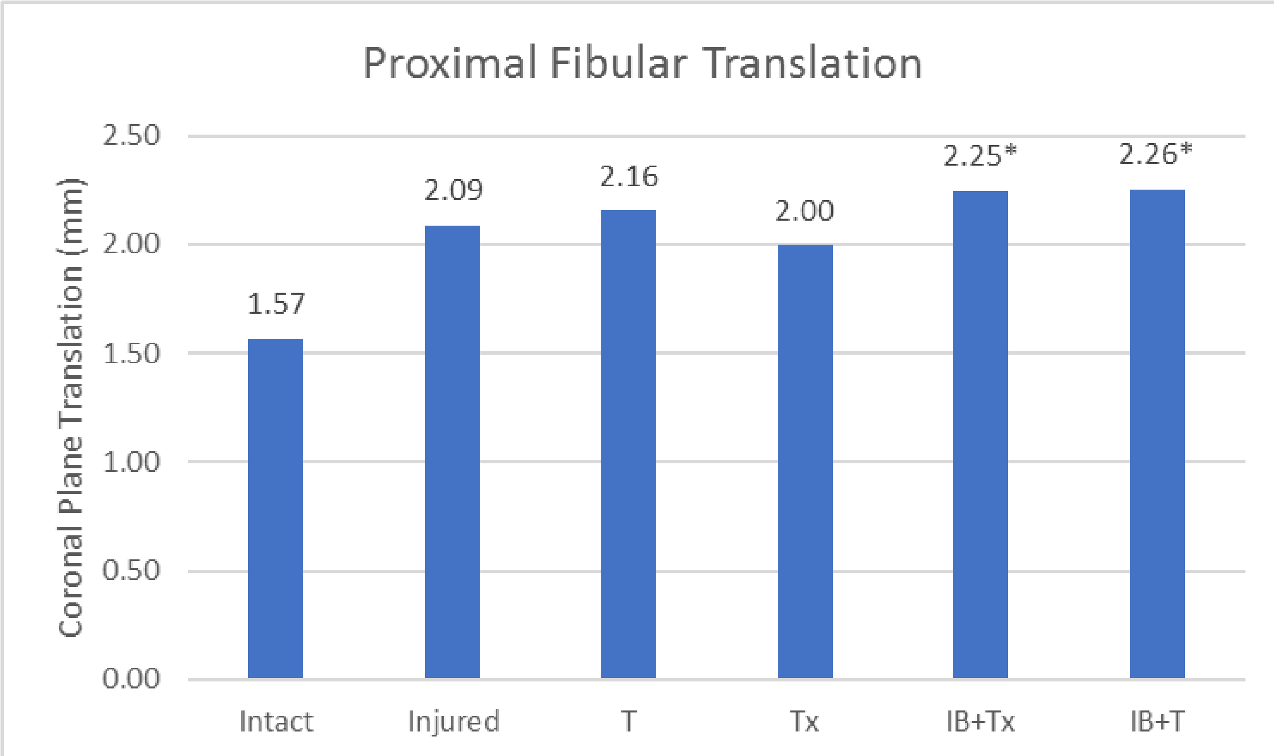

Figure 6. 3D Motion Tracking Data at 10 Nm of External Rotational Torque. 1x Suture-Button (T); 2x Suture-Button (Tx); 2x Suture-Buttons and Internal Brace (IB+Tx); 1x Suture-Button and Internal Brace (IB+T). (*P Value < .05 as Compared to Intact State)

Tibiofibular Clear Space

At 10 Nm of external rotational stress, Only the 2x suture-button and internal brace + 2x suture-button constructs were statistically different than the injured state. the internal brace + 2x suture-button construct came the closest to fully reducing the tibiofibular joint under 6 mm and was not significantly different than the intact state. Mean tibiofibular clear space: intact state (5.0 mm), injured state (8.6 mm), 1x suture-button (7.6 mm), 2x suture-buttons (6.8 mm), internal brace + 2x suture-buttons (6.3 mm), internal brace + 1x suture-button (7.2 mm) (Figure 7).

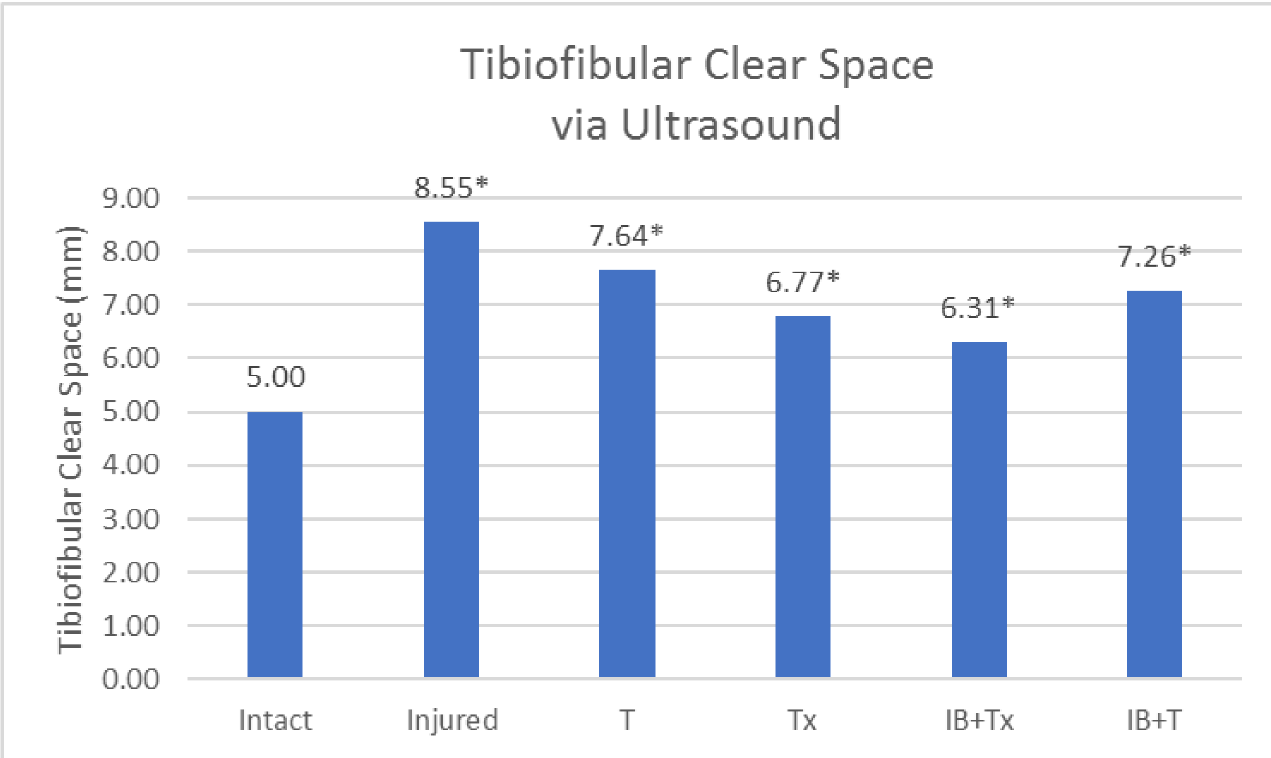

Figure 7. Ultrasound measurements of the tibiofibular clear space at 10 Nm of external rotational torque. (*P Value < .05 as Compared to Intact State)

Tukey Homogenous Groups			
	1	2	3
Injured		***	
T	***	***	
Tx	***		***
IB+Tx			***
IB+T	***	***	***

Figure 8. Tukey's Homogenous Groups of Ultrasound Measurements of the Tibiofibular Clear Space at 10 Nm of External Rotational Torque. (*** in the same column indicates homogeneity)

5.4. Discussion

Often science and medicine attempt to mimic nature for advancement due to its incredible effectiveness and efficiency. Ankle syndesmosis repair is no different, structure should be returned to restore function. Recently, Clanton et al investigated individual syndesmosis ligament contributions to stability and found the AITFL and PITFL to be significant contributors to fibular external and internal rotational restraint respectively.[18] Biomechanical evidence has shown increased and shifted tibiotalar contact pressures with increased fibular movement from syndesmosis injuries; which may lead to higher rates of osteoarthritis and ankle instability without treatment.[6, 19, 20] In addition, decreased syndesmosis motion was shown to predict poorer patient outcomes.[11, 12, 21, 22] This potentially permits a theoretical sweet spot that is neither too loose nor too rigid. This "sweet spot" is likely to be equivalent to physiological motion at the syndesmosis.

Development of syndesmosis treatment modalities has progressed from simple non-operative management for mild injuries to more rigid traditional cortical screw constructs to the most recent and less rigid suture-button implants. LaMothe et al compared screw and suture button fixation constructs and found screw fixation to be more rigid than native anatomy and suture-button techniques in translation and rotation.[15] The suture-button construct directs treatment towards restoring physiological motion and stability at the tibiofibular joint instead of absolute rigidity. This is thought to foster a soft tissue environment amenable to healing and expedited return to function.[8, 23, 24] However, evidence has shown the suture-button constructs to have increased external fibular rotation and increased posterior translation of the fibula than both the native ankle and screw constructs.[13, 15] Conceptually, the AITFL, PITFL, and suture-button constructs confer greatest constraint in parallel with their fiber orientation. This is a basic biomechanical concept and was situationally proven to be true with the syndesmosis by LaMothe et al and Clanton et al.[13, [15, 18] Suture-button constructs should then lend one to expect sagittal plane translational laxity and transverse plane rotational laxity as the suture orientation does not match the ligamentous fiber deficit with AITFL and PITFL injuries. These ligament injuries have become the new target for implants like the internal brace. The internal brace is a tension type restraint implant that is capable of being oriented in parallel with a damaged AITFL via suture anchors and suture. In theory, a combined internal brace and suture-button construct recreates anatomical restraints found at the syndesmosis to support restoration of physiological motion. Schottel et al provided evidence for this theory by finding increased rotational stability with repair of tibiofibular ligament tears as compared to screw fixation.[24] In essence, internal brace implants augment native tibiofibular ligaments in a synthetic manner similar to ligament repair.

The current study supports the addition of an internal brace to augment the ability of suture-button constructs as a mechanism to increase external rotational constraint of the fibula. This study also supports prior findings suggesting 1 and 2 suture-button constructs show minimal improvement in posterior translational and external rotational fibular constraint as compared to the injured state.[13, 15] This is of no surprise as the suture-button only construct is in excellent orientation to control lateral translational forces, but not force vectors that fall perpendicular to the suture trajectory. The combined suture-button and internal brace constructs had a statistically significant reduction in fibular external rotation while the suture-button only constructs were found to be no different than the injured state. In addition, the internal brace alone did not constrain posterior translation of the fibula to a physiological level (Figure 1). These findings demonstrate the importance of aligning tensile fixation implants in parallel to the force vectors in which they are expected to act. This data also highlights the importance of implant choice and alignment when striving to restore physiologic motion through mimicry of native structure via fixation. The suture-button implants mainly restore functionality similar to the IOL by maintaining fibular contact in the incisura and the internal brace acts in place of an AITFL to constrain rotation. The two of these constructs together come closer to restoring true physiological motion at the syndesmosis than all other constructs in our study. Our data also demonstrates the optimal construct seems to include 2x suture-buttons and the internal brace combined rather than a single tightrope-internal brace combination. This is likely due to the additive effect of rigidity, but we cannot rule out the effect of suture-button divergence as our study failed to corroborate increased rotational restraint with the inclusion of a divergent second suture-button due to study design. However, the 1 and 2 suture-button constructs did improve tibiofibular clear space measurements on ultrasound (Figures 7, 8C, 8D). The internal brace alone and in combination with one suture-button showed minor improvement in tibiofibular clear space (Figures 7, 8F).

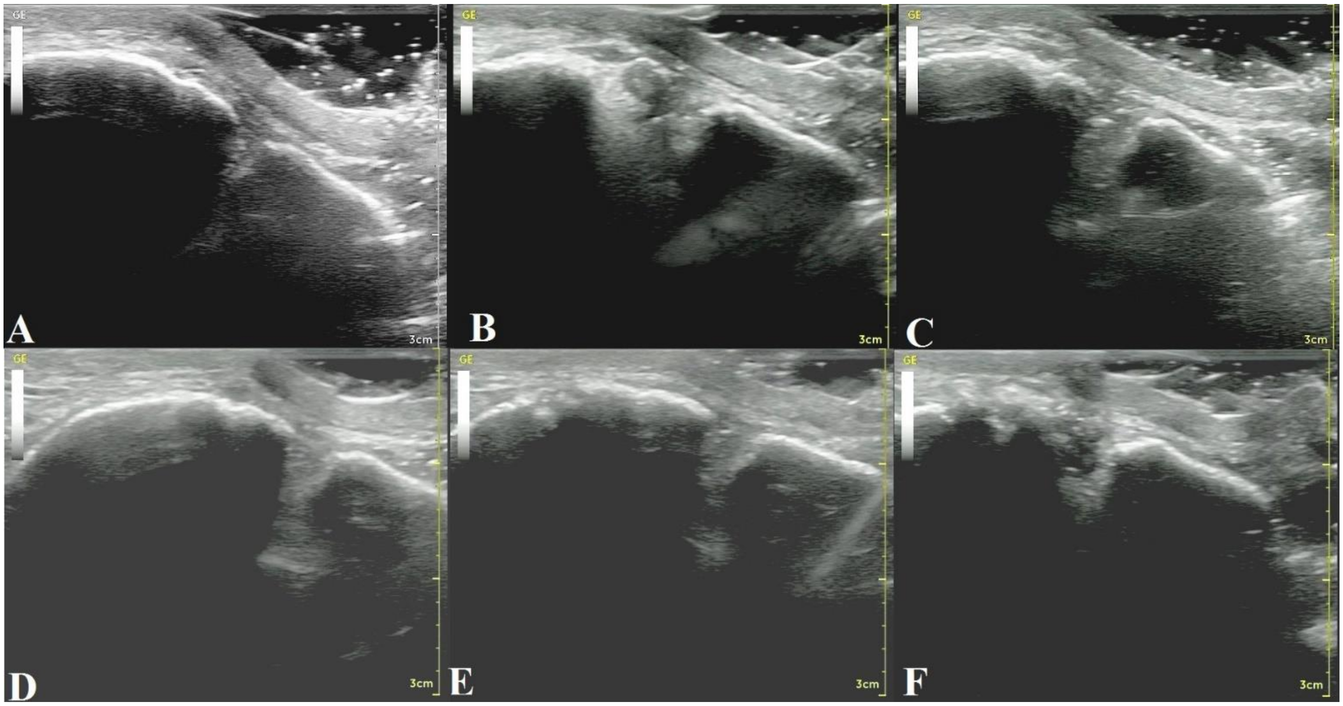

Figure 8. Ultrasound imaging of the tibiofibular clear space at 10 Nm of external rotational torque. [A]- Intact state; [B]- Injured state; [C]- 1x suture-button (T); [D]- 2x suture-button (Tx); [E]- 2x suture-button and internal brace (IB+Tx); [F]- 1x suture-button and internal brace (IB+T)

Upon analysis, our data indicates the addition of the internal brace to suture-button constructs does add statistically significant reductions in fibular flexion, lateral translation, external rotation, and posterior translation over suture-button only constructs (Figures 1-6). We can conclude that these two implants benefit each other in a mutually dependent mechanism that requires both suture-button and internal brace implants to achieve more physiologic stability. This can be explained by the surface anatomy of the fibular incisura as the fibula externally rotates and flexes it opens the anterior incisura and allows the fibula to translate posteriorly more freely. To counteract this effect, the suture-button acts to constrain lateral translation to maintain incisura joint surface congruence while the internal brace prevents rotations and anterior gaping. These findings can be further explained biomechanically by the resultant vector formed from the suture-button and internal brace restraints to posterior translation and external rotation. In addition, the combination of suture-button and internal brace showed excellent tibiofibular clear space reduction Figure 7. Clearly, the combined suture-button and internal brace construct provides an anatomically similar reconstruction of constraints found in the native ankle.

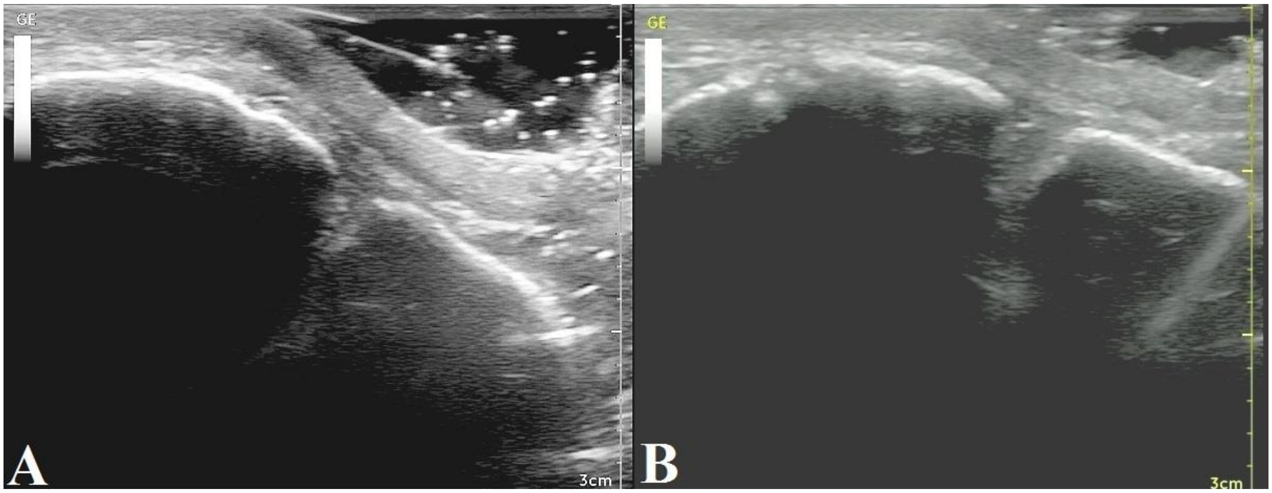

Figure 9. Ultrasound image of tibiofibular clear space at 10 Nm. [A]- Intact state; [B]- Internal brace.

The current study findings are new, but are also supported by the litany of syndesmosis literature when viewed as a whole.[8, 13, 15, 18, 23, 24] LaMothe et al described the inability of the suture-button only construct to restrain posterior translation and external rotation of the fibula, but did show evidence for excellent reduction and lateral translational constraint with the construct.[15] This aligns well with prior literature on the topic of suture-button orientation influencing restraint potential.[4, 8, 13-16, 23] Teramoto et al described these effects well and found aligning the suture-button in a more paralleled position to posterior fibular translation allowed greater reduction in posterior motion. However, this technique was described as clinically unrealistic due to proximity of the peroneal tendons and nerves.[16] The internal brace avoids this issue as it is on the anterior surface of the tibia and fibula, but still addresses the correct constraint trajectory. Clanton et al demonstrated both screw and suture-button constructs resulted in significant torsional stability improvement, but both failed to restore native syndesmosis kinematics.[13] These findings are supported by several similar studies, but none have examined the augmentation of AITFL function with an internal brace.[8, 9, 11, 13-16, 21, 23, 24] We hypothesize that changing the orientation of the internal brace to be more perpendicular to the long axis of the tibia may further rein in excess posterior fibular translation in the combined internal brace suture-button construct and will likely be a topic for future research.

There are multiple factors contributing to the limitations of the current study. There were no direct comparisons made to screw fixation or other constructs. The only comparisons made were to the native ankle, injured ankle, and the different combinations of suture-button and internal brace constructs. Not all the different variations in injury patterns and fixation constructs were examined. Therefore, limiting the ability of this study to make generalized statements on fixation. Additionally, the use of cadaveric material in an in vitro simulator does fully represent the in vivo condition. The simulation used in this study focused on the external rotational stress test and did not involve axial load, physiological maneuvers, or cyclic loading. However, this is a common occurrence for in vitro syndesmosis studies and our study model is similar to prior models used.[13, 15, 16, 18] Cadaveric material does not consider biologic healing or the postoperative effects of the surgery. The study was also limited by the age and sex of the cadaveric specimens used. Specimens were all male to reduce the occurrence of fragility fracture during experimentation by avoiding osteoporosis and were older than the prototypical demographics of this injury pattern, but enabled the use of larger amounts of torque up to 10 Nm in our protocol. The clinical implications of the biomechanical data presented herein are unknown and would require prospective studies to evaluate outcomes.

5.5. Conclusion

Overall, the most important finding of this study was the addition of an internal brace to suture-button constructs provided a mechanism to increase external rotational constraint of the fibula. In addition, neither the internal brace or the suture-button constructs independently contributed much posterior translational restraint to the fibula. This was by way of a mutually dependent mechanism with suture-button and internal brace implants. When the internal brace and suture-button constructs were found together they did restrain more translation and rotation than alone. This resulted in a more physiologically stable and mobile syndesmosis than by suture-button construct alone. Furthermore, this study provides a mechanistic understanding of how the combined suture-button and internal brace construct provides an anatomically similar reconstruction of constraints found in the native ankle. However, none of the constructs examined in this study could fully restore physiologic motion, therefore, refuting our initial hypothesis.

5.6. References

1. Gerber JP, Williams GN, Scoville CR, Arciero RA, Taylor DC. Persistent disability associated with ankle sprains: a prospective examination of an athletic population. *Foot Ankle Int.* 1998;19:653-660.

2. Hunt KJ, George E, Harris AH, Dragoo JL. Epidemiology of syndesmosis injuries in intercollegiate football: incidence and risk factors from National Collegiate Athletic Association injury surveillance system data from 2004-2005 to 2008-2009. *Clin J Sport Med.* 2013;23:278-282.

3. Waterman BR, Belmont PJ, Jr., Cameron KL, Svoboda SJ, Alitz CJ, Owens BD. Risk factors for syndesmotic and medial ankle sprain: role of sex, sport, and level of competition. *Am J Sports Med.* 2011;39:992-998.

4. McCullough CJ, Burge PD. Rotatory stability of the load-bearing ankle. An experimental study. *J Bone Joint Surg Br.* 1980;62-b:460-464.

5. Ogilvie-Harris DJ, Reed SC, Hedman TP. Disruption of the ankle syndesmosis: biomechanical study of the ligamentous restraints. *Arthroscopy.* 1994;10:558-560.

6. Ramsey PL, Hamilton W. Changes in tibiotalar area of contact caused by lateral talar shift. *J Bone Joint Surg Am.* 1976;58:356-357.

7. Rasmussen O. Stability of the ankle joint. Analysis of the function and traumatology of the ankle ligaments. *Acta Orthop Scand Suppl.* 1985;211:1-75.

8. Scranton PE, Jr., McMaster JG, Kelly E. Dynamic fibular function: a new concept. *Clin Orthop Relat Res.* 1976:76-81.

9. Xenos JS, Hopkinson WJ, Mulligan ME, Olson EJ, Popovic NA. The tibiofibular syndesmosis. Evaluation of the ligamentous structures, methods of fixation, and radiographic assessment. *J Bone Joint Surg Am.* 1995;77:847-856.

10. Van Heest TJ, Lafferty PM. Injuries to the ankle syndesmosis. *J Bone Joint Surg Am.* 2014;96:603-613.

11. Manjoo A, Sanders DW, Tieszer C, MacLeod MD. Functional and radiographic results of patients with syndesmotic screw fixation: implications for screw removal. *J Orthop Trauma.* 2010;24:2-6.

12. Song DJ, Lanzi JT, Groth AT, et al. The Effect of Syndesmosis Screw Removal on the Reduction of the Distal Tibiofibular Joint: A Prospective Radiographic Study. *Foot Ankle Int.* 2014;35:543-548.

13. Clanton TO, Whitlow SR, Williams BT, et al. Biomechanical Comparison of 3 Current Ankle Syndesmosis Repair Techniques. *Foot Ankle Int.* 2017;38:200-207.

14. Forsythe K, Freedman KB, Stover MD, Patwardhan AG. Comparison of a novel FiberWire-button construct versus metallic screw fixation in a syndesmotic injury model. *Foot Ankle Int.* 2008;29:49-54.

15. LaMothe JM, Baxter JR, Murphy C, Gilbert S, DeSandis B, Drakos MC. Three-Dimensional Analysis of Fibular Motion After Fixation of Syndesmotic Injuries With a Screw or Suture-Button Construct. *Foot Ankle Int.* 2016;37:1350-1356.

16. Teramoto A, Suzuki D, Kamiya T, Chikenji T, Watanabe K, Yamashita T. Comparison of different fixation methods of the suture-button implant for tibiofibular syndesmosis injuries. *Am J Sports Med.* 2011;39:2226-2232.

17. Phisitkul P, Ebinger T, Goetz J, Vaseenon T, Marsh JL. Forceps reduction of the syndesmosis in rotational ankle fractures: a cadaveric study. *J Bone Joint Surg Am.* 2012;94:2256-2261.

18. Clanton TO, Williams BT, Backus JD, et al. Biomechanical Analysis of the Individual Ligament Contributions to Syndesmotic Stability. *Foot Ankle Int.* 2017;38:66-75.

19. Hunt KJ, Goeb Y, Behn AW, Criswell B, Chou L. Ankle Joint Contact Loads and Displacement With Progressive Syndesmotic Injury. *Foot Ankle Int.* 2015;36:1095-1103.

20. Thordarson DB, Motamed S, Hedman T, Ebramzadeh E, Bakshian S. The effect of fibular malreduction on contact pressures in an ankle fracture malunion model. *J Bone Joint Surg Am.* 1997;79:1809-1815.

21. Miller AN, Paul O, Boraiah S, Parker RJ, Helfet DL, Lorich DG. Functional outcomes after syndesmotic screw fixation and removal. *J Orthop Trauma.* 2010;24:12-16.

22. Sagi HC, Shah AR, Sanders RW. The functional consequence of syndesmotic joint malreduction at a minimum 2-year follow-up. *J Orthop Trauma.* 2012;26:439-443.

23. Qamar F, Kadakia A, Venkateswaran B. An anatomical way of treating ankle syndesmotic injuries. *J Foot Ankle Surg.* 2011;50:762-765.

24. Schottel PC, Baxter J, Gilbert S, Garner MR, Lorich DG. Anatomic Ligament Repair Restores Ankle and Syndesmotic Rotational Stability as Much as Syndesmotic Screw Fixation. *J Orthop Trauma.* 2016;30:e36-40.

5.7. Supplemental Figures

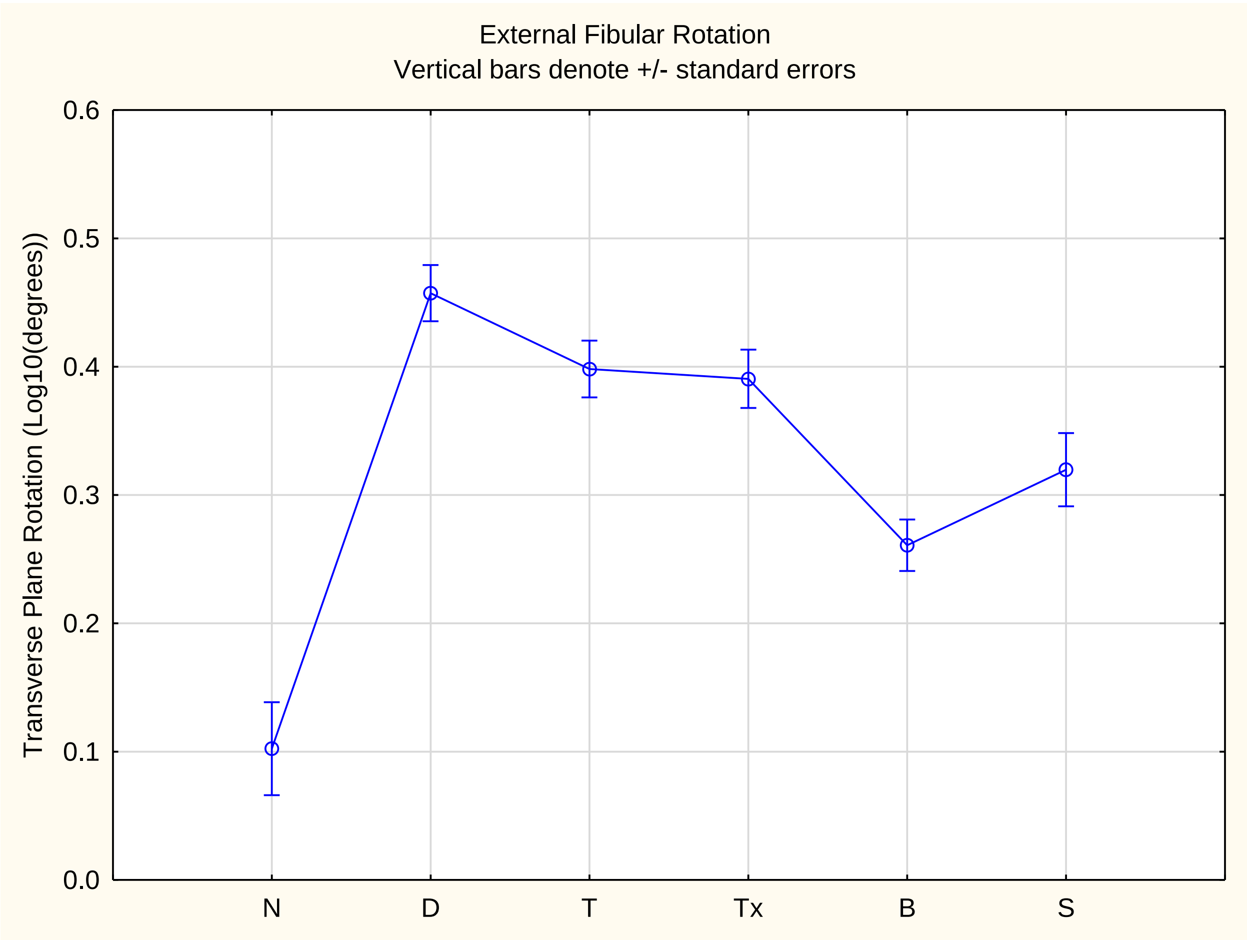

SF-1. Transformed (Log10) 3D Motion Tracking Data at 10 Nm of External Rotational Torque. Normal (N); Injured (D); 1x Suture-Button (T); 2x Suture-Button (Tx); 2x Suture-Buttons and Internal Brace (B); 1x Suture-Button and Internal Brace (S).

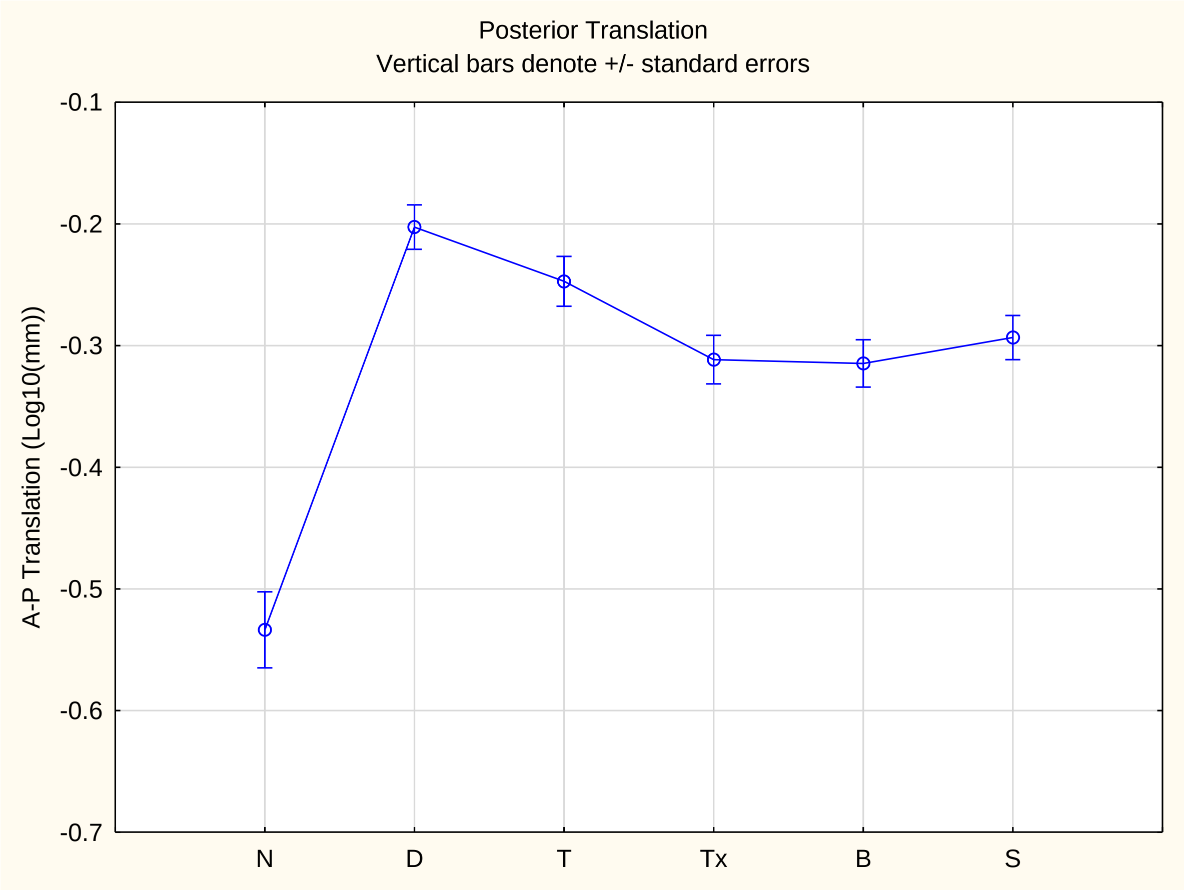

SF-2. Transformed (Log10) 3D Motion Tracking Data at 10 Nm of External Rotational Torque. Normal (N); Injured (D); 1x Suture-Button (T); 2x Suture-Button (Tx); 2x Suture-Buttons and Internal Brace (B); 1x Suture-Button and Internal Brace (S).

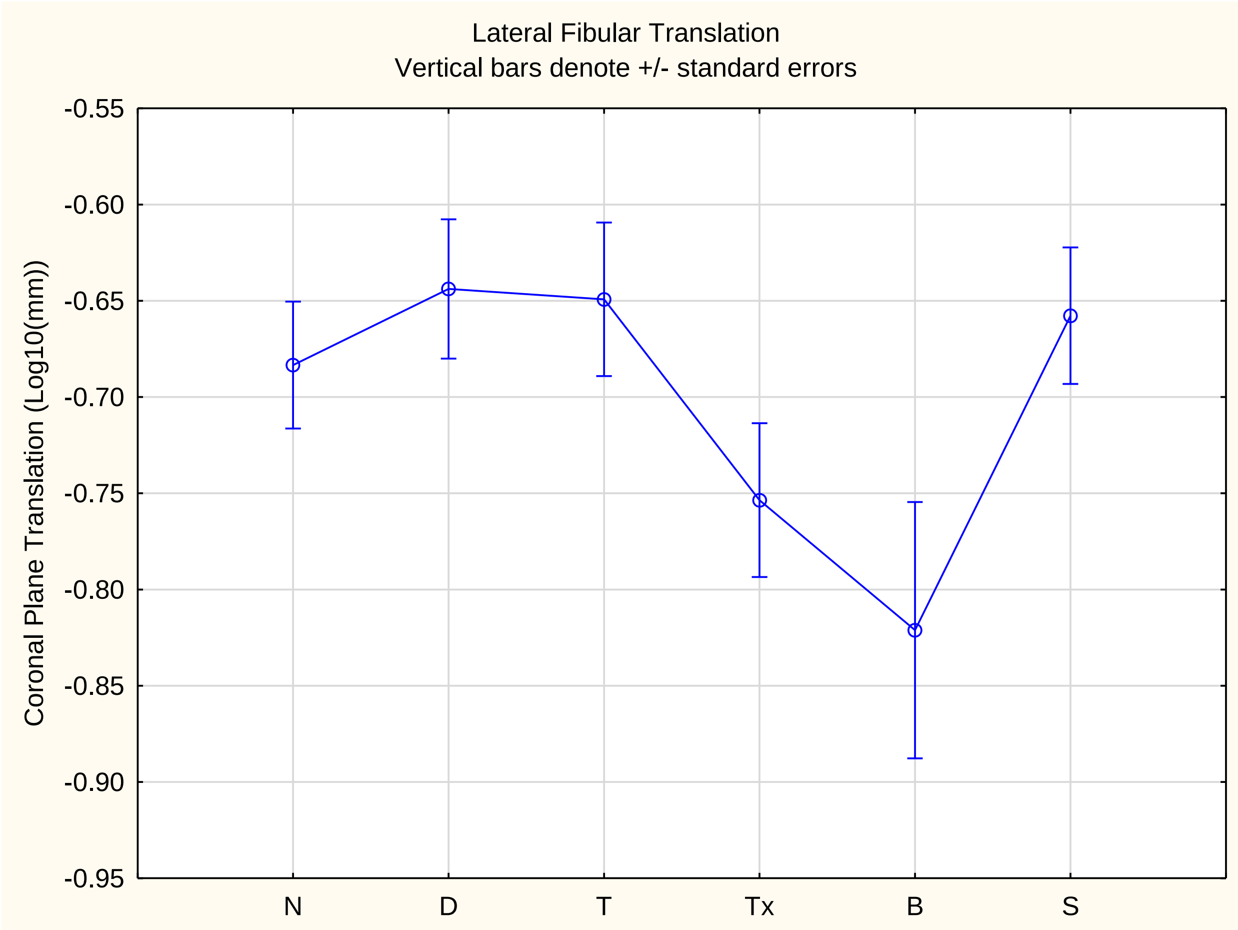

SF-3. Transformed (Log10) 3D Motion Tracking Data at 10 Nm of External Rotational Torque. Normal (N); Injured (D); 1x Suture-Button (T); 2x Suture-Button (Tx); 2x Suture-Buttons and Internal Brace (B); 1x Suture-Button and Internal Brace (S).

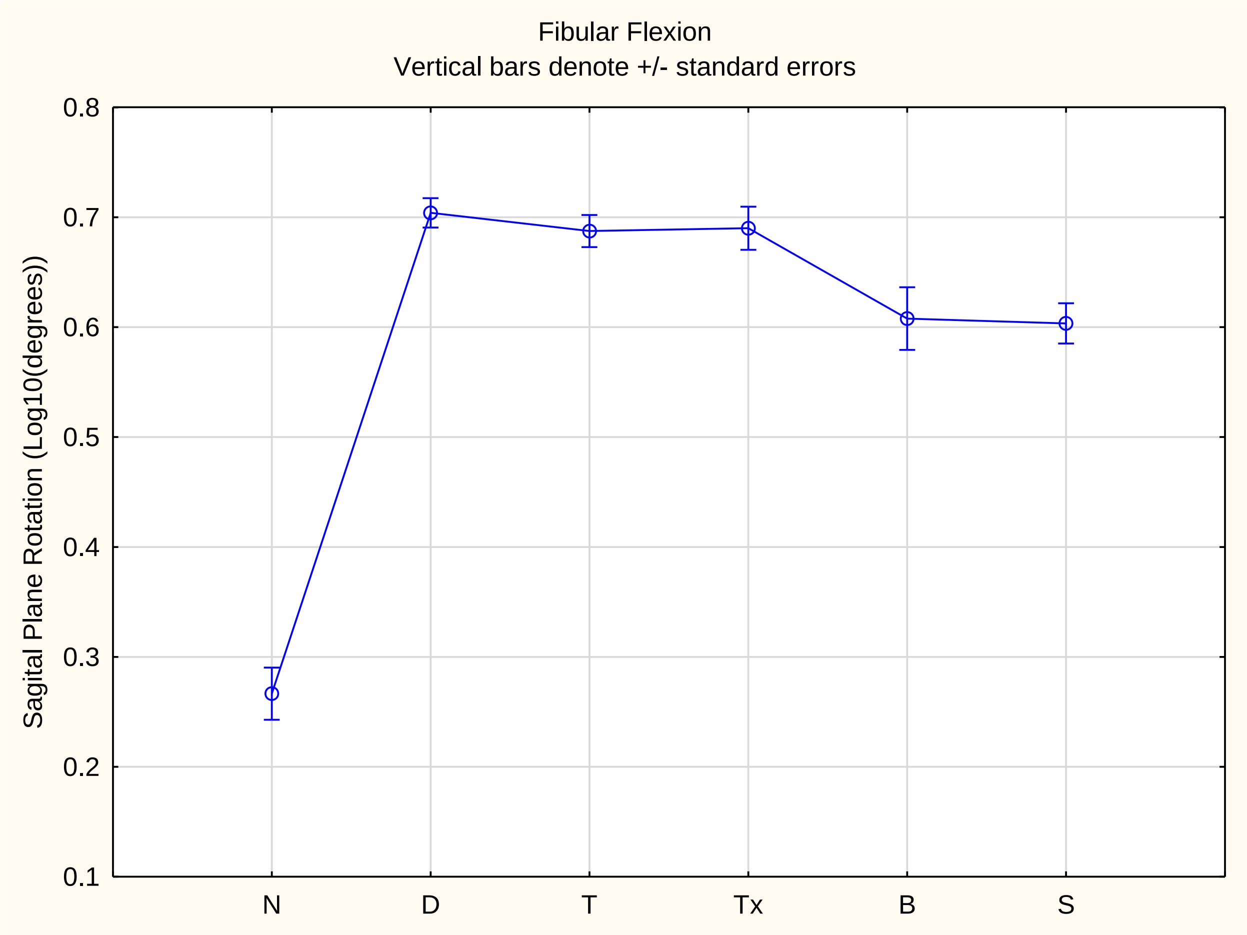

SF-4. Transformed (Log10) 3D Motion Tracking Data at 10 Nm of External Rotational Torque. Normal (N); Injured (D); 1x Suture-Button (T); 2x Suture-Button (Tx); 2x Suture-Buttons and Internal Brace (B); 1x Suture-Button and Internal Brace (S).

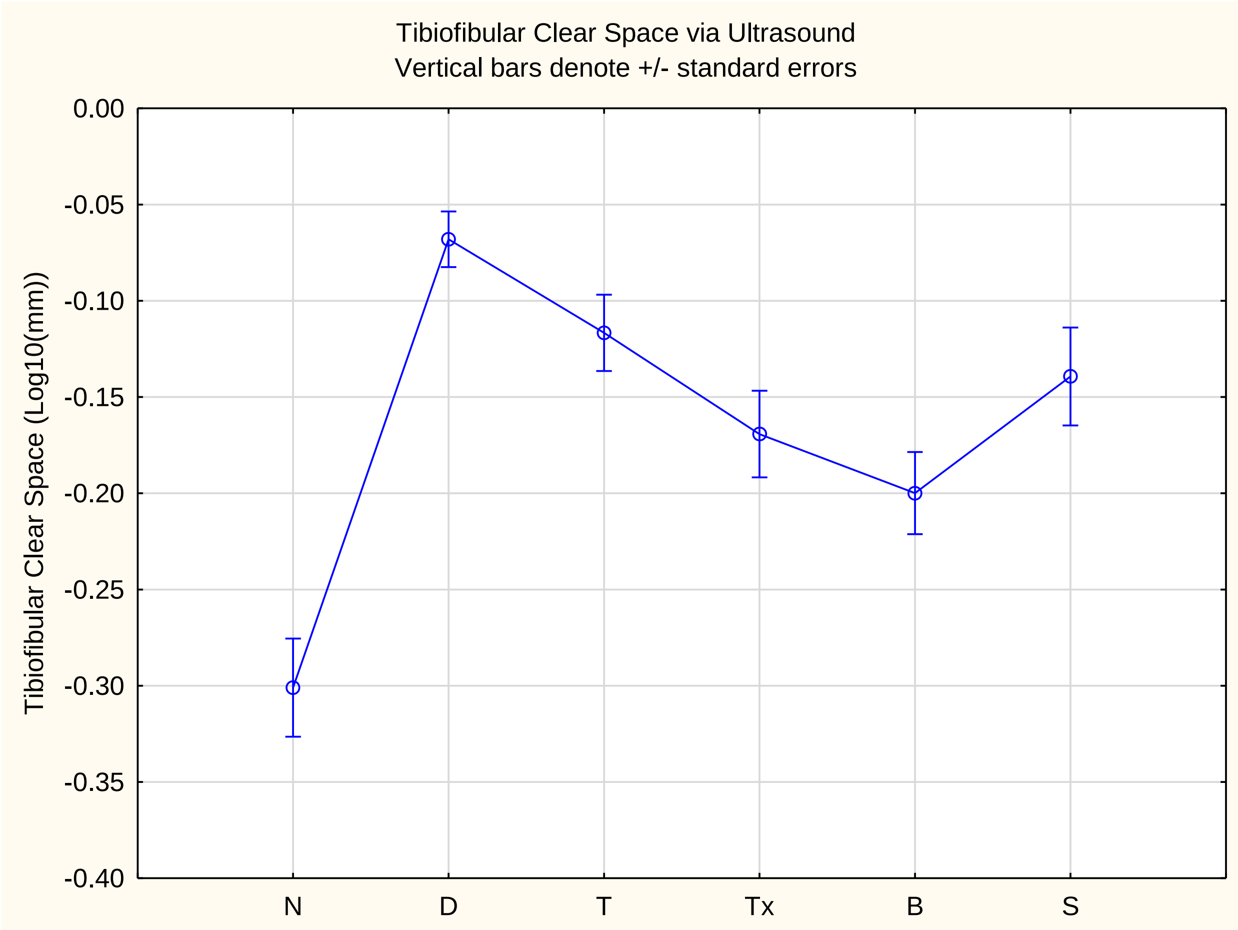

SF-5. Transformed (Log10) 3D Motion Tracking Data at 10 Nm of External Rotational Torque. Normal (N); Injured (D); 1x Suture-Button (T); 2x Suture-Button (Tx); 2x Suture-Buttons and Internal Brace (B); 1x Suture-Button and Internal Brace (S).

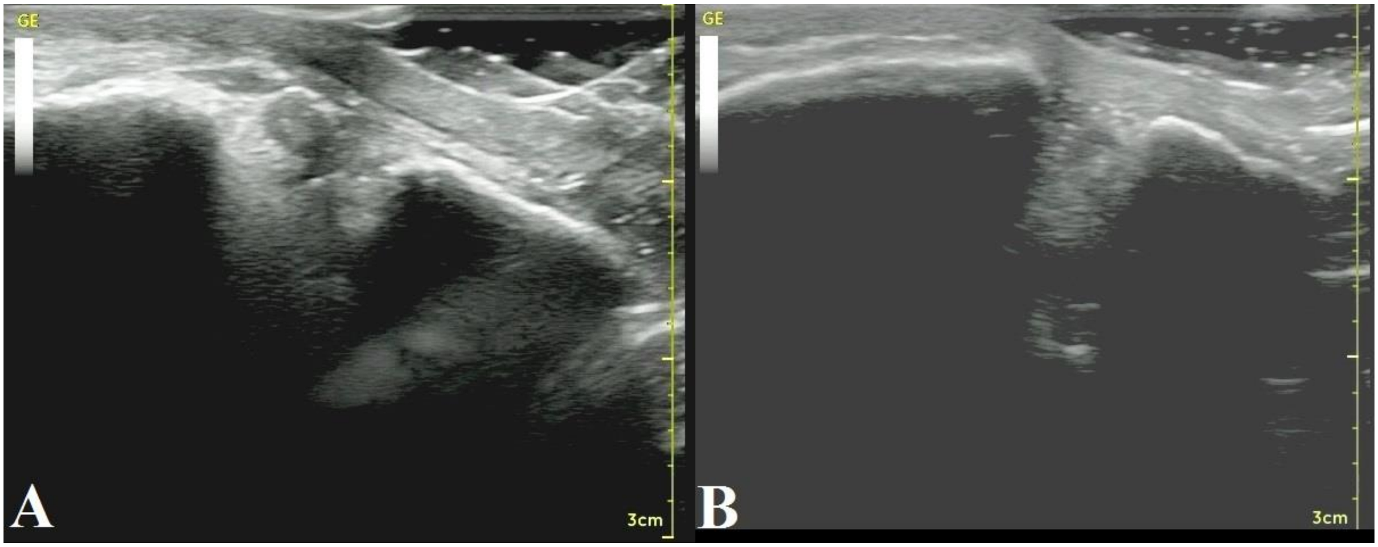

SF-6. Ultrasound Image Comparing [A] Injured state; [B] Internal Brace + 1x Suture-Buttons

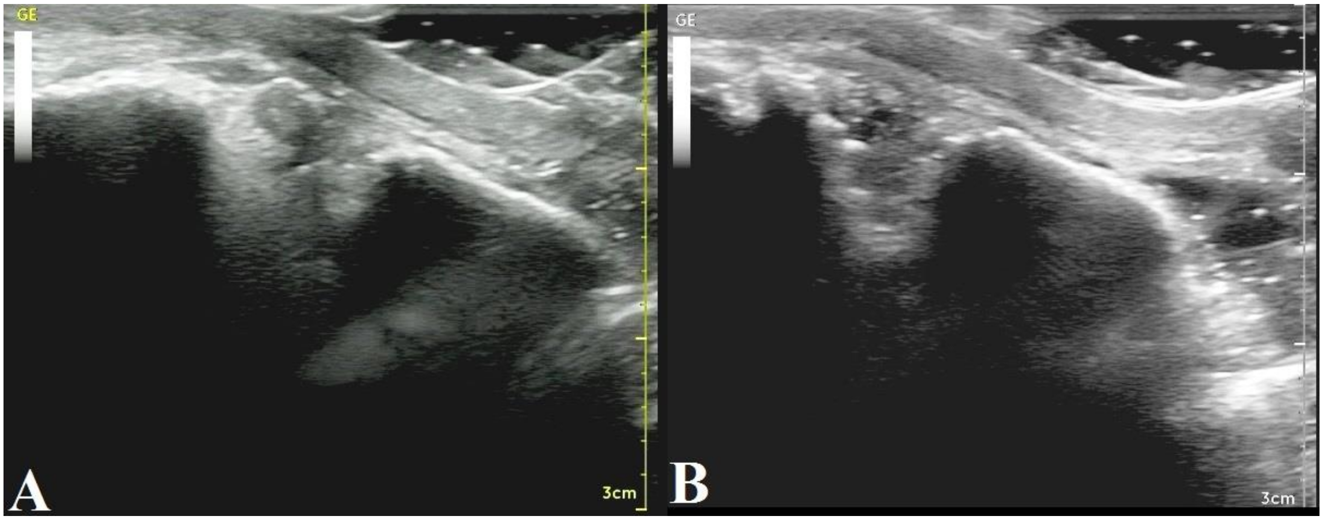

SF-7. Ultrasound Image Comparing [A] Injured state; [B] Internal Brace Alone

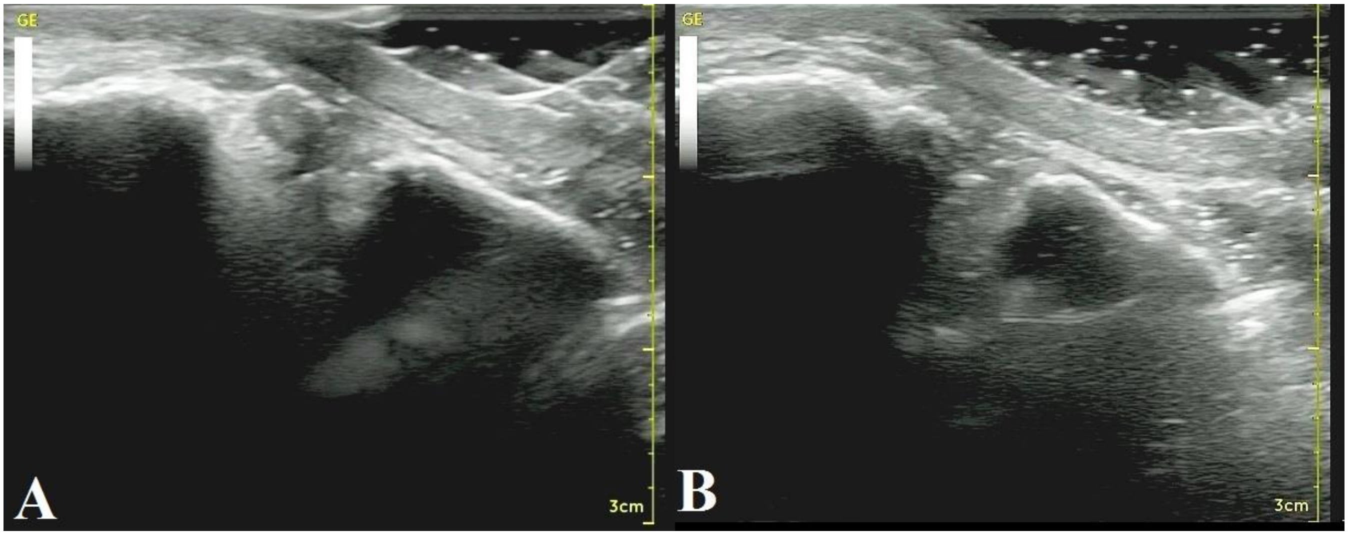

SF-8. Ultrasound Image Comparing [A] Injured state; [B] 1x Suture-Buttons

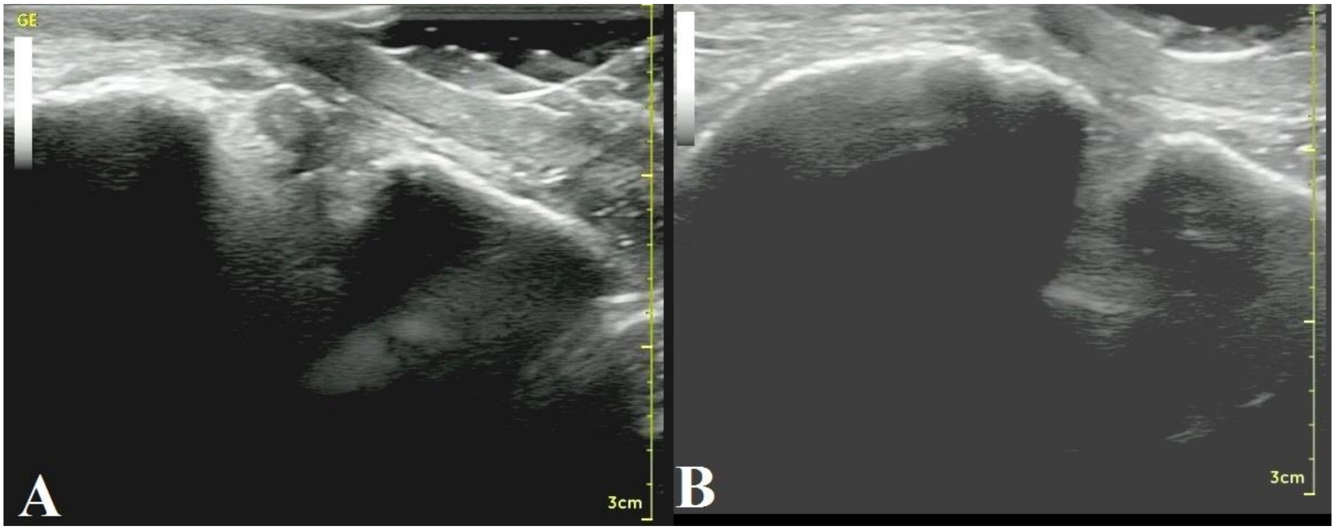

SF-9. Ultrasound Image Comparing [A] Injured State; [B] 2x Suture-buttons

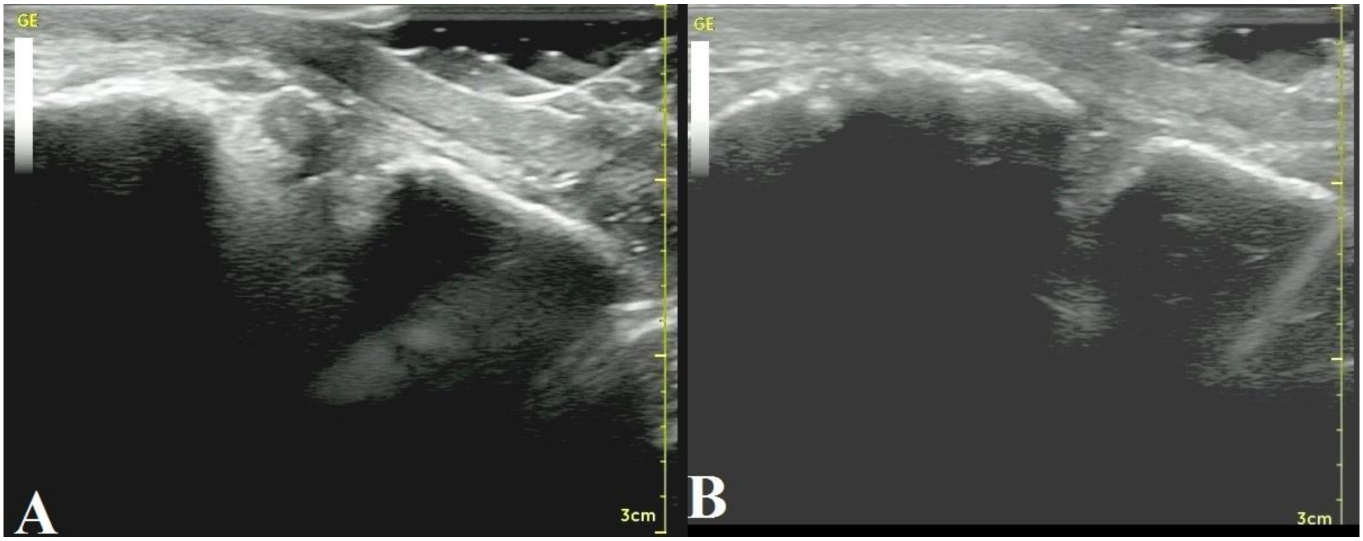

SF-10. Ultrasound Image Comparing [A] Injured state; [B] Internal Brace + 2x Suture-Buttons

Chapter 6

Future Work: Knee Model

Addison Wood, MS*[1]; Rustin Reeves PhD[1]; Rita Patterson PhD[1]; Russell Wagner MD[2]

From the [1]Department of Structural Anatomy and Rehabilitative Science,

University of North Texas Health Science Center, Fort Worth, Texas;

[2]John Peter Smith Hospital, Fort Worth, Texas

6.1. Specific Aims

Total knee arthroplasty (TKA) is most commonly performed on patients aged 50-80 years old for chronic knee pain and disability. It is considered one of the most successful surgeries performed. The long-term survival of TKA implants are generally over 90% at 15 years of follow up. [17, 18] Advances over the past 20 years in implant design, surgical technique, and patient selection have led to these outstanding outcomes. Today, orthopaedic surgeons are faced with an increasingly younger patient population with severe joint degeneration. This new demographic of patients does not achieve the same level of success with TKA as prototypical patients.[19-23] This population is expected to increase over the next decade which presents new challenges for TKA.[24] Younger patients have higher average physical activity levels and require a wider range of functional motion than their older peer.[21] These patients deserve definitive treatment, but TKA does not achieve that level of success with current methods. To accomplish this, the knowledge base on the effects of posterior tibial slope (PTS) and implant design must be further elucidated. *The primary objective of this study is to provide a conceptual strategy for better knee flexion using a combination of implant design and surgical technique.* Younger patients demand physiologic motion of their prosthetic knees to keep up with their activity levels. Surgeons take advantage of PTS and implant design to increase the functional range of motion of the prosthetic knee. However, the literature provides a limited view of the collective effects of these two variables. This study can provide objective data to orthopaedic surgeons on the appropriate combination of prosthesis and PTS to achieve physiologic motion during TKA. Furthermore, future prosthesis design may be influenced by our findings to improve patellofemoral (PF) interaction. *I propose a hypothesis in which maintaining more native anatomy and geometry during TKA provides the most physiological motion of the knee.* This study focuses on 4 major implant designs currently used in the United

States. These designs encompass the divergent methodologies of constraining the knee via implant to control motion versus using native anatomic structures to control motion. Bicruciate retaining (BCR) and posterior cruciate retaining (PCR) implants make use of native structures to help guide tibiofemoral (TF) and PF motion. Anterior stabilized (AS) designs retain the PCL, but makes use of an anterior polyethylene lip to constrain motion. Posterior stabilized (PS) designs do not retain native cruciate structures and attempt to control motion through a cam-post mechanism. Data acquired from this study can be used to implement implant design changes and guide surgeons on decision making.

Specific Aim 1: To determine the combination of implant design and posterior tibial slope that provides the most physiological patellofemoral motion during TKA. Hypothesis: Cruciate retaining implant designs provide the most physiological motion by retaining the PTS found in the native knee. Sequential TKA with 4 different implant designs is performed on cadaver specimens utilizing each specimen's native motion as a control. Deep knee flexion is simulated from 0-120 degrees using a knee rig used by Shalhoub et al.[25] Dynamic motion is recorded by an electromagnetic tracking system with 6 degrees of freedom. PF motion and TF motion is then reconstructed and analyzed after each design is tested at 0, 4, and 8 degrees of PTS using a shim system from our previous work. We expect the BCR and PCR designs to be the most similar to the native knee with the AS and PS bearings being the least similar. We also postulate the mechanism of this increased physiologic motion *to be the retention of native cruciate anatomy.*

Specific Aim 2: To assess changes in cruciate ligament strain as a function of posterior tibial slope and implant design. Hypothesis: Minimalizing PTS will provide the most benefit to the BCR design and maximizing PTS will benefit PCR, AS, and PS designs. Experimentation takes place using the same model as specific aim 1 with the addition of strain sensors. Synchronized data will be collected in the dynamic model as the knee completes a cycle of deep knee flexion. Cruciate strain is assessed for an increased risk of rupture as indicated by increased strain at different combinations of PTS and implant design. We expect the BCR design to benefit the most from restricting PTS at or below the native PTS to reduce ACL strain. All other designs are expected to benefit the most from having a PTS at or above the level of native. The point at which PTS becomes detrimental to cruciate strain in each implant design is of crucial importance to implant survivability.

6.2. Background & Significance

Reduction in pain and achieving a functional range of motion are goals for the more than 600,000 TKAs performed each year in the United States. The majority of these surgeries are performed on patients older than 65, but a growing proportion of TKAs are being performed on patients younger than 65.[5, 10] It is projected that the majority of TKAs will be performed on patients younger than 65 over the next 2 decades.[5, 6, 8] Younger TKA patients generally desire higher activity levels and a wider range of motion as compared to older patients.[5] The long-term survivability of implants in younger patients has been reported to be over 90% at 10 years follow up with a decrease in survival to 85% at 15 years.[5, 10] The average life expectancy in the United States is 79.8 years. Patients under 65 can therefore expect to outlast their TKA implants and receive revision surgery. In summary, patients younger than 65 require longer implant survivability and demand more from their implants with higher activity levels and range of motion. This new patient demographic undergoing TKA presents new challenges to orthopaedic surgeons and implant manufacturers. Surgical technique, implant selection, and implant design must be maximized to meet the needs of younger patients.

The effect PTS has on the PF joint is largely unknown yet most surgeons incorporate dome degree of PTS using either surgical technique or implant selection.[11] The PTS is defined as the angle formed from the intersection of the tibial plateau surface with the long axis of the tibia in the sagittal plane. This angle is changed during surgery by altering the angle of the saw blade during resection of the tibial plateau. The PTS of the polyethylene insert of the implant can also be altered by the manufacturer. Past studies have shown that altering the PTS increases posterior femoral translation (PFT) and maximum flexion achieved during TKA.[11, 12] This same pattern of PFT is found during physiological motion of the native knee.[12] Patellar tracking may be altered by changing the PTS during TKA, but no evidence currently exists on the topic. Changing PTS during TKA may therefore be a viable method to create more physiological motion. Our study will track the patella through deep knee flexion as PTS and implant design are changed. This will provide insight on how to maintain physiological patellar movement during TKA. Native physiological patellar tracking is guided by the structural anatomy of the knee. In the prosthetic knee, the majority of the anatomical features have changed as well as the motion. Abnormal patellar tracking is an important factor to consider during TKA as it can be implicated in the need for revision surgeries in as many 7.3% of cases.[2] Currently, proper surgical technique and implant alignment can prevent some of these complications, but not all.[1, 2, 13] Implant manufacturers may be influenced to alter their designs and surgical technique recommendations for TKA with the addition of this basic knowledge to the literature.

Achieving physiologic knee flexion has been a challenge in arthroplasty. Attaining this motion in the prosthetic knee is made difficult with the vast array of surgical techniques and implant designs to choose from. Currently, only 80% of patients are satisfied with their TKA, leaving room for improvement.[4] Maximizing physiologic motion in the prosthetic knee may help meet patient's expectations of maintaining activity levels after surgery. This is especially important for younger TKA patients[5]. A major determinant of knee motion after TKA is implant design.[12, 14-16] Implant selection is largely driven by surgeon preference and native structural anatomy. The 4 implants examined in this study provide a spectrum of comparison between anatomical guided and prosthetic guided motion. The cruciate retaining designs employ native anatomy to guide motion. The PS design uses its prosthetic cam-post mechanism to guide motion in place of native cruciate anatomy. It is highly debated whether these designs provide any benefit over one another.[14-17] Our study seeks accurate comparison of these implant designs when PTS is varied. This comparison is currently not available in the literature due to major methodological differences between studies.[18, 19] To address this knowledge gap our study analyzes kinematics and cruciate strain together across all designs. Cruciate strain is important to monitor while altering PTS as it has been debated that increasing the PTS can lead to higher than normal cruciate strain.[20-23] This higher than normal strain can lead to early failure and revision due to rupture of the cruciate ligament(s).[21, 22] Therefore it is pertinent to know which combination of PTS and implant design affords the best physiological motion and cruciate strain.

6.3. Innovation

As recently reviewed, the PTS literature reveals widespread differences in the methods used for measuring patellofemoral kinematics.[18, 19] This makes accurate comparison between studies impossible. This is an extremely important point to be made as *there are no studies comparing the effects of PTS across multiple implant designs.* This leaves the potential for inaccurate conclusions to be made. Our study combines the use of a knee rig, muscle loading scheme, and coordinate system that have proven accurate in past studies.[9, 18] This study would provide the most accurate and broad assessment of multiple implant designs and PTS in the current literature. In addition, there is conflicting evidence on the effects of PTS on cruciate strain.[20-22, 24] The cruciate ligaments are integral to the stability and motion of any cruciate retaining design. Protecting the cruciate ligaments is of upmost importance to the long-term survivability of these implants.[14, 20, 24] Furthermore, no data currently exists regarding how cruciate strain is effected by PTS in the BCR design. Our data may provide definitive evidence to guide surgeons with respect to cruciate integrity after PTS alteration.

We specifically chose the spectrum of implant designs for this study to illustrate different strategies an orthopaedic surgeon may employ to address anatomical considerations of each individual patient. These implants also contribute data towards the argument on whether it is better to conserve the cruciate ligaments to control motion or to allow bearing constraints to drive that motion. We examine this paradigm by testing a range of implants from fully cruciate retaining to a fully cruciate sacrificing design with 2 intermediate designs (PCR & AS) in between. Surgeons will be able to view the data and directly make conclusions as to what is the best combination of bearing design and PTS for their patients.

6.4. Approach

Previous Work: Nine fresh frozen cadaver knees underwent a modified PCR-TKA. The posterior tibial slope was cut to 10 degrees and a shim system was used to incrementally adjust the PTS 1 degree at a time. A Polhemus tracking system was used to measure flexion, extension, rotation, and translation of the knee joint. A weight and pulley apparatus applied a simulated force to the quadriceps and hamstrings. Each specimen was subjected to the simulated force while only the PTS was changed. The maximum flexion and amount of PFT were then recorded at each level of PTS. Primary outcomes of this study were maximum flexion and PFT as a function of PTS.

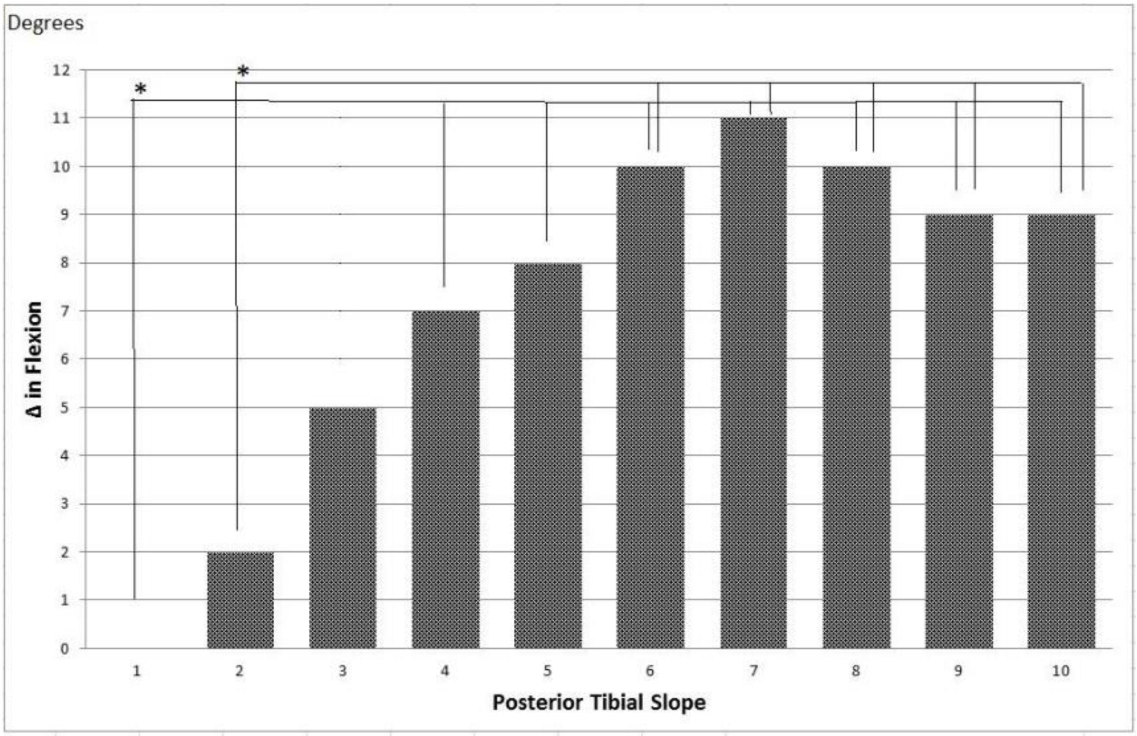

Figure 1. Effects of increasing the posterior tibial slope on the A-P translation of the femur.

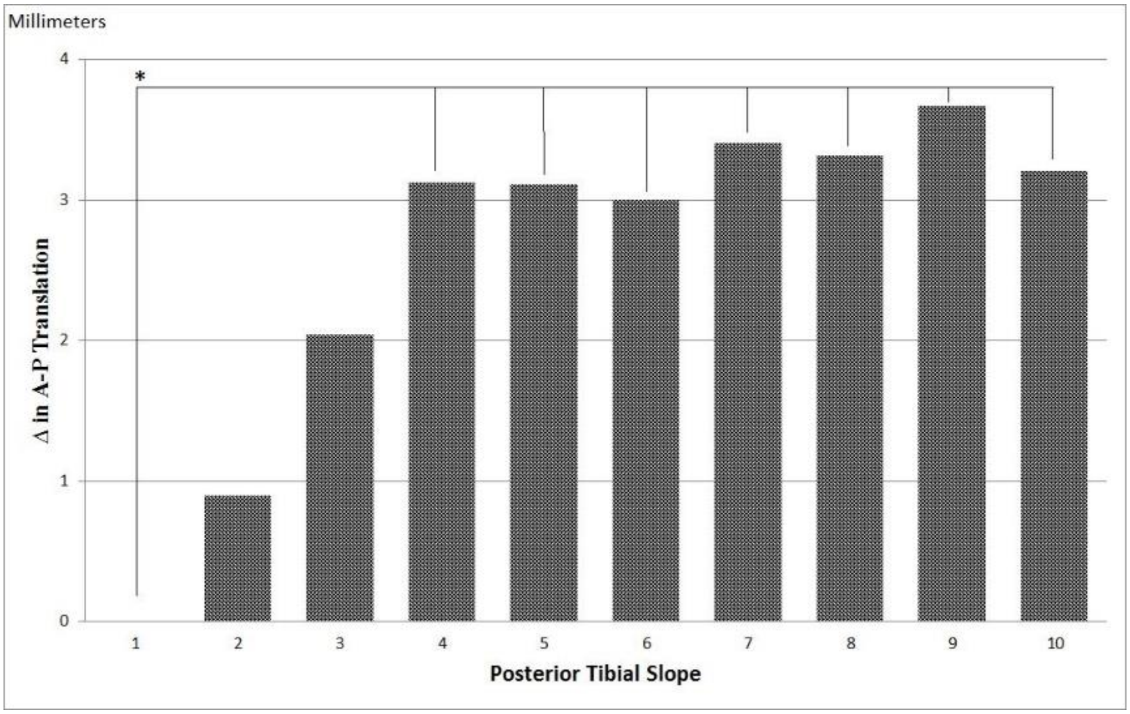

Figure 2. Effects of increasing the posterior tibial slope on the maximum flexion of the knee joint.

Total flexion decreased beyond 7 degrees of PTS; however, this was not statistically significant. PFT also increased significantly with increased posterior tibial slope. Achieving optimal posterior tibial slope in CR-TKA is an important variable in obtaining maximal flexion range of motion. The findings in this cadaveric study suggest that PTS provides for improved flexion range of motion by limiting posterior tibiofemoral impingement via increased rollback. Although flexion and rollback may be improved with initial increases of PTS up to 6 degrees, our data suggest that further increases in PTS fail to improve flexion and rollback.

Current Study:

Specimen Preparation Fresh frozen cadaver specimens are thawed overnight to room temperature prior to testing. Specimens with evidence of prior knee surgery, abnormal ligament contracture, coronal or sagittal plane deformity, and severe obesity are omitted from the study. All specimens undergo fluoroscopic evaluation prior to experimentation to rule out deformity. The quadriceps muscle groups are dissected into vastus medialis (VM), vastus lateralis (VL), rectus femoris (RF), and vastus intermedius (VI) muscle heads. The hamstrings muscle heads are dissected into biceps femoris (BF) and Semimembranous (SM) portions. All muscle heads are then attached via clothe and resin glue to loops for later attachment to tension cables. Tracking sensor anchor pins are implanted into predrilled holes with epoxy resin in the femur, tibia and patella. Computed tomography (CT) is then performed to verify baseline PTS and recreate a 3-dimensional model of the specimen. A graphite rod is cemented into the medullary canal using methyl methacrylate for attachment to the knee rig. Differential variable reluctance transducers (DVRT) are installed into the ACL and PCL to record dynamic strain data. These sensors are attached through a locking barb mechanism. Leads are passed through the medial peripatellar incision to the data acquisition system. Specimens are forced through maximum flexion-extension for 20 cycles by hand prior to testing.

Knee Rig Set-up and Validation A knee rig (KR) shown to be a valid in-vitro model for dynamic deep knee flexion is built from aluminum as reported by Shalhoub et al. (Fig. 3).[9] The specimen is secured to the KR via the cemented graphite rod at the proximal femur. A weight and pulley system is used to orient and load the quadriceps and hamstring muscles individually as reported by Farahmand et al.[25] Muscle loads are distributed based upon cross sectional area of the muscle bodies. Muscle vectors are formed from loading the quadriceps and hamstrings in anatomical orientation. The rig allows unrestrained motion at the knee and ankle as anatomy dictates.

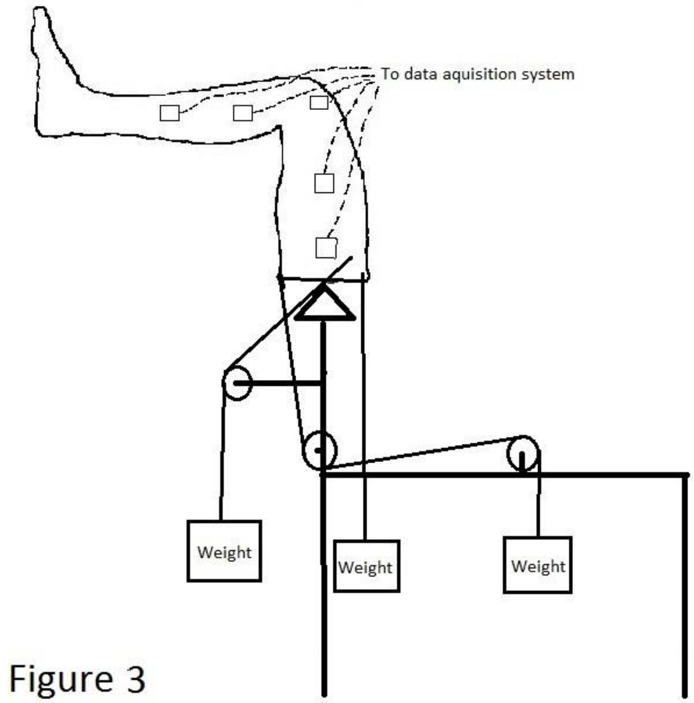

Figure 3.

The knee flexion moment is due to gravity as hamstring and quadriceps loads are equal at 175N. To induce motion the knee is fully extended manually and then released. Flexion is restricted to a maximum rate of 10 degrees per a second. Prior to measurement of prosthetic knee kinematics, the KR will undergo repeatability testing using native specimens. Each specimen is mounted to the KR with all sensors attached and undergo 3 cycles of motion. The specimen is detached from the KR and sensors are removed. The specimens then have their sensors reattached and is remounted to the KR with repeated measurements performed. This mounting-detachment process is repeated 5 times to ensure repeatability between specimen data recording sessions. Native knee kinematic data is then compared to published data to validate the model.

<u>Study Protocol</u> Native knee kinematic data is first recorded in the KR alongside the cruciate strain data. This data is used as a control to compare prosthetic knees against. Each knee will serve as its

own control. Sequential TKA is then performed in the following order: BCR, PCR, AS, PS. The PTS is varied for each implant design at 0, 4, and 8 degrees. PF and TF Kinematics and cruciate strain are evaluated at each of these levels of PTS for every implant design. 5 cycles of motion are completed at each level of PTS to ensure accurate measurement. Custom made shims from our previous work are used to change PTS without effecting implant alignment. These shims are secured inferior to the tibial plate using nails and decrease the PTS as they are added. Using CT data, a 3d reconstruction of the native specimen and the location of the motion tracking sensors is formed. Data from the tracking system is then integrated with the CT data. This allows the reconstruction of the motion of each specimen with each implant design at every level of PTS. The location of the patella in the trochlear groove and a coordinate system for describing PF and TF motion are formed using this integration of tracking system and CT data.

<u>Surgical Protocol</u> A medial peripatellar approach is used to allow installation of strain and retropatellar force sensors. To simulate joint capsule closure towel clamps are used. After initial data gathering and validation of native knee motion BCR surgery will proceed. To reduce costs, trial sets of implants will be used for all experimentation. Surgery is carried out according to Biomet recommendations for all implant designs. Soft tissue balancing and implant alignment will remain constant throughout experimentation. The PTS is cut to 8 degrees using a surgical jig and verified using a manual compass. After completion of BCR data gathering the bone island and ACL is removed using an oscillating saw to allow fitment of the PCR/AS tibial plate. Data is then recorded on the PCR implant and then the polyethylene trays are swapped to allow testing of the AS design without any further modification. The PS design is tested last as an additional femoral block of bone and PCL must be removed to allow fitment of the femoral cam component.

Alternative Methods: A camera-reflector system could be used in place of the electromagnetic tracking system. This system was not chosen as it requires multiple personnel to run and would require significant laboratory changes to be made. However, it could be made available should insurmountable issues occur with the electromagnetic system. A microscribe system could be used in place of the CT scans to coordinate tracking sensor position with anatomical position. This system was not chosen due to significant time requirements and feasibility in accessing pertinent anatomical structures with the microscribe system.

Data Collection and Analysis Results will be analyzed initially using descriptive statistics. Data will be analyzed by 2-way repeated measures ANOVA with a post hoc TUKEY test to determine significant changes from the native knee in flexion, PFT, and patellofemoral motion as PTS is varied in each implant design. Regression analysis will be used to determine if there is a correlation between PTS and cruciate strain. CT data will be used to calculate TF and PF kinematics with 6 degrees of freedom. This is made possible by the location of the tracking sensor pin placement prior to CT scanning. With these reference points the patella can be described in relation to the trochlear groove. The native knee motion is considered physiologic and acts as the control for all comparisons made in the study.

Limitations Cadaveric specimens may vary in soft tissue integrity, bone integrity, hidden prior injuries, undetectable deficits to the human eye, and may cause inconsistencies during TKA surgery. Cadaveric specimens do not contain living tissues and therefore do not represent the metabolic and remodeling processes that would be present in living tissue. Simulated tension on the hamstrings and quadriceps muscles used in this study do not fully represent the dynamic activation of muscle during flexion extension cycles in vivo. Boney alignment in each specimen is limited as the angles of cuts are not changed throughout the experiment.

6.5. References

1. Gerber JP, Williams GN, Scoville CR, Arciero RA, Taylor DC. Persistent disability associated with ankle sprains: a prospective examination of an athletic population. *Foot Ankle Int.* 1998;19:653-660.
2. Hunt KJ, George E, Harris AH, Dragoo JL. Epidemiology of syndesmosis injuries in intercollegiate football: incidence and risk factors from National Collegiate Athletic Association injury surveillance system data from 2004-2005 to 2008-2009. *Clin J Sport Med.* 2013;23:278-282.
3. Waterman BR, Belmont PJ, Jr., Cameron KL, Svoboda SJ, Alitz CJ, Owens BD. Risk factors for syndesmotic and medial ankle sprain: role of sex, sport, and level of competition. *Am J Sports Med.* 2011;39:992-998.
4. McCullough CJ, Burge PD. Rotatory stability of the load-bearing ankle. An experimental study. *J Bone Joint Surg Br.* 1980;62-b:460-464.
5. Ogilvie-Harris DJ, Reed SC, Hedman TP. Disruption of the ankle syndesmosis: biomechanical study of the ligamentous restraints. *Arthroscopy.* 1994;10:558-560.
6. Ramsey PL, Hamilton W. Changes in tibiotalar area of contact caused by lateral talar shift. *J Bone Joint Surg Am.* 1976;58:356-357.
7. Rasmussen O. Stability of the ankle joint. Analysis of the function and traumatology of the ankle ligaments. *Acta Orthop Scand Suppl.* 1985;211:1-75.
8. Scranton PE, Jr., McMaster JG, Kelly E. Dynamic fibular function: a new concept. *Clin Orthop Relat Res.* 1976:76-81.

9. Xenos JS, Hopkinson WJ, Mulligan ME, Olson EJ, Popovic NA. The tibiofibular syndesmosis. Evaluation of the ligamentous structures, methods of fixation, and radiographic assessment. *J Bone Joint Surg Am.* 1995;77:847-856.

10. Van Heest TJ, Lafferty PM. Injuries to the ankle syndesmosis. *J Bone Joint Surg Am.* 2014;96:603-613.

11. Manjoo A, Sanders DW, Tieszer C, MacLeod MD. Functional and radiographic results of patients with syndesmotic screw fixation: implications for screw removal. *J Orthop Trauma.* 2010;24:2-6.

12. Song DJ, Lanzi JT, Groth AT, et al. The Effect of Syndesmosis Screw Removal on the Reduction of the Distal Tibiofibular Joint: A Prospective Radiographic Study. *Foot Ankle Int.* 2014;35:543-548.

13. Clanton TO, Whitlow SR, Williams BT, et al. Biomechanical Comparison of 3 Current Ankle Syndesmosis Repair Techniques. *Foot Ankle Int.* 2017;38:200-207.

14. Forsythe K, Freedman KB, Stover MD, Patwardhan AG. Comparison of a novel FiberWire-button construct versus metallic screw fixation in a syndesmotic injury model. *Foot Ankle Int.* 2008;29:49-54.

15. LaMothe JM, Baxter JR, Murphy C, Gilbert S, DeSandis B, Drakos MC. Three-Dimensional Analysis of Fibular Motion After Fixation of Syndesmotic Injuries With a Screw or Suture-Button Construct. *Foot Ankle Int.* 2016;37:1350-1356.

16. Teramoto A, Suzuki D, Kamiya T, Chikenji T, Watanabe K, Yamashita T. Comparison of different fixation methods of the suture-button implant for tibiofibular syndesmosis injuries. *Am J Sports Med.* 2011;39:2226-2232.

17. Le DH, Goodman SB, Maloney WJ, Huddleston JI. Current modes of failure in TKA: infection, instability, and stiffness predominate. *Clin Orthop Relat Res.* 2014;472:2197-2200.

18. Sharkey PF, Lichstein PM, Shen C, Tokarski AT, Parvizi J. Why are total knee arthroplasties failing today--has anything changed after 10 years? *J Arthroplasty.* 2014;29:1774-1778.

19. Parvizi J, Nunley RM, Berend KR, et al. High level of residual symptoms in young patients after total knee arthroplasty. *Clin Orthop Relat Res.* 2014;472:133-137.

20. Matsuda S, Kawahara S, Okazaki K, Tashiro Y, Iwamoto Y. Postoperative alignment and ROM affect patient satisfaction after TKA. *Clin Orthop Relat Res.* 2013;471:127-133.

21. Keeney JA, Eunice S, Pashos G, Wright RW, Clohisy JC. What is the evidence for total knee arthroplasty in young patients?: a systematic review of the literature. *Clin Orthop Relat Res.* 2011;469:574-583.

22. Kurtz S, Mowat F, Ong K, Chan N, Lau E, Halpern M. Prevalence of primary and revision total hip and knee arthroplasty in the United States from 1990 through 2002. *J Bone Joint Surg Am.* 2005;87:1487-1497.

23. Wainwright C, Theis JC, Garneti N, Melloh M. Age at hip or knee joint replacement surgery predicts likelihood of revision surgery. *J Bone Joint Surg Br.* 2011;93:1411-1415.

24. Kurtz SM, Lau E, Ong K, Zhao K, Kelly M, Bozic KJ. Future young patient demand for primary and revision joint replacement: national projections from 2010 to 2030. *Clin Orthop Relat Res.* 2009;467:2606-2612.

25. Shalhoub S, Maletsky LP. Variation in patellofemoral kinematics due to changes in quadriceps loading configuration during in vitro testing. *J Biomech.* 2014;47:130-136.

Chapter 7

7. Conclusion

The central objective of this dissertation was to achieve physiologic kinematics post-operatively in an in vitro simulation. To achieve this goal, the underlying determinants of physiological kinematics were first examined through anatomical variation and muscular architecture studies. These initial studies indicated significant variation exists between specimens and that muscular architecture can play a major role as input in vitro simulations. This wide diversity and importance of anatomical structural differences between subjects led us to deepen our understanding of structure governing function in our pursuit of attaining physiological kinematics after reconstructive surgery of the lower extremity.

We tested the effectiveness of an osteotome to prevent iatrogenic posterior cruciate ligament damage during surgery and found an absolute risk reduction of 50%. We had expected the effectiveness to be higher and searched for a reason why our expectations and results did not match. The answer was anatomical variation. The posterior tibial slope can vary widely from -3-16° and if the osteotome is not placed at least 2 cm deep there is the potential for the saw blade to pass underneath the osteotome and damage the posterior cruciate ligament.

We pursued the importance of anatomical individuality further by describing the muscular architecture of the popliteus muscle. In vitro simulations and many orthopaedic surgical techniques demand a high level of precise and detailed anatomy to properly guide them. The popliteus muscle is a unique and complicated structure that likely does not get the attention it deserves. At a foundational level, we provided evidence for the inclusion of the popliteus as a dynamic structure rather than just static. The PCSA and trajectory of the popliteus muscle were described and compared to the semimembranosus muscle to form a robust database of popliteus information that may be helpful in designing future in vitro simulations to include the popliteus muscle.

The UNT HSC Ankle Joint Simulator was designed and built to simulate an external rotational stress test that could be monitored with ultrasound, fluoroscopy, and motion tracking. The simulator fixes the tibia rigidly and allows free movement of the fibula to allow a torque to be applied through the tibiotalar joint thereby stressing the tibiofibular joint. The simulator has performed well with several kinematic studies on Lauge-Hansen ankle fractures, ligamentous stability, diagnostic sensitivity and specificity, and syndesmosis fixation studies already been completed using the rig.

The comparative ankle syndesmosis fixation study was performed using the UNT HSC Ankle simulator with the goal of achieving physiologic kinematics. To achieve this goal, different combinations of suture-button and internal brace fixation constructs were used to restore the function of injured ligamentous structures. The constructs were compared to the intact and injured ankle states to find optimal restoration of function. The internal brace with 2x suture-buttons was found to be statistically superior in restraining external fibular rotation and fibula flexion to suture-button only constructs. In addition, the combined internal brace with 2x suture-buttons construct was equivalent in all other degrees of restraint to suture-button only constructs. The combined internal brace with 2x suture-buttons construct was the most similar to the intact state out of all constructs examined, but still failed to achieve magnitude of anterior to posterior translational restraint of the intact state. This study solidified the notion of recreating structure to restore function in my mind. The suture-button implant has similar functionality to the interosseous ligament and provided acceptable fixation on its own, but fails to restore physiologic stability and motion on its own as other ligaments, in addition to the IOL, are typically involved in an injury to the syndesmosis. The addition of the internal brace to suture-button fixation provided an avenue to return ligament functions lost outside of the IOL, namely AITFL function. The study also reaffirmed the ability of ultrasound to detect changes in tibiofibular clear space due to syndesmosis disruption. These findings are clinically useful and provides a detailed understanding of the structure guiding function at the syndesmosis.

The revolving theme of this dissertation is anatomic structure drives physiologic function. Through the course of all of this work I have gained a wide breadth of technical skills and a deep knowledge of knee and ankle function. Perhaps the greatest asset gained was the ability to switch the paradigm around and not immediately focus on function when approaching a reconstructive surgery problem. I now look at structure first and come up with an idea of what kind of function that structure may provide before utilizing what is already known. This has a profound effect on my approach to methodology and practical applications in surgery. It is this line of thinking that I will take with me in pursuit of future lower extremity research.